

*Hanf*

PNL-8789

UC-602

---

**Investigation of Exposure Rates  
and Radionuclide and Trace Metal  
Distributions Along the Hanford  
Reach of the Columbia River**

A. T. Cooper  
R. K. Woodruff

---

September 1993

Prepared for the U.S. Department of Energy  
under Contract DE-AC06-76RLO 1830

Pacific Northwest Laboratory  
Operated for the U.S. Department of Energy  
by Battelle Memorial Institute



PNL-8789

## DISCLAIMER

This report was prepared as an account of work sponsored by an agency of the United States Government. Neither the United States Government nor any agency thereof, nor Battelle Memorial Institute, nor any of their employees, makes any warranty, expressed or implied, or assumes any legal liability or responsibility for the accuracy, completeness, or usefulness of any information, apparatus, product, or process disclosed, or represents that its use would not infringe privately owned rights. Reference herein to any specific commercial product, process, or service by trade name, trademark, manufacturer, or otherwise does not necessarily constitute or imply its endorsement, recommendation, or favoring by the United States Government or any agency thereof, or Battelle Memorial Institute. The views and opinions of authors expressed herein do not necessarily state or reflect those of the United States Government or any agency thereof.

PACIFIC NORTHWEST LABORATORY  
*operated by*  
BATTELLE MEMORIAL INSTITUTE  
*for the*  
UNITED STATES DEPARTMENT OF ENERGY  
*under Contract DE-AC06-76RLO 1830*

Printed in the United States of America

Available to DOE and DOE contractors from the  
Office of Scientific and Technical Information, P.O. Box 62, Oak Ridge, TN 37831;  
prices available from (615) 576-8401. FTS 626-8401.

Available to the public from the National Technical Information Service,  
U.S. Department of Commerce, 5285 Port Royal Rd., Springfield, VA 22161.

INVESTIGATION OF EXPOSURE RATES  
AND RADIONUCLIDE AND TRACE METAL  
DISTRIBUTIONS ALONG THE HANFORD REACH  
OF THE COLUMBIA RIVER

A. T. Cooper  
R. K. Woodruff

September 1993

Prepared for  
the U.S. Department of Energy  
under Contract DE-AC06-76RLO 1830

Pacific Northwest Laboratory  
Richland, Washington 99352

## SUMMARY

Studies have been conducted to investigate exposure rates, and radionuclide and trace metal distributions along the Columbia River where it borders the Hanford Site. The last major field study was conducted in 1979. With recently renewed interest in various land use and resource protection alternatives, it is important to have data that represent current conditions.

Radionuclides and trace metals were surveyed in Columbia River shoreline soils along the Hanford Site (Hanford Reach). The work was conducted as part of the Surface Environmental Surveillance Project, Pacific Northwest Laboratory. The survey consisted of taking exposure rate measurements and soil samples primarily at locations known or expected to have elevated exposure rates.

Exposure rate measurements ranged from 4 to 11  $\mu\text{R/hr}$  at the Vernita back-ground area, to 8 to 28  $\mu\text{R/hr}$  at the White Bluffs Slough area along the Hanford Reach. In all, 12 discrete radioactive particles were detected. Eleven of the particles were found on 100-D Island. One particle was found at the White Bluffs Slough area. The particle from White Bluffs Slough and one particle from 100-D Island were identified as  $^{60}\text{Co}$  with activities of 16 and 1.7  $\mu\text{Ci}$ , respectively. The remaining 10 particles were not removed for analysis.

Doses from exposure to the two particles collected were calculated for various potential exposure scenarios. The dose-limiting exposure scenario was determined to be a particle that is inhaled and deposited in the front part of the nose. The dose from this scenario would exceed the limit of 75  $\mu\text{Ci-hr}$  exposure to a skin surface from a particle as listed by the National Council on Radiation Protection and Measurements. This limit could also be reached for other plausible although improbable exposure scenarios including contact with bare skin for 5 hr, exposure through the lining of a pocket for 30 hr, and exposure through a sleeping bag for 44 hr. The largest effective dose equivalent from particle exposure was 60 mrem through ingestion, compared to a public standard of 100 mrem. The probability of the public actually coming in contact with such particles, however, is considered very low.

Exposure rate measurements taken adjacent to the 100-N Area on the water surface of the Columbia River, which is unrestricted for public use, ranged from

4.1 to 20.1  $\mu\text{R/hr}$ . These exposures have been attributed to radiation from liquid waste disposal facilities in the 100-N Area rather than from shoreline contamination. The estimated dose from fishing near the 100-N Area (over the area surveyed), 8 hr/d for a year, would be approximately 45 mrem, or about one half of the limit for public exposures.

Areas with elevated (compared to background) soil concentrations of major radioactive constituents (i.e.,  $^{22}\text{Na}$ ,  $^{60}\text{Co}$ ,  $^{90}\text{Sr}$ ,  $^{137}\text{Cs}$ ,  $^{152}\text{Eu}$ ,  $^{154}\text{Eu}$ , and  $^{239,240}\text{Pu}$ ) include 100-D Island, the Hanford Townsite shoreline, and the White Bluffs Slough area. The potential external exposure dose rates from continuous occupancy at a hypothetical location with soil containing the maximum concentrations measured at any location was calculated to be approximately 14 mrem/yr or less.

The only sampled location having a significantly elevated concentration of any trace metal (i.e., chromium) was near the 100-F floodplain area. While standards have not been written for freshwater sediments, the maximum chromium concentration was about 30% of the Washington State standard for marine sediments.

The data were examined (correlation of concentrations) to determine whether it is reasonable to assume that the highest concentrations of nongamma-emitting radionuclides and trace metals occur in the same places as the highest concentrations of gamma-emitting radionuclides. The results indicated that elevated  $^{239,240}\text{Pu}$  concentrations were associated (correlated) with and therefore predicted by the presence of several gamma-emitting radionuclides. Uranium,  $^{90}\text{Sr}$ , and trace metals concentrations were not correlated with the concentrations of gamma-emitting radionuclides. The lack of correlation with uranium and strontium suggests that they could have been distributed differently in the environment, but the lack of correlation may also be due to the relatively few locations with significantly elevated concentrations.

Several areas along the Hanford Reach still show detectable impacts from past Hanford operations. No short-lived radionuclides were detected, and no significant variation among trace metal concentrations was found, indicating that there are no recent depositions of radioactive and/or trace metal contaminants along the Hanford Reach.

## ACKNOWLEDGMENTS

Several individuals made valued contributions to this study and report. Gerald Simiele was the original study leader. He developed the original study design, but left to be employed by Roy F. Weston Co., Albuquerque, New Mexico, before the study was completed.

Field measurements and soil sampling was conducted by staff of the Field Sampling and Analysis Group, E. W. Lusty, Supervisor. Fieldwork was performed by Marshall Almarode, Gordon Andersen, Larry Belt, Wade Hankel, John Harrison, Jim Jahnke, Ted Lakey, Jose Lopez, Dan Mackliet, Dana Mueller, and John Reck. Their efforts during a very warm summer are greatly appreciated. Thanks also goes to Trevor VanArsdale for technical assistance.

Soil samples were analyzed for radionuclides by International Technology Corporation, Richland, Washington; analyses for trace metals were performed by Data Chem Laboratories, Salt Lake City, Utah. The  $^{60}\text{Co}$  particle analyses were performed by Elwood Lepel, Pacific Northwest Laboratory (PNL), Nuclear Chemistry Section.

The discrete radioactive particle dose calculations summarized in the report and contained in Appendix E were prepared by James Durham and Joseph Soldat, PNL, Health Physics Department.

Roger Dirkes and Richard Gilbert peer reviewed the report for technical content and Regina Lundgren edited the report. Their numerous comments were a valuable contribution to the report technically and editorially.

## CONTENTS

SUMMARY . . . . .	iii
ACKNOWLEDGMENTS . . . . .	v
1.0 INTRODUCTION . . . . .	1.1
2.0 STUDY OBJECTIVES . . . . .	2.1
3.0 APPROACH . . . . .	3.1
3.1 LOCATIONS . . . . .	3.1
3.2 SAMPLING METHODS . . . . .	3.17
3.2.1 External Gamma Surveys . . . . .	3.17
3.2.2 Discrete Particle Surveys . . . . .	3.17
3.2.3 Soil Sampling . . . . .	3.17
3.3 SOIL SAMPLE PREPARATION AND COMPOSITING . . . . .	3.18
4.0 RESULTS AND DISCUSSION . . . . .	4.1
4.1 EXPOSURE RATE SURVEY . . . . .	4.1
4.1.1 Comparison With 1988 Aerial Survey . . . . .	4.1
4.1.2 Comparison of Exposure Rates With Upstream and Historical Data . . . . .	4.3
4.1.3 Instrument Correlations . . . . .	4.4
4.2 DISCRETE RADIOACTIVE PARTICLE ANALYSIS . . . . .	4.9
4.3 100-N AREA SURVEY . . . . .	4.12
4.4 SOIL CONCENTRATION SURVEY . . . . .	4.14
4.4.1 Radionuclides . . . . .	4.14
4.2.2 Trace Metals . . . . .	4.23
5.0 REFERENCES . . . . .	5.1
APPENDIX A - EXPOSURE RATE DATA . . . . .	A.1

APPENDIX B - SOIL SAMPLE RADIONUCLIDE CONCENTRATION DATA AND  
SUPPLEMENTAL FIGURES . . . . . B.1

APPENDIX C - SOIL SAMPLE TRACE METAL CONCENTRATION DATA AND  
SUPPLEMENTAL FIGURES . . . . . C.1

APPENDIX D - ANALYTE CONCENTRATION CORRELATION MATRIX . . . . . D.1

APPENDIX E - DOSE CALCULATIONS . . . . . E.1

FIGURES

3.1	Survey Track Locations 1 Through 3	3.3
3.2	Survey Track Locations 4 Through 12	3.5
3.3	Survey Track Locations 13 Through 31	3.7
3.4	Survey Track Locations 32 Through 37	3.9
3.5	Survey Track Locations 38 Through 44	3.11
3.6	Survey Track Locations 45 Through 51	3.13
3.7	Survey Track Locations 52 Through 56	3.15
3.8	Soil Compositing Logic	3.19
4.1	1988 EG&G Aerial Radiological Survey of the 100-N Area	4.2
4.2	Individual Exposure Measurements Taken from Vernita to Richland	4.5
4.3	Median Exposure Rates at Each Survey Track	4.5
4.4	Log-Normal Distribution of Exposure Rate Measurements	4.6
4.5	Correlation of Ludlum $\mu R$ and Bicron $\mu rem$ Measurements	4.8
4.6	Correlation of Reuter Stokes PIC and Bicron $\mu rem$ Measurements	4.8
4.7	Exposure Rates on the Columbia River Adjacent to the 100-N Area, $\mu R/hr$	4.13
4.8	Sodium-22 ( $^{22}Na$ ) Concentrations in Soils	4.16
4.9	Cobalt-60 ( $^{60}Co$ ) Concentrations in Soils	4.16
4.10	Zinc-65 ( $^{65}Zn$ ) Concentrations in Soils	4.17
4.11	Cesium-137 ( $^{137}Cs$ ) Concentrations in Soils	4.17
4.12	Europium-152 ( $^{152}Eu$ ) Concentrations in Soils	4.18
4.13	Europium-154 ( $^{154}Eu$ ) Concentrations in Soils	4.18
4.14	Strontium-90 ( $^{90}Sr$ ) Concentrations in Soils	4.19
4.15	Uranium-234 ( $^{234}U$ ) Concentrations in Soils	4.19
4.16	Uranium-235 ( $^{235}U$ ) Concentrations in Soils	4.20

4.17 Uranium-238 ( <sup>238</sup> U) Concentrations in Soils . . . . .	4.20
4.18 Plutonium-239,240 ( <sup>239,240</sup> Pu) Concentrations in Soils . . . . .	4.21
4.19 Barium Concentrations in Soils . . . . .	4.24
4.20 Beryllium Concentrations in Soils . . . . .	4.24
4.21 Cadmium Concentrations in Soils . . . . .	4.25
4.22 Chromium Concentrations in Soils . . . . .	4.25
4.23 Cobalt Concentrations in Soils . . . . .	4.26
4.24 Lead Concentrations in Soils . . . . .	4.26
4.25 Manganese Concentrations in Soils . . . . .	4.27
4.26 Comparison of Maximum Trace Metal Concentrations Between Soils Along the Hanford Reach and Soils from Background Areas Across the Hanford Site . . . . .	4.30

TABLES

3.1 Analyses and Methods . . . . .	3.20
4.1 Comparison of Exposure Rates . . . . .	4.4
4.2 Comparison of Maximum Shoreline and Background Regional Soil Concentrations, pCi/g . . . . .	4.22
4.3 External Dose Rates from Radionuclides in Soils . . . . .	4.23
4.4 Trace Metals Comparisons, mg/kg . . . . .	4.29

## 1.0 INTRODUCTION

In 1943, the Hanford Site in southeast Washington State was selected by the U.S. Army Corps of Engineers, Manhattan District, as the site for future nuclear reactors to produce plutonium. The area was chosen because of its distance from major cities, the relatively small local population, the reliable electricity from Grand Coulee Dam, and convenient access to the water of the Columbia River as a reactor cooling source and an effluent sink for the reactors' byproducts (Becker 1990). By February 1945, three reactors (B, D, F) were operating and producing plutonium.

A total of eight single-pass-cooling reactors would eventually line the Hanford Reach of the Columbia River, the stretch of river from Priest Rapids Dam to just upstream from the city of Richland. These reactors discharged significant amounts of heat, radioactivity, and chemicals directly into the river. Suspension of insoluble chemicals, trace metals, and radionuclides in the river led to deposition in shoreline soils downstream of each discharge point. The last such reactor (100-KE) ceased operations in 1971. Since that time, the radionuclide burden of the shoreline soils along the Hanford Reach has been decreasing as the radioactive material decays. Short-lived radionuclides, which accounted for the major component of radiation exposure, have since decayed to negligible levels (Sula 1980).

The most recent aerial survey of the Site, conducted in 1988 (EG&G 1990), indicated that previously identified areas of elevated radioactivity continued to exist as a result primarily of longer-lived radionuclides. The aerial survey, however, is a relative indicator of contamination, and only for gamma-emitting radionuclides.

The last major field study to quantify external gamma rates and radionuclides along the Columbia River in shoreline soils was performed in 1979 (Sula 1980). With recently renewed interest in various land use and resource protection alternatives, one being the designation of the Hanford Reach as a National Wild and Scenic River, it is important to have data that represent the current conditions on the Hanford Site. A wide range of potential uses for the Site is identified by the Hanford Future Site Uses Working Group (1992).

This report describes a study conducted as an activity of the Hanford Site Surface Environmental Surveillance Project to investigate exposure rates and radionuclide and trace metal distributions along the Hanford Reach. The study was designed as a field survey rather than as a statistically based sampling design. The results provide current external exposure rates, characterize radionuclide concentrations, and provide new data on the concentrations of trace metals in shoreline soils along the Hanford Reach. Trace metals are of interest because of their use and disposal to the river and soil column in reactor and chemical-processing operations.

## 2.0 STUDY OBJECTIVES

The current study was performed during July through October 1992 with the following specific study objectives:

1. Exposure Rates—Assess potential human exposure rates at specific locations along the Hanford Reach, examine the differences in exposure rates between locations, assess changes in exposure rates since prior studies, and quantify exposure rates in areas identified by aerial surveys as having elevated radioactivity.
2. Discrete Radioactive Particle Analysis—Record the frequency of occurrence of discrete radioactive particles, measure their activity, and compare the frequency of particle occurrences to data from prior studies.
3. 100-N Area Survey—Assess potential human exposure rates on the surface of the Columbia River along the section that borders the 100-N Area (N Reactor).
4. Soil Concentrations—Investigate the effect of Hanford operations on concentrations of radionuclides and trace metals in soils at specific locations along the Hanford Reach, and examine the differences in concentrations between locations.
5. Concentration Correlations—Determine if the concentrations of major gamma emitting radionuclides are correlated with the concentrations of other radionuclides and trace metals, i.e., does the presence of gamma emitters predict the presence of other radionuclides and trace metals.

### 3.0 APPROACH

The approach to the study was to choose locations and sampling methods that would help characterize external dose rates and radionuclide and trace metal distributions.

#### 3.1 LOCATIONS

The areas of the Hanford Reach surveyed are best described as islands, flood plains, sloughs, low-lying peninsulas, and exposed river shoreline. The Hanford Reach has an occasional sandy beach, but in general the terrain along the Reach is dominated by embedded layers of rocks.

The area chosen for background sampling was the southern shoreline ranging from the Priest Rapids Dam to the Vernita Bridge. This area was chosen for background sampling because it is upstream of the Hanford Site, not impacted by Hanford operations, and geographically and geologically similar to the survey areas to be investigated. A total of 21 soil samples were taken from three locations (Tracks 1, 2, and 3, Figure 3.1) to form three composite samples for analysis and comparison to downstream samples (see sampling methods below). A total of 51 exposure rate measurements (each measurement was the visually averaged exposure rate along a 100-m track, see sampling methods below) from eight background locations were averaged to provide an exposure rate background value for comparison to downstream values.

The 53 survey locations, downstream of the Vernita Bridge, (Tracks 4 through 56) are shown in Figures 3.2 through 3.7. The locations range geographically from the northern stretch of the Hanford Reach (near the 100-D Reactor) to the southwestern stretch near the city of Richland water intake (commonly known as the Richland Pumphouse). The locations sampled were chosen by examining historical survey information (Sula 1980), the 1988 aerial radiological monitoring system report (EG&G 1990), public use/access information, and evaluations of Columbia River flow characteristics and sedimentation zones. Areas with known radiation exposure levels greater than background levels were given sampling priority (EG&G 1990), although other areas were also sampled.

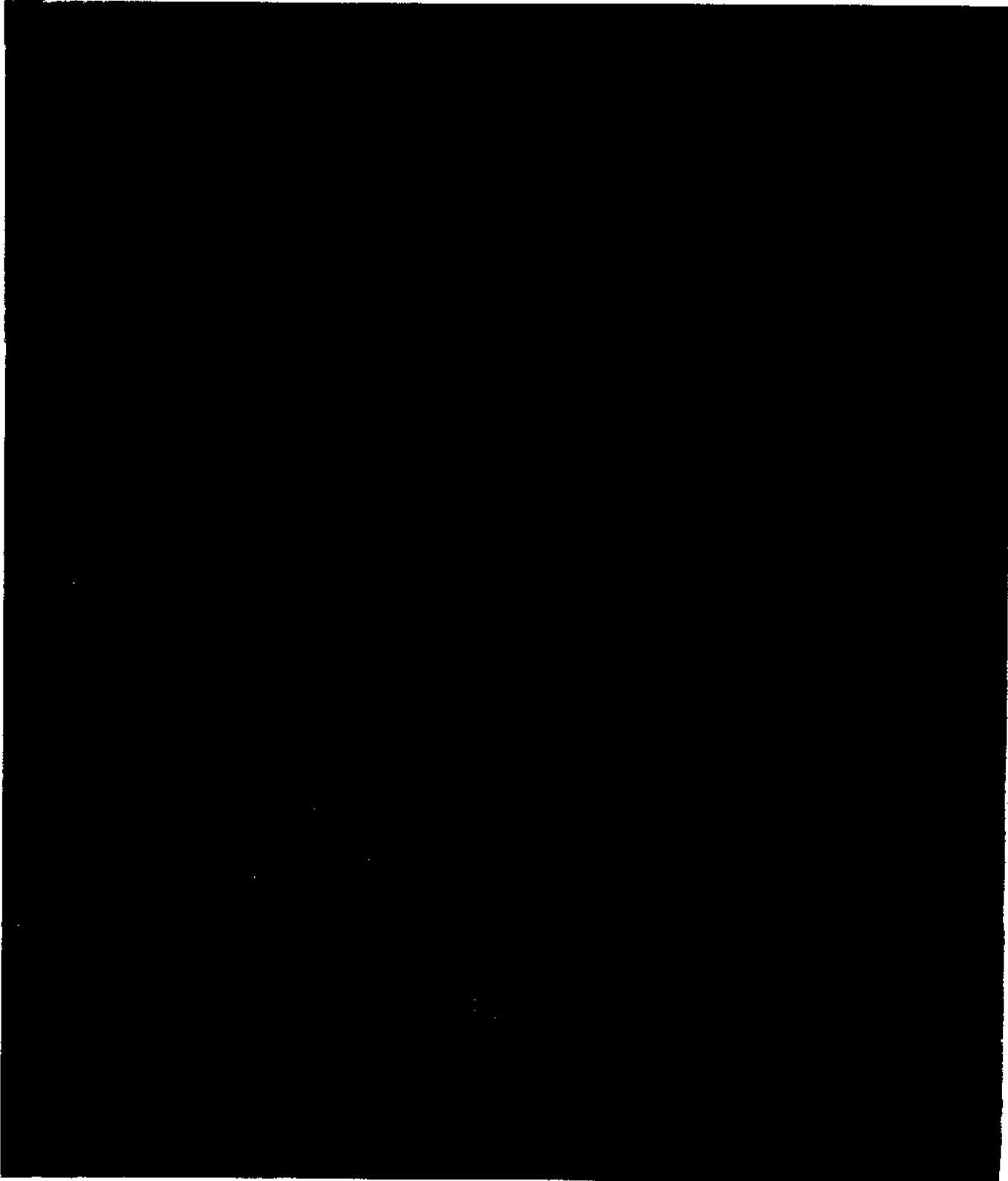


FIGURE 3.1. Survey Track Locations 1 Through 3

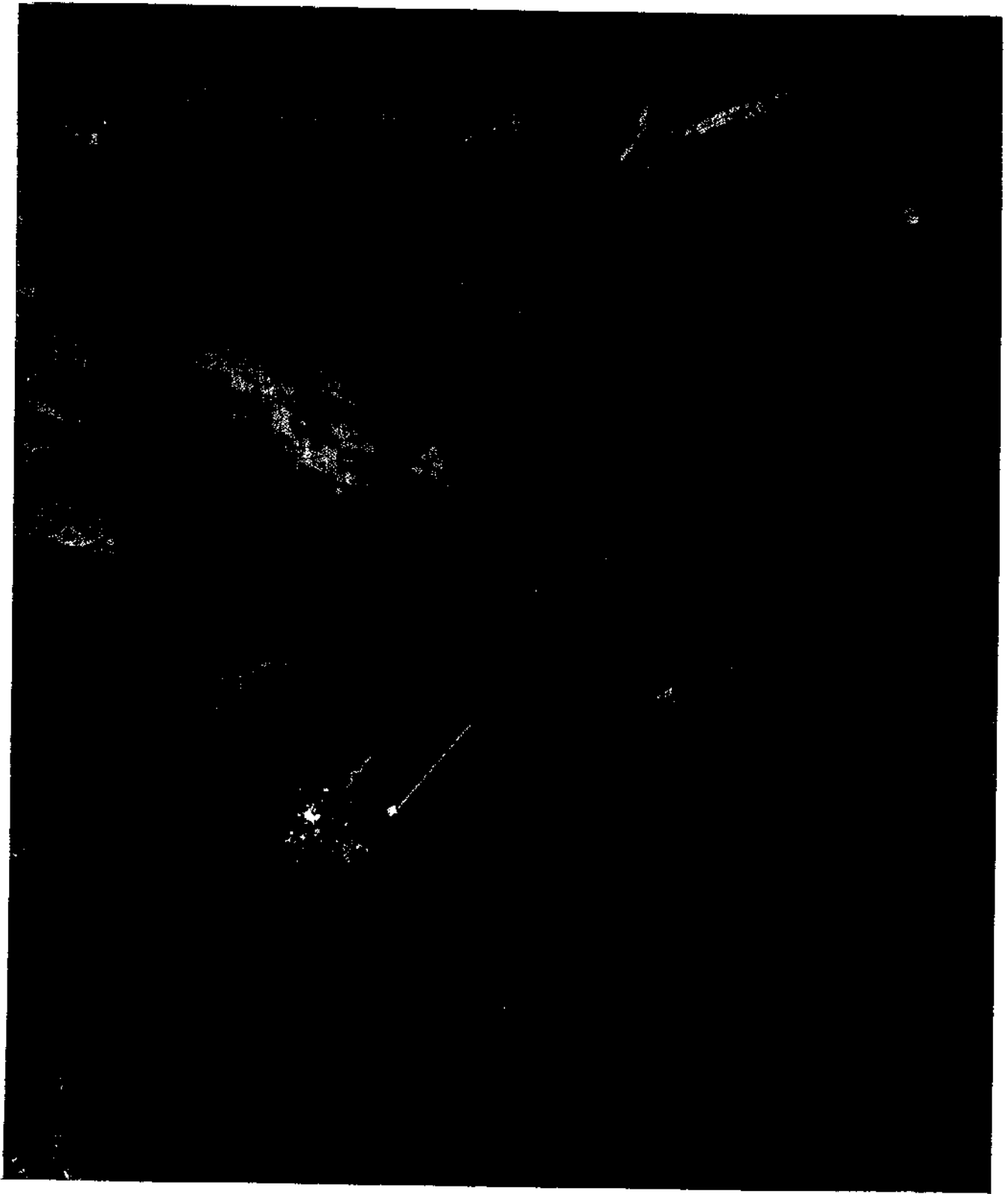


FIGURE 3.2. Survey Track Locations 4 Through 12

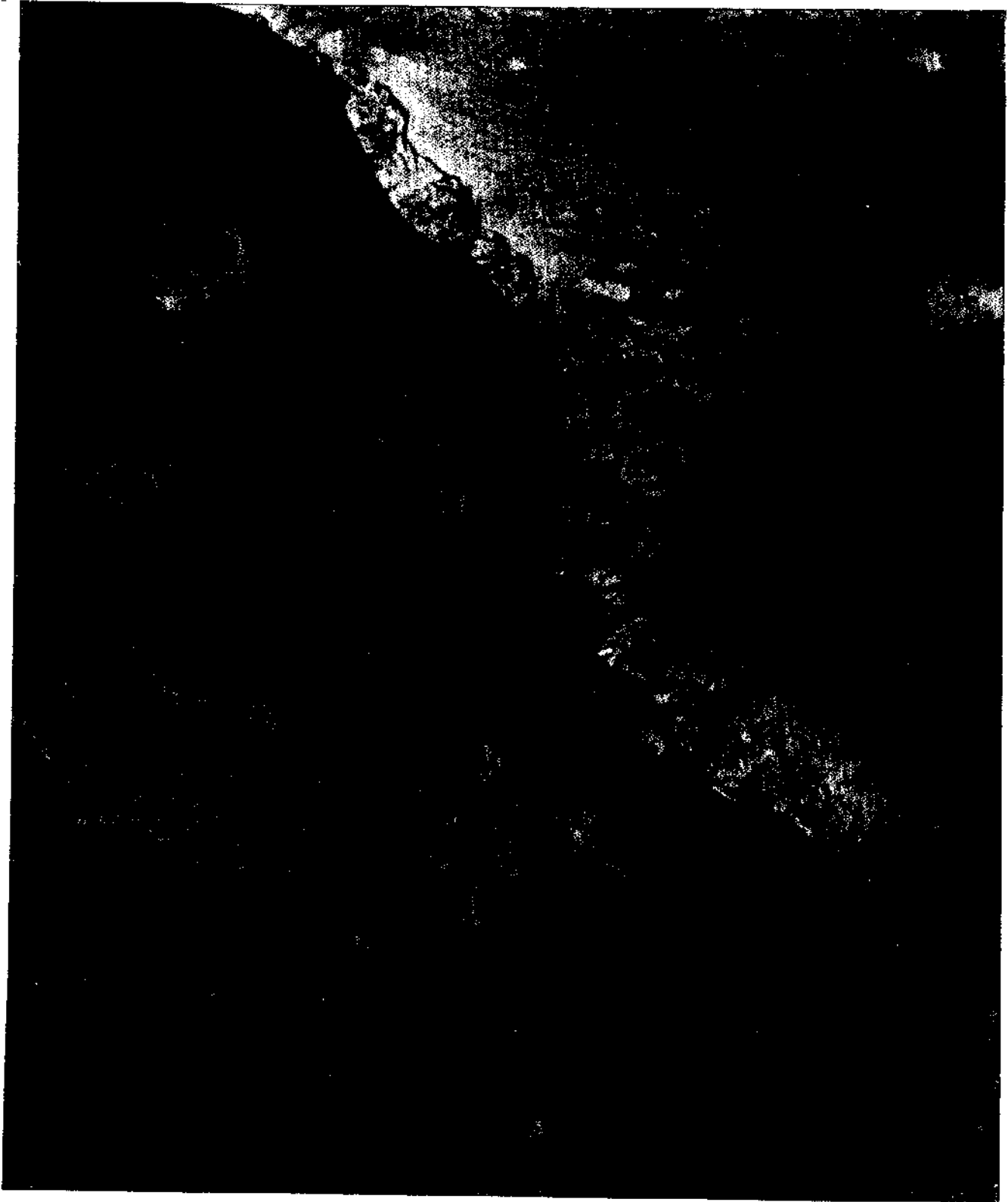


FIGURE 3.3. Survey Track Locations 13 Through 31

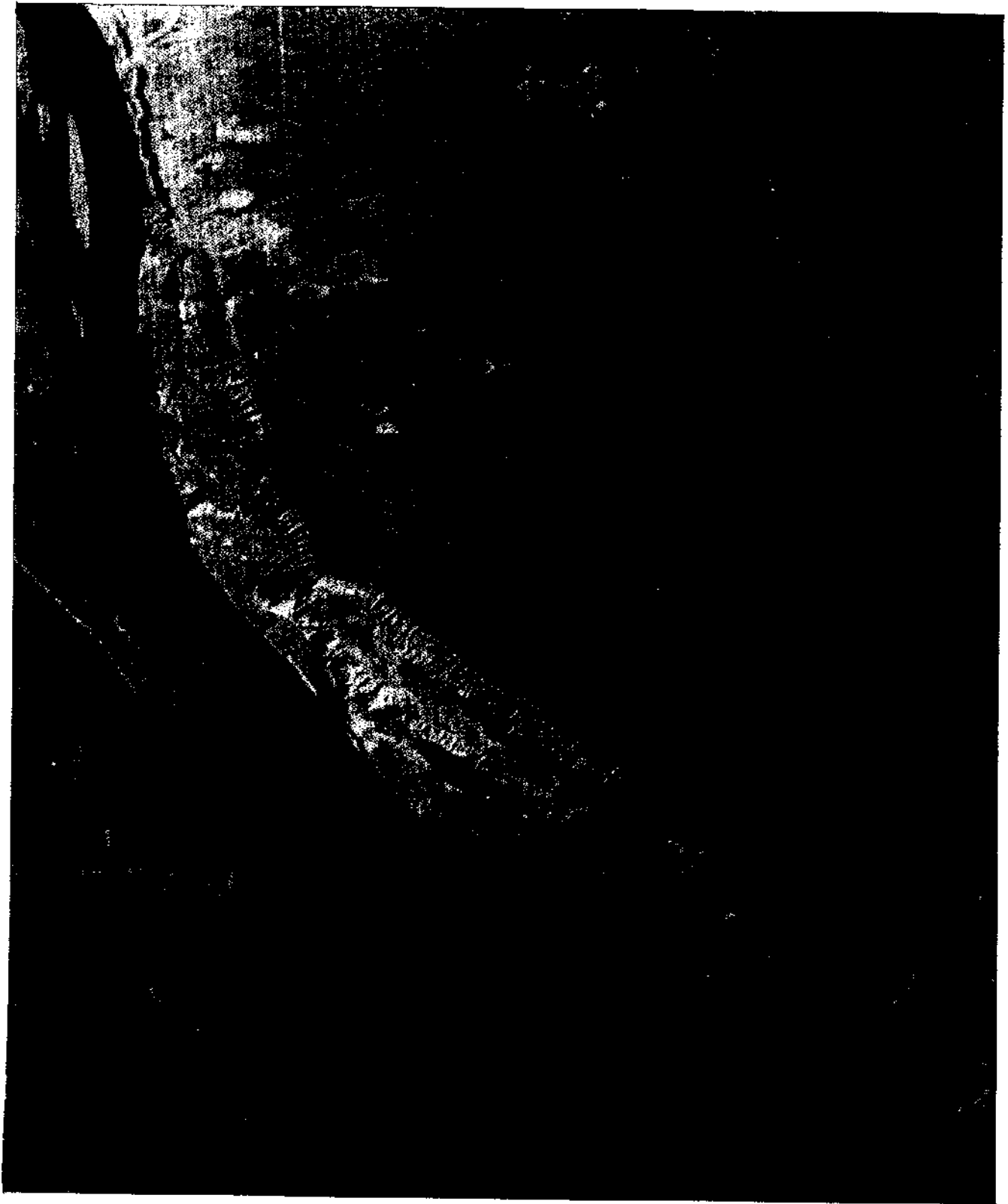


FIGURE 3.4. Survey Track Locations 32 Through 37

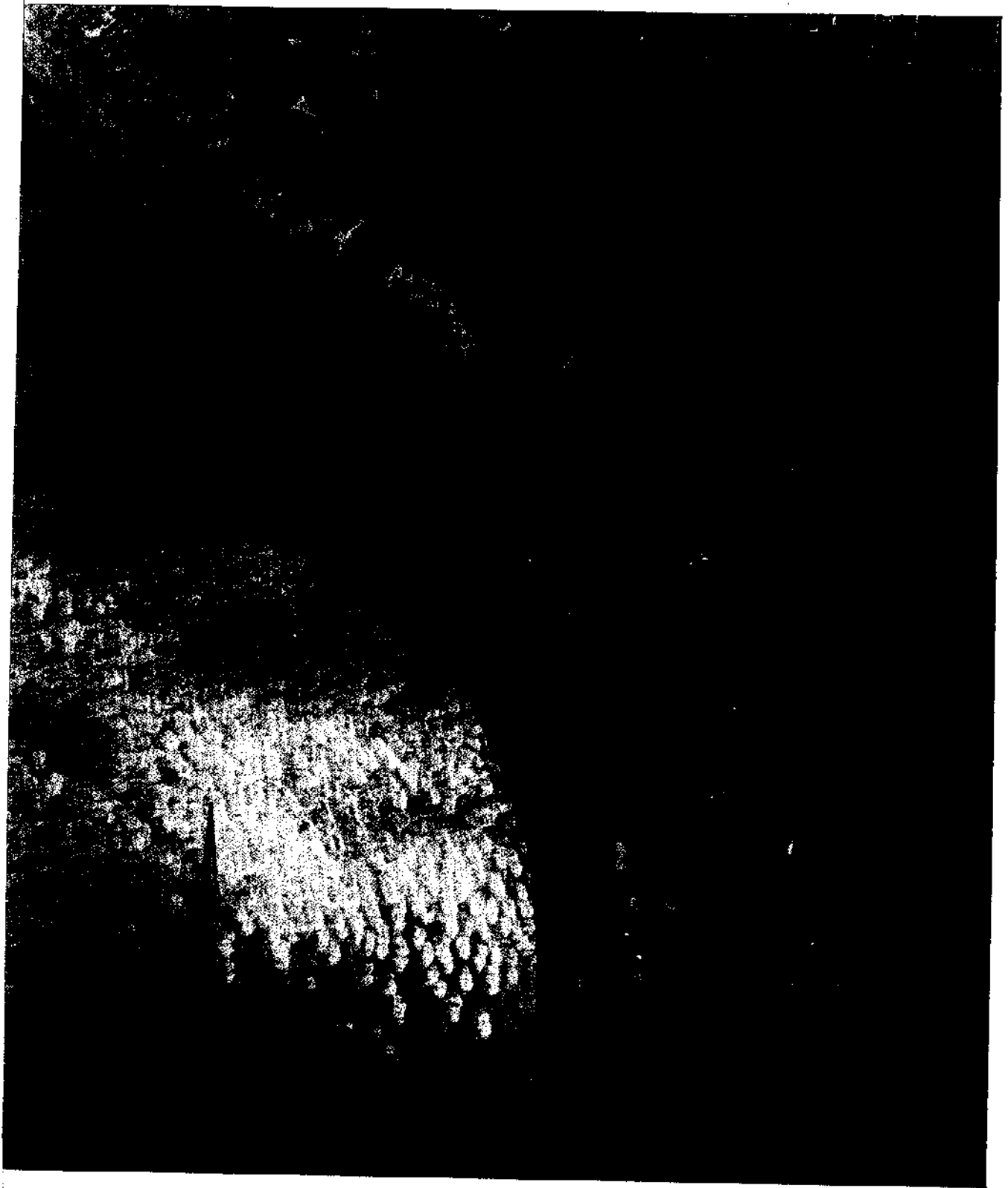


FIGURE 3.5. Survey Track Locations 38 Through 44

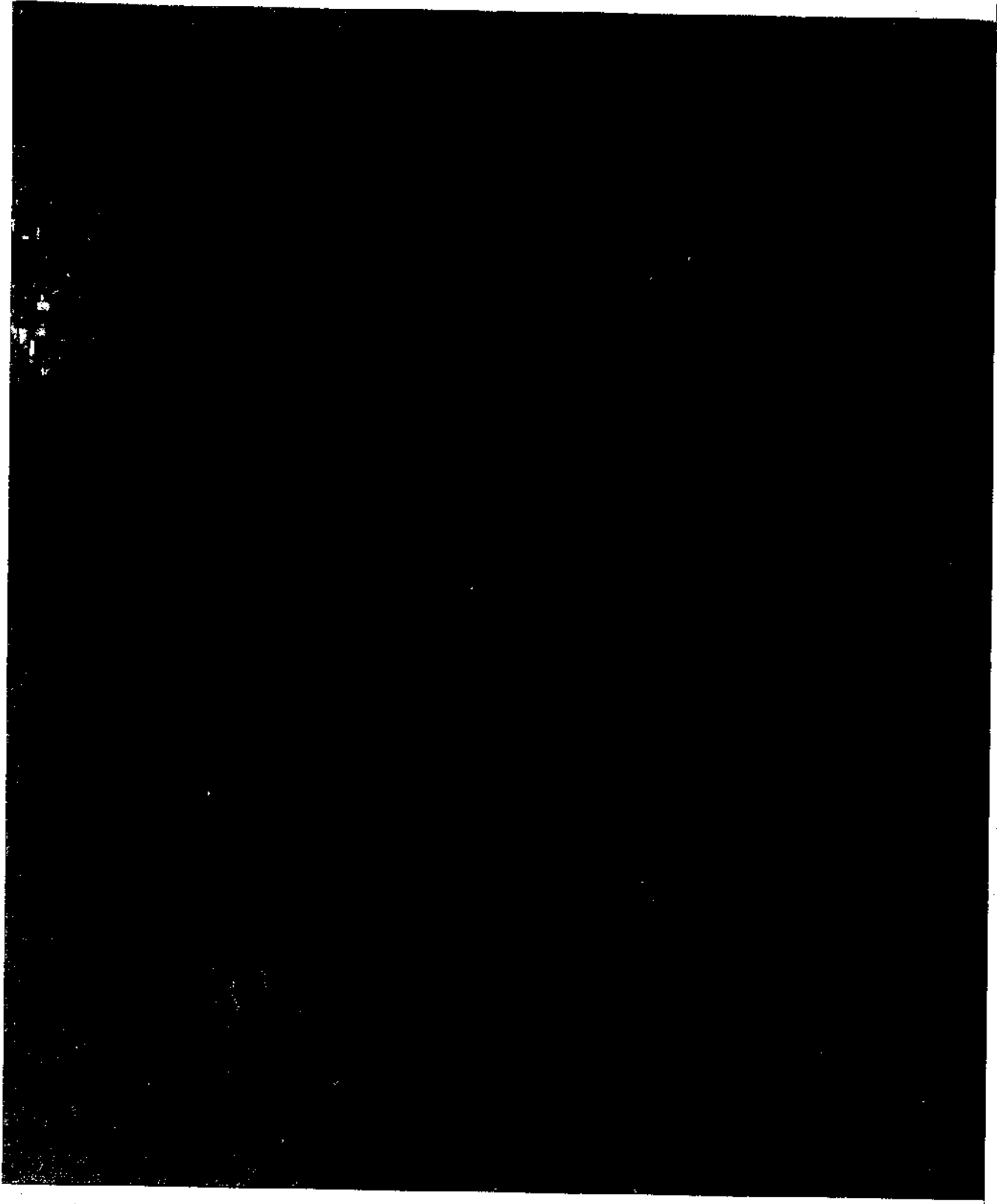


FIGURE 3.6. Survey Track Locations 45 Through 51

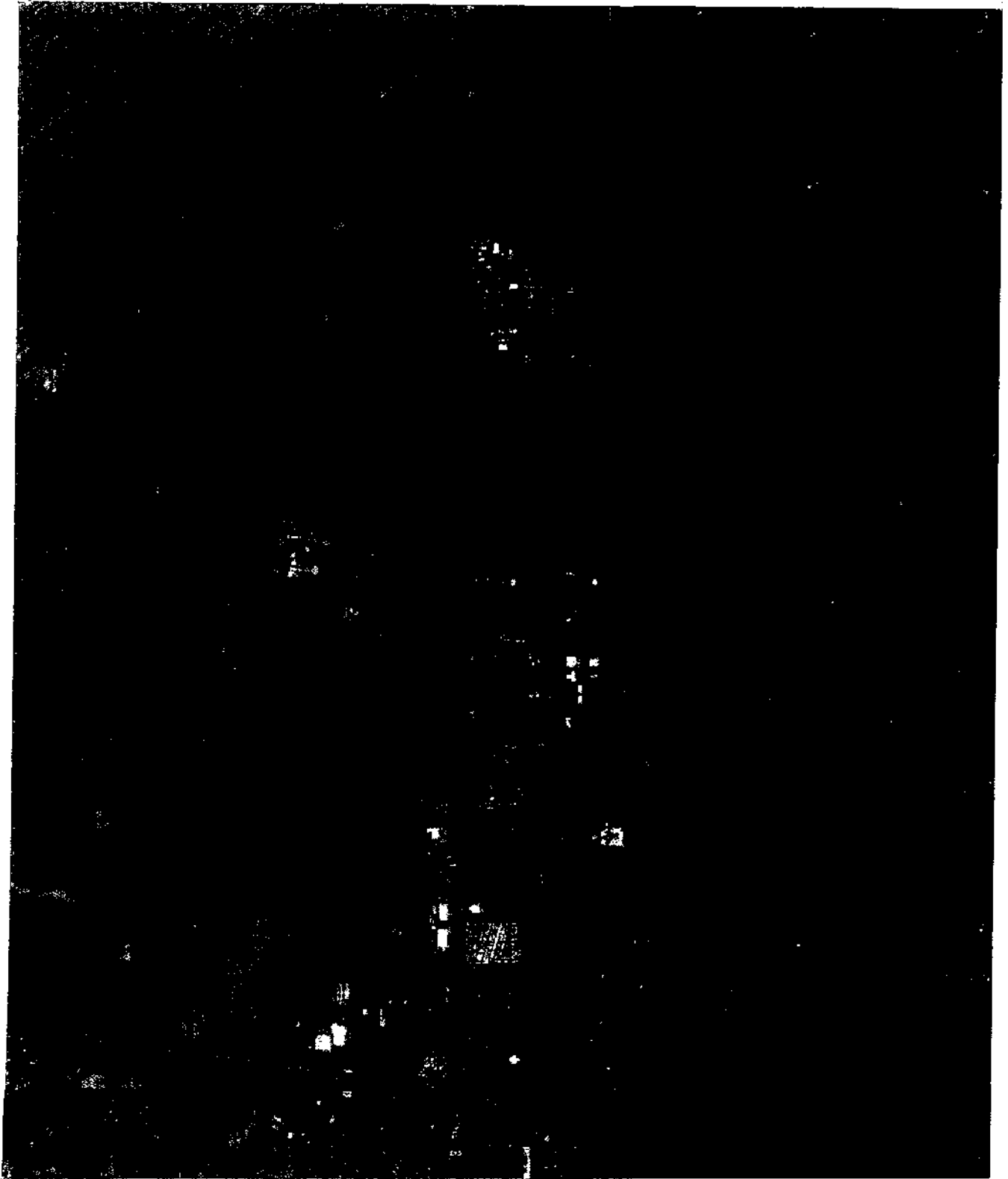


FIGURE 3.7. Survey Track Locations 52 Through 56

## 3.2 SAMPLING METHODS

Sampling methods for external gamma surveys, discrete particle surveys, and soil sampling are discussed below.

### 3.2.1 External Gamma Surveys

External gamma measurements were made using Model 12S, portable Ludlum  $\mu$ R meters with audio output. The instruments were calibrated with a  $^{137}\text{Cs}$  source at the mR level and pulse-calibrated at the  $\mu$ R level. Daily battery checks and background measurements were made to ensure each instrument's reliability.

The survey tracks as shown in Figures 3.2 through 3.7 consisted of two survey lines 20 m apart and typically extending approximately 1000 m. Each line was surveyed with a  $\mu$ R meter, at a height of approximately 1 m, by walking along the line and observing exposure rates. The instrument readings along the lines were visually averaged (based on the technician's judgement) over 100 m and recorded. The  $\mu$ R meter readings from both survey lines were mathematically averaged to ensure that bias from a single instrument would not greatly affect the data.

In some instances a Bicron  $\mu$ rem meter was used to provide data for comparison to the  $\mu$ R meter. The  $\mu$ rem meter was used to provide a measure of dose and is a more portable equivalent of the pressurized ionization chamber (PIC), as will be shown later.

### 3.2.2 Discrete Particle Surveys

Discrete radioactive particle surveys were conducted every 100 m along the track. The particle surveys began at a point midway between the two survey lines and covered the area circumscribed by a circle of 10 m radius from the center point. The surveys were conducted with the  $\mu$ R meters at a height of approximately 0.25 m.

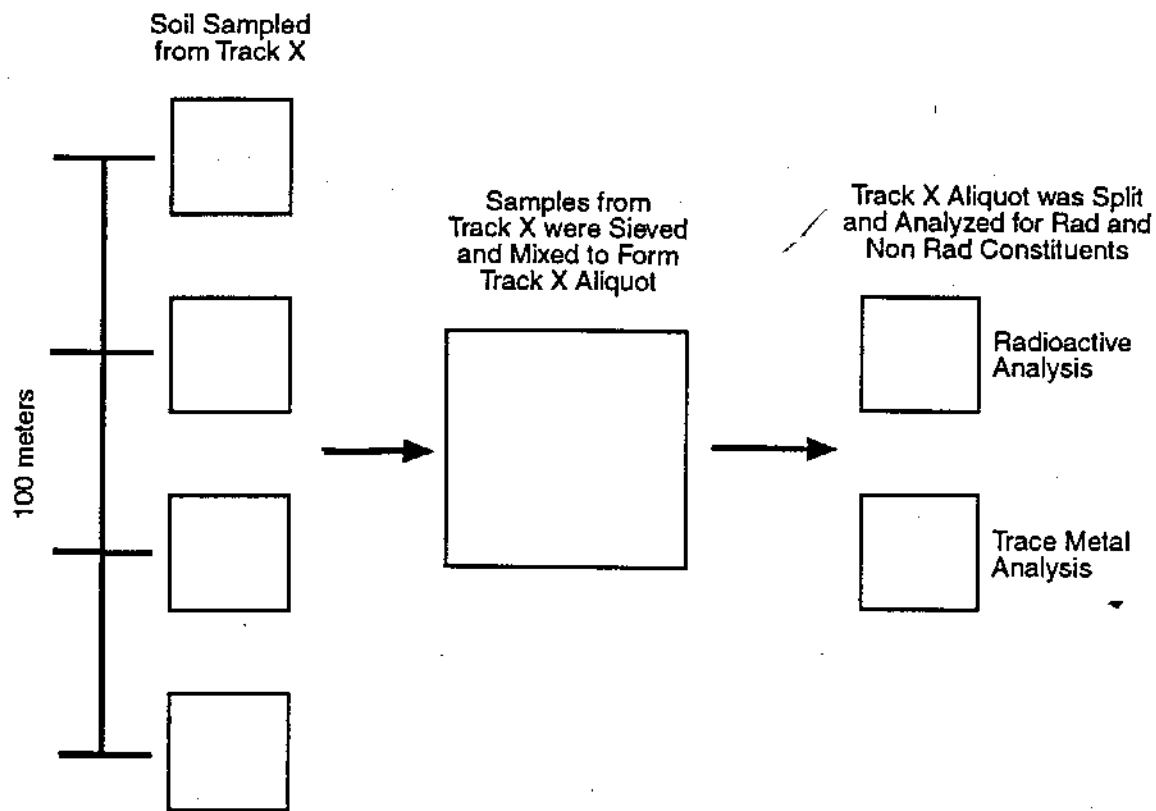
### 3.2.3 Soil Sampling

Soil samples were also taken at 100-m intervals at a point between the survey lines (at the same location as the particle surveys). The area sampled was defined as a circular area with a 10-m radius. The soil samples were taken with a device called a "cookie cutter." The cookie cutter takes a

sample 10 cm in diameter and 2.5 cm in depth. At many locations, soil samples were taken with a shovel; this was due to the layered beds of rocks that dominate the Columbia River area. Smaller areas (i.e., short stretches of shoreline) that displayed a potential for soil contamination based on the aerial survey results were sampled/surveyed on a 50-m basis.

### 3.3 SOIL SAMPLE PREPARATION AND COMPOSITING

The soil was placed in a plastic bag and taken from the field for refrigeration. The soil taken at each interval along a track was sieved with a 2.36-mm screen. Approximately 250 g from each sieved sample were composited to form an aliquot for that particular track. The aliquot from each track was thoroughly mixed, subsampled, and sent for analysis. Figure 3.8 illustrates the logic of the sample compositing. Table 3.1 lists the analyses performed on each sample and the methods involved. Radionuclide and trace metal analyses in soil are reported as pCi and  $\mu\text{g/g}$  dry weight, respectively. The analysis results are given in Appendixes B and C.



S8305055.2

**FIGURE 3.8.** Soil Compositing Logic

TABLE 3.1. Analyses and Methods

<u>Analyses</u>	<u>Methods of Analysis</u>
<u>Radioactive</u>	
Gamma analysis	Gamma spectroscopy
<sup>90</sup> Sr	Chemical separation/gas flow proportional counter
Isotopic uranium	Chemical separation/alpha spectroscopy
Isotopic plutonium	Chemical separation/alpha spectroscopy
<u>Chemical</u>	
Trace metals	EPA Method 6010 <sup>(a)</sup> /Inductively Coupled Plasma Atomic Emission Spectroscopy
Mercury	EPA Method 7471 <sup>(a)</sup> /Manual Cold Vapor Technique
Lead	EPA Method 7421 <sup>(a)</sup> /Atomic Absorption Furnace Technique

(a) From EPA (1982).

## 4.0 RESULTS AND DISCUSSION

Results for the exposure rate survey, discrete radioactive particle analysis, the 100-N Area survey, and soil concentration survey are presented in the following subsections.

### 4.1 EXPOSURE RATE SURVEY

Results for the exposure rate survey were compared with the 1988 aerial survey results, and background and historical data.

#### 4.1.1 Comparison With 1988 Aerial Survey

The largest determining factor in choosing the survey areas in this study was the exposure measurements taken by EG&G during July/August of 1988. EG&G used an elaborate NaI detection system attached to a helicopter to conduct an aerial radiological survey of the Hanford area. The NaI detection system was calibrated to suppress natural background and therefore only detected sources of anthropogenic, gamma-emitting radioactivity. The aerial data were presented as isopleths overlaid onto a map of the Hanford Site. The data provided the information needed to select tracks for subsampling areas with elevated exposure rates.

Figure 4.1 shows the categories EG&G used to differentiate between relative levels of exposure rates. All the tracks in the current study were in areas classified by EG&G as either category A or B. Category A, 0 to 700 cps, designates areas with no detectable amounts of anthropogenic radioactivity. Of the 53 tracks in the current survey, 20 are located in the areas identified by EG&G as having relative exposure rates falling in the A category. The average exposure rates of the 20 Category A tracks ranged from 9 to 14  $\mu\text{R/hr}$  in the current survey.

Twenty-three tracks are located in category B areas (700 to 2200 cps). The exposure rates of these tracks ranged from 11 to 24  $\mu\text{R/hr}$  in the current survey. The remaining 10 tracks in the current study had average exposure rates ranging from 11 to 17  $\mu\text{R/hr}$  and were not located within the EG&G survey area.

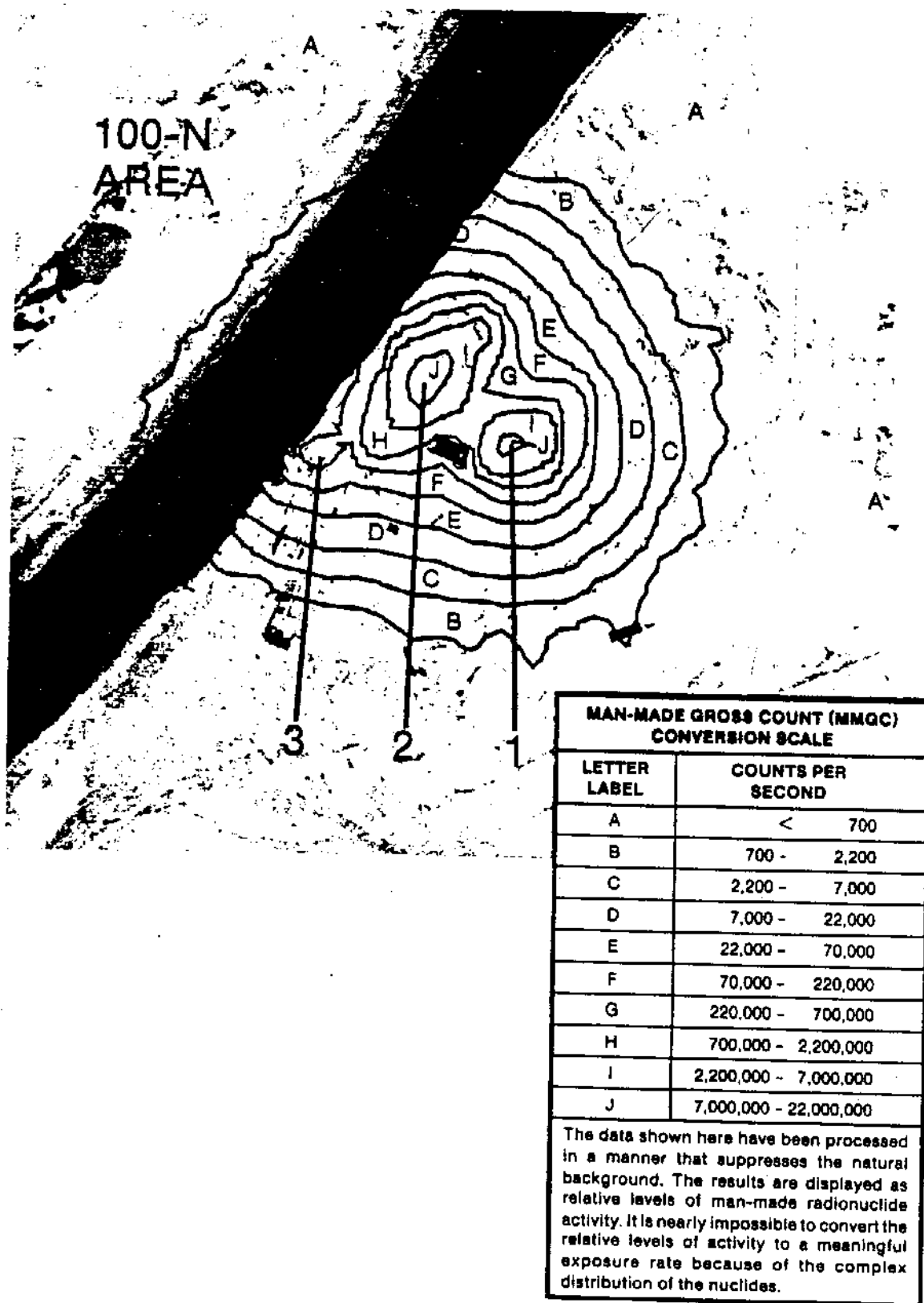


FIGURE 4.1. 1988 EG&G Aerial Radiological Survey of the 100-N Area

When interpreting the isopleths presented on the EG&G survey (see Figure 4.1), it is important to realize that the isopleths do not accurately delineate areas of contaminated soil, and probably do not accurately represent the distribution of external exposure rates that would be measured by an instrument 1 m above the ground because of ground surface scattering and shielding effects. The isopleths tend to form a "bull's eye" around the source of gamma emissions, with higher exposure rates nearest the center of the "bull's eye" as shown in Figure 4.1. Figure 4.1 illustrates the effect a point source(s), in this case a facility, can have on exposure rates as reported by an aerial survey, even though areas within the isopleths are not necessarily contaminated. In general, the aerial survey was an aid in locating areas with elevated exposure rates but did not stringently define contaminated areas.

#### 4.1.2 Comparison of Exposure Rates With Upstream and Historical Data

In 1978 and 1979 an extensive radiological survey was conducted of the shoreline and islands along the Hanford Reach (Sula 1980). Table 4.1 shows the six locations with the highest exposure rate measurements from the current survey compared with the measurements reported by Sula. Differences in survey locations and number of instrument readings make direct comparison of the exposure rates in Table 4.1 inappropriate but a decreasing trend of exposure rates is evident. Because Sula also used the Ludlum Model 12S  $\mu\text{R}$  meter and the methods he used were very similar to the methods used in this survey, the differences in exposure rates shown in Table 4.1 are most probably a result of the decay of radionuclides rather than data bias from instrument or human error.

Figure 4.2 shows the individual exposure rate measurements observed from upstream of the Vernita Bridge to downstream near the Richland Pumpouse. As expected, areas along the Hanford Reach measure approximately 5 to 15  $\mu\text{R}/\text{hr}$  higher than the background locations. Overall, exposure rate measurements ranged from 4 to 11  $\mu\text{R}/\text{hr}$  at the background locations, to 8 to 28  $\mu\text{R}/\text{hr}$  along the Hanford Reach. The tracks with the highest exposure rate measurements were the White Bluffs Slough (tracks 22 and 23), 28 and 20  $\mu\text{R}/\text{hr}$ ; Hanford Peninsula (Track 33), 20  $\mu\text{R}/\text{hr}$ ; and the Hanford Townsite shoreline (Track 37), 18  $\mu\text{R}/\text{hr}$ . Appendix A lists the exposure rates as measured at each location.

**TABLE 4.1.** Comparison of Exposure Rates

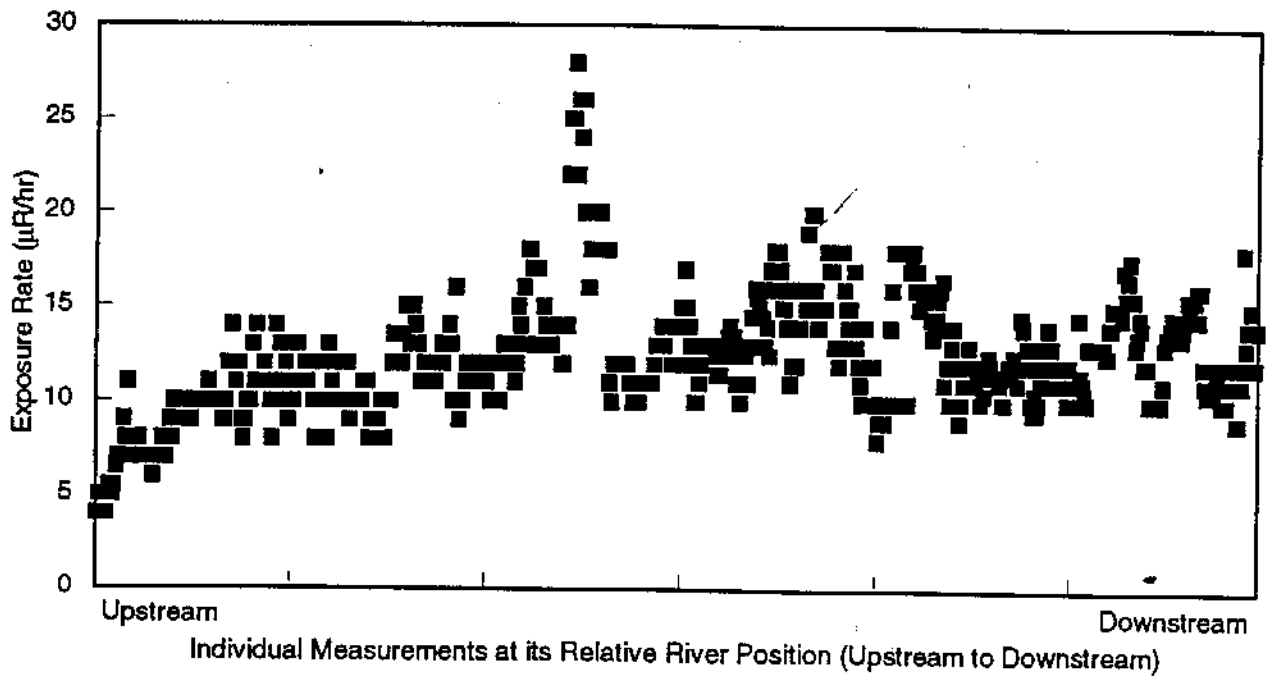
	1978/1979 Maximum, $\mu\text{R/hr}$ (from Sula 1980)	Current Survey Maximum, $\mu\text{R/hr}$	Location in Current Survey
White Bluffs Slough	32	28	Tracks 20, 21, 22, and 23
Hanford Peninsula	30	20	Tracks 32, 33, and 34
Hanford Townsite shoreline	24	18	Track 37
Hanford Townsite slough	19	18	Track 35
Savage Island	28	18	Tracks 38
Wooded Island	18	18	Tracks 49, and 50

Figure 4.3 displays the median exposure rates at each track bounded by 95% confidence limits. The exposure rates were found to be log-normally distributed as shown in Figure 4.4, so the data were log-transformed. Because the data were log-normally distributed, the median was selected as the measure of central tendency rather than using the arithmetic mean. The median was determined by calculating the mean of the log-transformed values. The confidence limits were determined by log-transforming the data and determining the confidence limits as described by Havilcek and Crane (1988), i.e.,  $CL = \text{mean} \pm t^*(SEM)$ .

The exposure readings taken at the background locations (51 measurements) were pooled and a median calculated. Each downstream median was calculated using approximately 10 measurements (see Appendix A). All the downstream tracks had median exposure rates greater than the upper 95% confidence limit of the median background value. The White Bluffs Slough area had the highest median exposure rates (Tracks 22 and 23) at 20 and 18.5  $\mu\text{R/hr}$ , respectively.

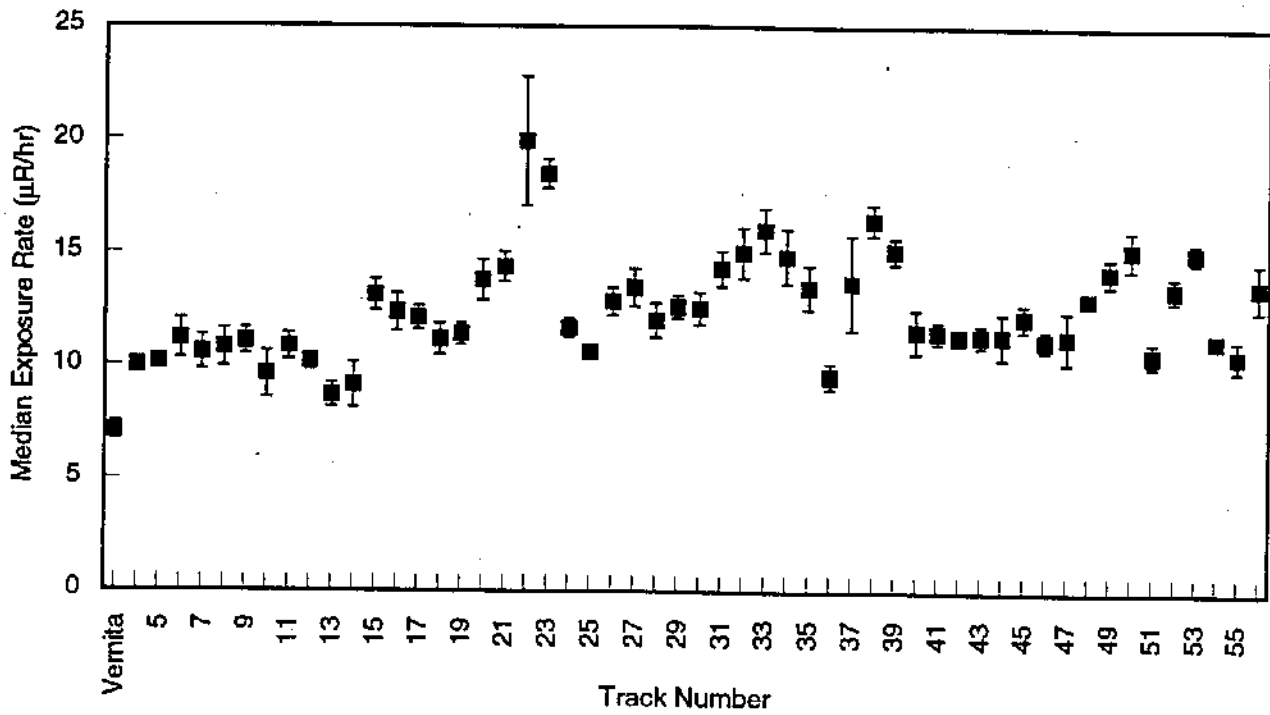
#### 4.1.3 Instrument Correlations

For the past 15 years, the Surface Environmental Surveillance Project has relied upon the Model 12S, portable Ludlum  $\mu\text{R}$  meter for environmental exposure measurements. The Ludlum  $\mu\text{R}$  meter was chosen for the current survey



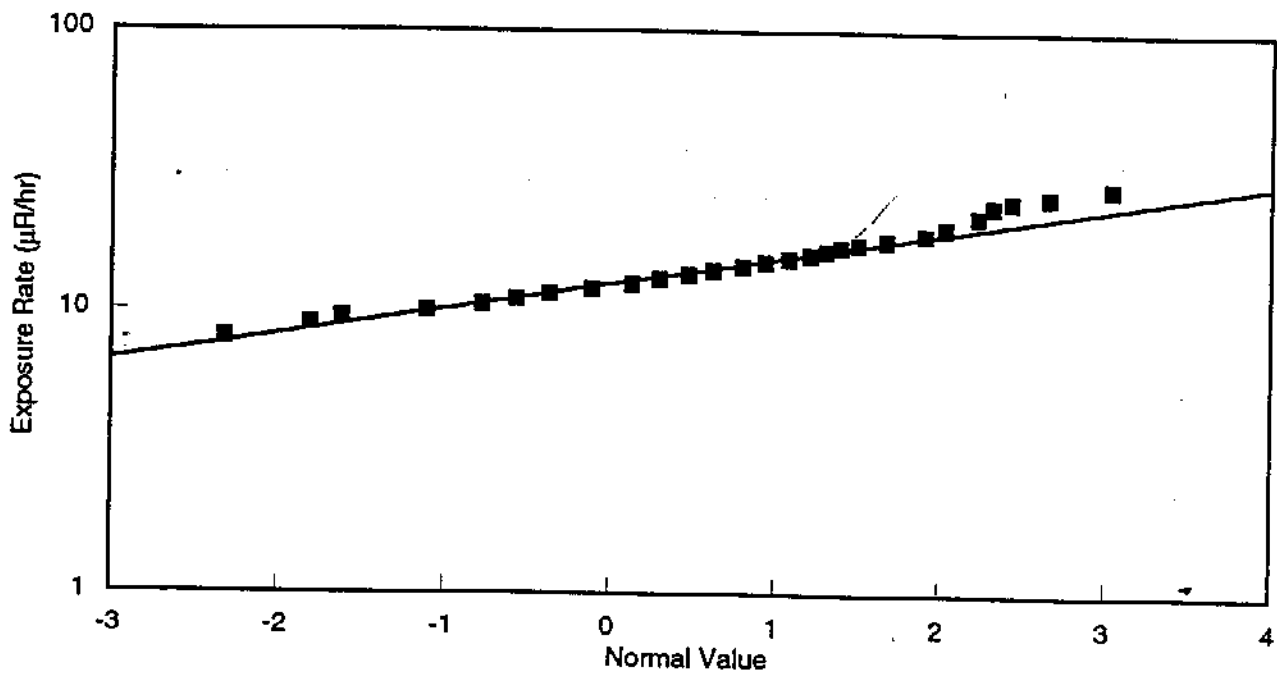
S9306049.1

FIGURE 4.2. Individual Exposure Measurements Taken from Vernita to Richland



S9306049.2

FIGURE 4.3. Median Exposure Rates at Each Survey Track



S9306049.41

**FIGURE 4.4.** Log-Normal Distribution of Exposure Rate Measurements

so that data could be compared to historical results. Note that in Sula (1980) the Ludlum  $\mu\text{R}$  measurements were corrected (standardized) to the Reuter Stokes Pressurized Ionization Chamber (PIC). The exposure rates discussed above are all based on the Ludlum  $\mu\text{R}$  meter (i.e., Sula's results were back-corrected for comparison to the  $\mu\text{R}$  values in the current study). Sula standardized his Ludlum  $\mu\text{R}$  measurements to the PIC based on his reporting of a significant correlation between the Ludlum and the PIC. In the current study, a correlation between the Ludlum  $\mu\text{R}$  meter and the PIC was not found and therefore direct comparisons between uncorrected Ludlum  $\mu\text{R}$  measurements were made. Note also that the finding of no correlation between the Ludlum  $\mu\text{R}$  meter and the PIC was demonstrated in an indirect but appropriate manner which is described below.

Theoretically, values of exposures in roentgens ( $\mu\text{R}$ ) can be considered essentially numerically equal to absorbed doses in rads or dose equivalents in rem. Therefore, an instrument measuring exposure ( $\mu\text{R}$ ) should provide similar measurements as an instrument measuring dose ( $\mu\text{rem}$ ). Through comparison of

instrument measurements it was found that the Ludlum  $\mu R$  meter did not provide similar readings to the Bicron  $\mu rem$  meter.

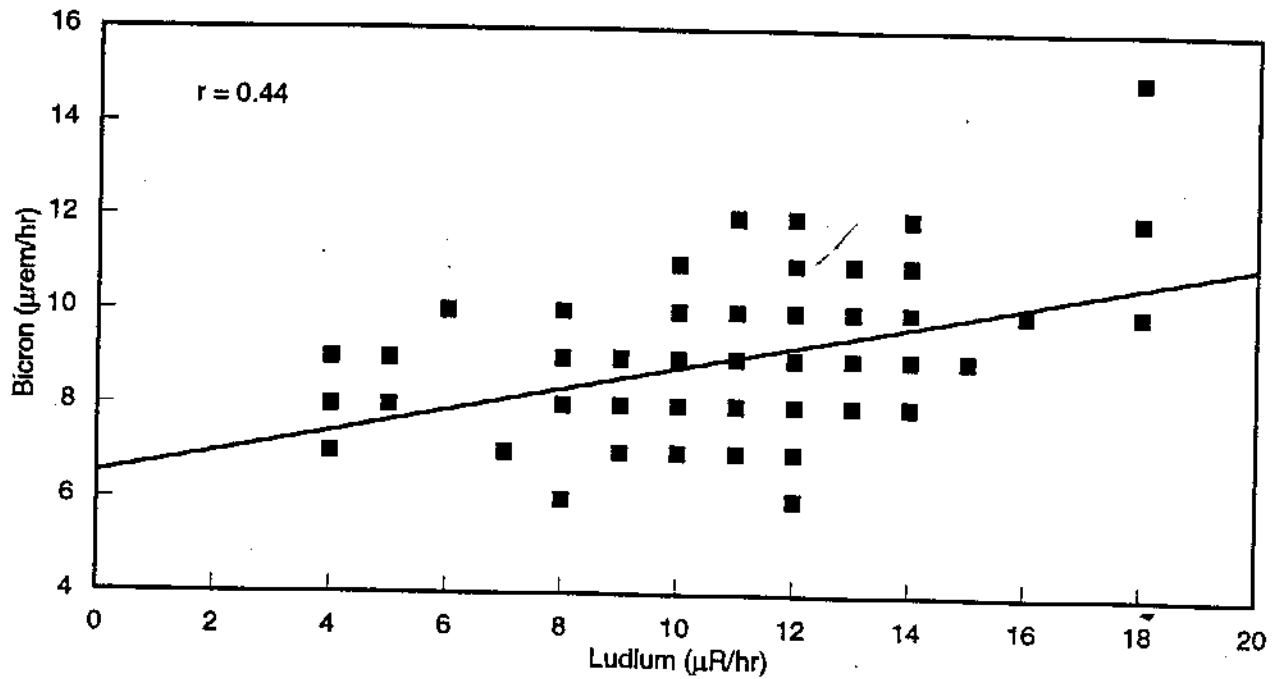
During this survey simultaneous data were not taken with the  $\mu R$  meter and the PIC. Simultaneous data were collected with the  $\mu R$  meter and the Bicron  $\mu rem$  meter. Simultaneous data were also collected with the Bicron  $\mu rem$  meter and the PIC. In short, the Bicron  $\mu rem$  meter was found to be correlated with the PIC. But the Bicron  $\mu rem$  meter was not found to be correlated to the Ludlum  $\mu R$  meter. These correlations are not surprising given the knowledge of the energy response curves for each instrument.

The Ludlum  $\mu R$  meter contains a NaI scintillator that is very sensitive to changes in exposure rates; however, because it over-responds to low-energy photons, it is a poor quantifier of the true exposure rate. The Bicron  $\mu rem$  meter is a portable hand-held instrument and has an energy response curve very similar (i.e., flat) to the PIC over the ranges of 0.1 to 1 Mev. The Bicron  $\mu rem$  meter uses a plastic scintillation detector that has a very flat energy response to low-energy photons. The flat energy response curve of the Bicron (and PIC) allows for a more accurate estimate of the true exposure rates, especially when a wide range of energy levels are being measured. The PIC is an 8-L ionization chamber and is the 'industry standard' for measuring environmental dose rates.

Figure 4.5 shows the relationship between the  $\mu R$  measurements and the  $\mu rem$  measurements. As expected, the scatter of the data points indicates a very poor correlation ( $r = 0.44$ ). The lack of correlation shown is expected because of the over-response of the Ludlum  $\mu R$  meter to the wide range of low-energy photons from natural radioactive decay chains that are present in the environment (i.e. thorium, neptunium, uranium, and actinium).

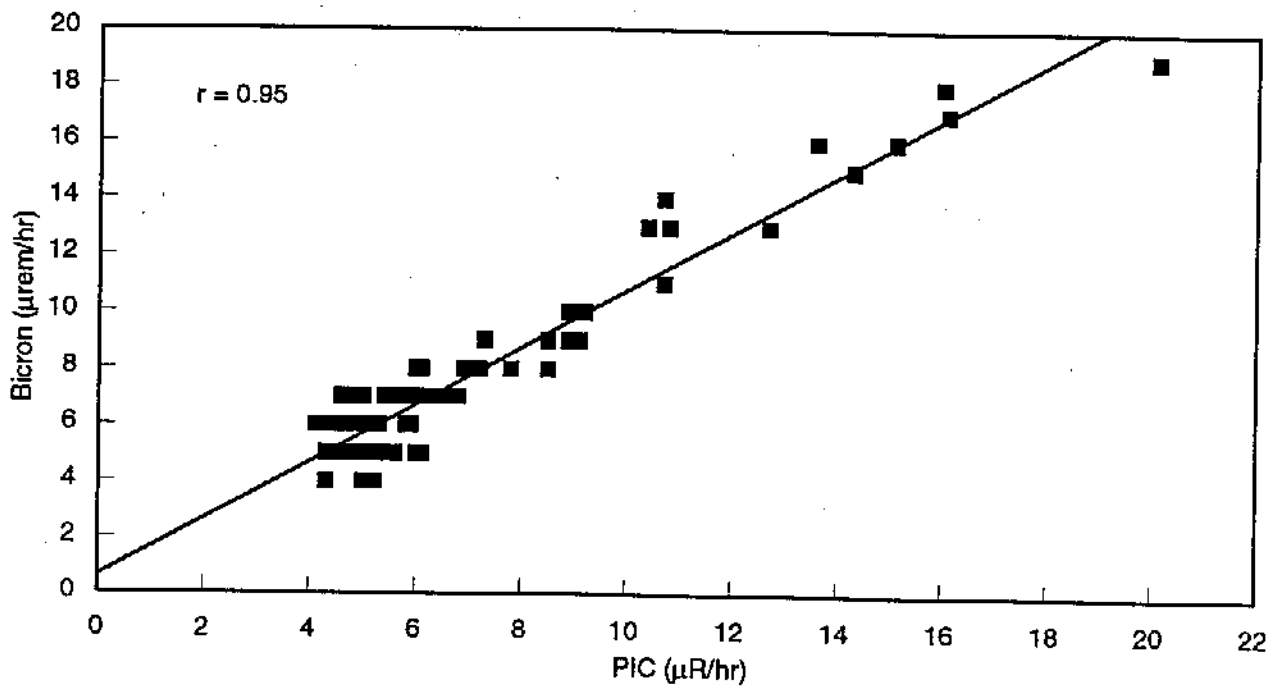
Figure 4.6 shows a very strong correlation ( $r = 0.95$ ) between the PIC measurements and the Bicron  $\mu rem$  measurements made along the Columbia River adjacent to the 100-N Area (discussed later). The strong correlation between the  $\mu rem$  meter and the PIC indicates that the Bicron  $\mu rem$  meter is a good estimator of the true exposure rate/dose rate.

These results indicate that the  $\mu R$  meter should only be used as a detector not as an estimator of the true exposure/dose rates. When possible,



S9306049.42

FIGURE 4.5. Correlation of Ludlum  $\mu R$  and Bicron  $\mu rem$  Measurements



S9306049.43

FIGURE 4.6. Correlation of Reuter Stokes PIC and Bicron  $\mu rem$  Measurements

the PIC should be used as an estimator of the true exposure/dose rates, but because the PIC and associated electronics weigh about 70 lb, use of the PIC is not always practical. The Bicron  $\mu$ rem meter can be used in place of the PIC (because the energy response curves are very similar) when many exposure readings need to be taken over large areas.

#### 4.2 DISCRETE RADIOACTIVE PARTICLE ANALYSIS

In the 1978/1979 survey, Sula reported finding 188 particles of discrete contamination along the Hanford Reach. Sula removed and analyzed seven particles from 100-D Island. The particles were barely visible to the naked eye (diameter approximately 0.1 mm) and contained  $^{60}\text{Co}$  at activities ranging from 1.7 to 23  $\mu\text{Ci}$ .

The terrain on 100-D Island is very rocky, with no significant vegetation in most areas. During the current survey, a total of 11 particles were detected on the island (Tracks 4 and 5). One particle was removed from the island for analysis. The particle was located approximately 10 cm beneath the ground and measured 400  $\mu\text{R/hr}$  at the ground surface. The particle was isolated to a few grains of sandy material and was identified as  $^{60}\text{Co}$  with an activity of  $1.7 \mu\text{Ci} \pm 0.8\%$ . The exposure rates at the ground surface of the 10 other particles, which were not disturbed, ranged from 60 to 300  $\mu\text{R/hr}$ . Since the conclusion of this survey, Westinghouse Hanford Company, the Site operations contractor, has begun 100% survey coverage of 100-D Island. To date, with approximately half of the island surveyed, 106 discrete radioactive particles have been removed.

One other discrete particle was found at the White Bluffs Slough (Track 20) during the current survey. The particle was about 10 cm beneath the ground. The particle was found to contain  $16 \pm 4.5\% \mu\text{Ci}$  of  $^{60}\text{Co}$  (1360  $\mu\text{R/hr}$  at the ground surface). Sula reported finding two discrete particles in the White Bluffs Slough area in the 1978/1979 survey.

Various exposure scenarios were hypothesized to assess potential human radiological doses from the two particles found and quantitated. These scenarios included:

1. inhalation of particles of a size that would deposit in the nose, naso- and oropharynx regions, and bronchial regions of the respiratory system
2. ingestion by swallowing
3. various modes of external skin exposure (direct contact, exposure through cloth such as in a pocket, and exposure through a sleeping bag). These assessments were made using LUDEP (Birchall et al. 1991), MIRDOSE (Watson et al. 1984), and VARSKIN 2 (Durham 1992) computer models, respectively.

The dose-limiting exposure scenario was determined to be a particle that is inhaled and deposited in the front part of the nose, where the residence times may be as long as 48 hours. No regulatory guidance exists for this mode of public exposure to discrete radioactive particles. The only available and applicable health context found was for occupational exposures. For occupational exposures, the limit is 75  $\mu\text{Ci-hr}$ , or  $1 \text{ E}+10$  beta particles emitted to a skin surface from the surface of the particle (NCRP 1989). Because the exposure limit is based on deterministic (not cancer-inducing) damage, and because doses at or below the limit will not produce skin damage, it is reasonable to use the same limit for public protection.

For a 48-hr residence time, the maximum dose to the nose was calculated by the VARSKIN 2 code to be 2000 rad ( $41 \text{ rad/hr} \times 48 \text{ hr}$ ) for the  $16\text{-}\mu\text{Ci}$  particle and 360 rad for the  $1.7\text{-}\mu\text{Ci}$  particle. If the limit for public exposure to discrete radioactive particles was the same as the limit for occupational exposure (i.e.,  $75 \mu\text{Ci-hr}$ ), the limit would be exceeded by about a factor of 10 for the  $16\text{-}\mu\text{Ci}$  particle. The exposure from the  $1.7\text{-}\mu\text{Ci}$  particle in the nose would be very close to the NCRP limit (when credit is taken for self-absorption as permitted in NCRP 1989). The smallest particle that could approach the exposure limit is about  $1.6\text{-}\mu\text{Ci}$ , if self-absorption of the source is ignored.

For the external skin exposure scenarios it was found that the  $75\text{-}\mu\text{Ci-hr}$  exposure limit for the  $16\text{-}\mu\text{Ci}$  particle could be reached in time periods that are plausible for these exposure scenarios. Specifically, the limit was reached in about 5, 30, and 44 hr for the skin contact, through the pocket, and through a sleeping bag exposure scenarios, respectively.

The maximum effective dose equivalent (EDE) for a particle exposure scenario was 60 mrem if a 16  $\mu\text{Ci}$  particle were ingested. The calculated EDE does not exceed the annual limit for exposure to the general public (100 mrem), and therefore the probability of cancer induction is not a concern with these discrete radioactive particles.

The doses calculated above assume that a particle comes into contact with a person. A number of factors qualitatively indicate that this is extremely unlikely. One mitigating factor is the fact that the area where particles were found is not currently open for public access. Also, the two particles collected were well below the surface; therefore, they were not available for inhalation or contact and the beta radiation leading to external dose would have been totally attenuated. In addition, the occurrence of particles, except on 100-D Island, was very low: only one particle was detected in over 120,000  $\text{m}^2$  of area surveyed. Another factor is a suggestion in the results shown in Appendix E of Sula (1980) that the particles found then were larger and more asymmetrical (less inhalable) than assumed in these calculations (the current study did not determine the size or shape of the two particles collected). Finally the 75- $\mu\text{Ci-hr}$  limit is at a level where no effect is observed. Higher levels would be required to cause any observable effect (e.g., a small discoloration of the skin), and much higher levels to cause a small break in the skin.

While these mitigating factors make it extremely unlikely that a member of the public would come in contact with such particles, there is a small probability that similar particles exist at other publicly accessible locations along the river. To fully understand the likelihood of discrete radioactive particle exposure, a detailed radiation survey of the accessible areas along the Columbia River should be conducted. One method of making such a determination is to perform a thorough contamination survey of the publicly accessible shorelines of the Columbia River. An appropriate instrument and scan speed that would allow detection of particles that have an activity of 1  $\mu\text{Ci}$  or more could be used. Particles with activities less than 1  $\mu\text{Ci}$  should not, in all probability, pose a health hazard and would not result in exposure of the public in excess of limits. Some further refinement of the dose assessment could also be conducted by characterizing the particle sizes and

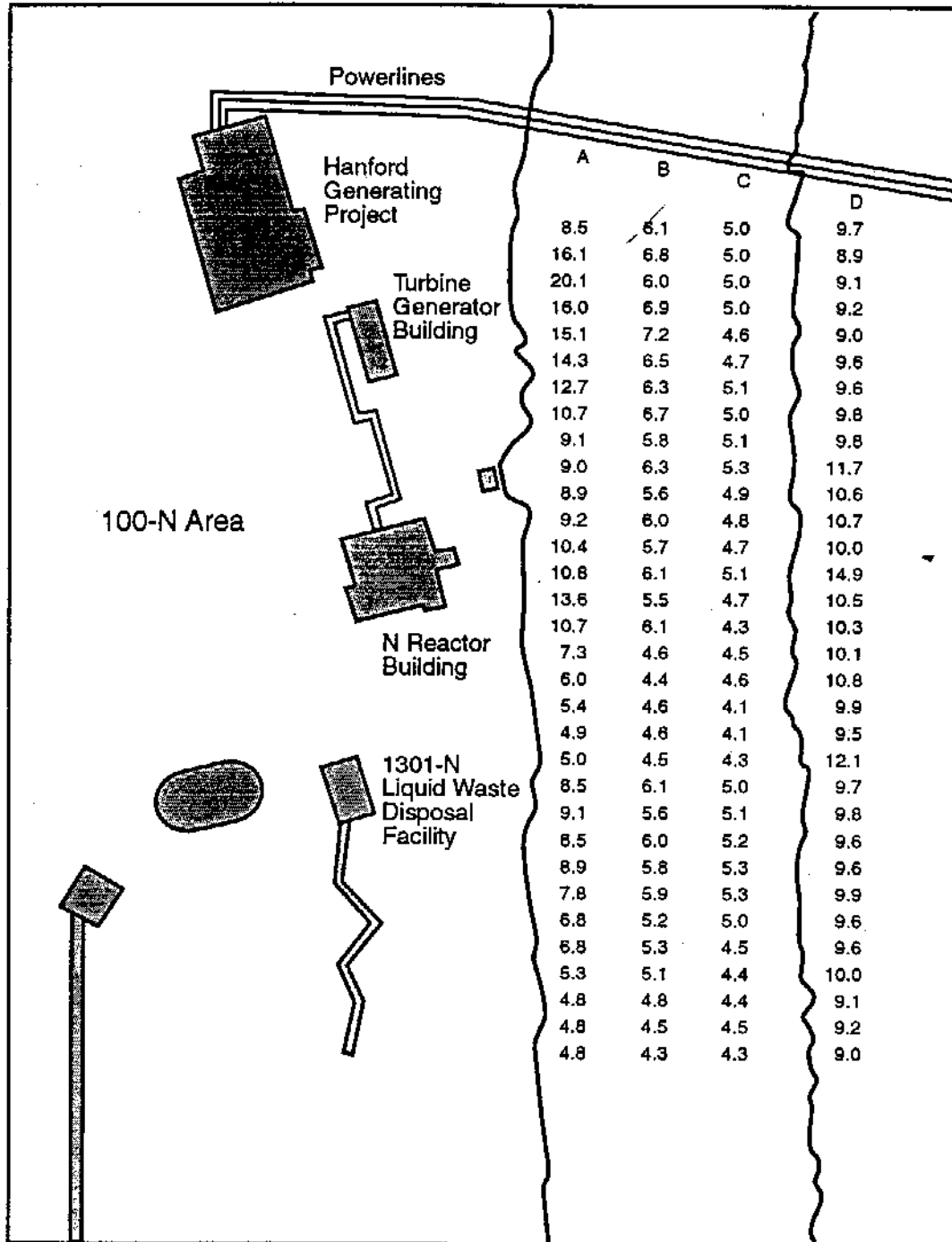
activities, frequency of occurrence along the river, and the settings in which they are found (buried or exposed on the surface).

#### 4.3 100-N AREA SURVEY

In recent history, the highest exposure rates from Hanford operations observed at a location near where the public has access have been on the river at the 100-N Area shoreline (Woodruff et al. 1993). Thermoluminescent dosimeter (TLD) measurements have been made at this location since 1990. In 1992, the maximum annual average dose rate measured by TLDs on the shoreline was 324 mrem (or about 40  $\mu\text{rem/hr}$ ). The DOE public dose standard is 100 mrem/yr for routine exposures and 500 mrem/yr under special circumstances. The shoreline is not accessible to the public, but the adjacent river is open to the public for recreational uses. The source of the elevated exposures is sky shine from liquid waste disposal trenches and other facilities located above the river and back from the bluff line in the 100-N Area. As such, questions exist about the expected decrease in exposure rates with distance from the shoreline. Measurements were made by boat on the adjacent Columbia River to describe exposure rates over the publicly accessible water body.

Figure 4.7 shows four tracks running from the powerlines upstream of the 100-N Area to a distance of about 1500 m downstream. The distance between measurement points along a track was approximately 50 m. The exposure rates shown in Figure 4.7 were measured with a PIC ( $\mu\text{R/h}$ ), although measurements were also taken with the Bircon  $\mu\text{rem}$  meter for comparison. Track A was located approximately 75 m from the Hanford shoreline, and Track C was located approximately 75 m from the opposite shoreline. Track B was located midway between Tracks A and C. Track D was on the shoreline opposite the 100-N Area.

Because there is essentially no terrestrial component to the radiation field on the river, the exposure rates on the river will be lower than the exposure rates measured on land. This is assuming there is no external source of exposure such as radiation from the 100-N Area. The minimum rate shown in Figure 4.7 is 4.1  $\mu\text{R/hr}$ . Exposure measurements taken at other river locations (away from the 100-N Area) indicated rates of 3.5 to 4.0  $\mu\text{R/hr}$  in the center of the river, and 4.0 to 4.5 along (within 15.25 m) the shoreline. So one can



S9305055.1

FIGURE 4.7. Exposure Rates on the Columbia River Adjacent to the 100-N Area,  $\mu\text{R/hr}$

attribute approximately 3.5 to 4  $\mu\text{R/hr}$  of the measurements on Track B and 4.0 to 4.5  $\mu\text{R/hr}$  on Tracks A and C to natural background.

The exposure rates along Track C are primarily attributable to the cosmic component with some contribution from the 100-N Area. Because of the 100-N Area source, the exposure rates along Track B are slightly higher than those along Track C. This increase in exposure rates from the 100-N Area source is more evident along Track A.

Because the 100-N Area shoreline is off limits to the public, the exposure rates shown along Track A are typical of exposure rates a fisher would encounter. The highest exposure rate measured was 20.1  $\mu\text{R/hr}$ . This measurement appears adjacent to the Washington Public Power Supply System turbine generator building. Another increase occurs farther downstream adjacent to the N Reactor building, and there is an apparent final increase in the area of the 1301-N Liquid Waste Disposal Facility. The maximum measurement of 20.1  $\mu\text{R/hr}$  minus an estimated natural background of 4  $\mu\text{R/hr}$  extrapolates to an annual dose contribution of approximately 45 mrem, assuming one fishes for 8 hr/d every day of the year at that location.

The exposure rates on the shoreline opposite the 100-N Area (Track D) have both terrestrial and cosmic contributions, and potentially a contribution from the 100-N Area. Background measurements ranged from 4 to 11  $\mu\text{R/hr}$  and averaged 9.7. Two locations along Track D exceeded this range somewhat, as shown in Figure 4.7. These areas were not investigated.

#### 4.4 SOIL CONCENTRATION SURVEY

Soil concentrations were analyzed for radionuclides and trace metals.

##### 4.4.1 Radionuclides

Of the 56 tracks in the current survey, 23 are located in the areas identified by EG&G as having exposure rates greater than background. Each of the 23 areas were found to have soil concentrations of  $^{60}\text{Co}$  and  $^{152}\text{Eu}$  greater than the upstream background concentrations. Elevated concentrations of  $^{137}\text{Cs}$  are evident in 13 of the 23 survey locations,  $^{154}\text{Eu}$  in 9,  $^{22}\text{Na}$  in 7, and  $^{65}\text{Zn}$  in 4. Elevated concentrations of  $^{90}\text{Sr}$  are evident in 2 of the 23 Category B tracks,  $^{234}\text{U}$  in 2,  $^{238}\text{U}$  in 2, and  $^{239,240}\text{Pu}$  in 3.

Figures 4.8 through 4.13 show the concentrations of the elevated gamma emitters in soils along the Hanford Reach, beginning with the background locations (1, 2, and 3) and ending with the island directly downstream of the Richland Pumphouse (Track 56). Figures 4.14 through 4.18 show the concentration of  $^{90}\text{Sr}$ , uranium, and plutonium in soils. Figures B.1 through B.10 of Appendix B show similar figures for the other radionuclides that did not show apparent elevations in concentrations.

The concentrations shown in Figures 4.8 through 4.18 are the concentrations of the soil composites taken from each track. The concentration values are bounded by the 2 sigma error, which combines the counting error and the propagated analytical error, and defines the 95% confidence intervals.

Certain tracks are of particular interest because they showed elevated concentrations for more than one radionuclide. Track 4, located on 100-D Island, had soil concentrations of  $^{22}\text{Na}$ ,  $^{60}\text{Co}$ ,  $^{137}\text{Cs}$ ,  $^{152}\text{Eu}$ , and  $^{154}\text{Eu}$  that were higher than those at the background tracks and most of the survey locations along the Hanford Reach. The higher concentrations in the soils on 100-D Island can be attributed to the underground piping system that runs from the 100-D Reactor to 100-D island. The piping was used to release cooling water from the 100-D Reactor back into the Columbia River.

Track 37, along the Hanford Townsite shoreline, has elevated soil concentrations of  $^{22}\text{Na}$ ,  $^{60}\text{Co}$ ,  $^{137}\text{Cs}$ ,  $^{152}\text{Eu}$ , and  $^{154}\text{Eu}$ . The survey area along the Hanford Townsite shoreline had thick matted layers of vegetation. Therefore, it is hypothesized that when the radioactive contamination was deposited the vegetation trapped the contamination and did not allow it to reenter the Columbia River by natural erosion processes.

Tracks 22 and 23, along the White Bluffs Slough area, have elevated concentrations of  $^{60}\text{Co}$ ,  $^{137}\text{Cs}$ , and  $^{152}\text{Eu}$ . The White Bluffs Slough is located south of the 100-H Reactor. The slough is normally above water but during high water the Columbia River will flow between the 100-H floodplain and the Hanford shoreline, thus forming the marshy slough area. Because the 100-H Reactor outfall is located directly upstream of the slough, it is hypothesized that during high water periods the effluent stream from the reactor entered

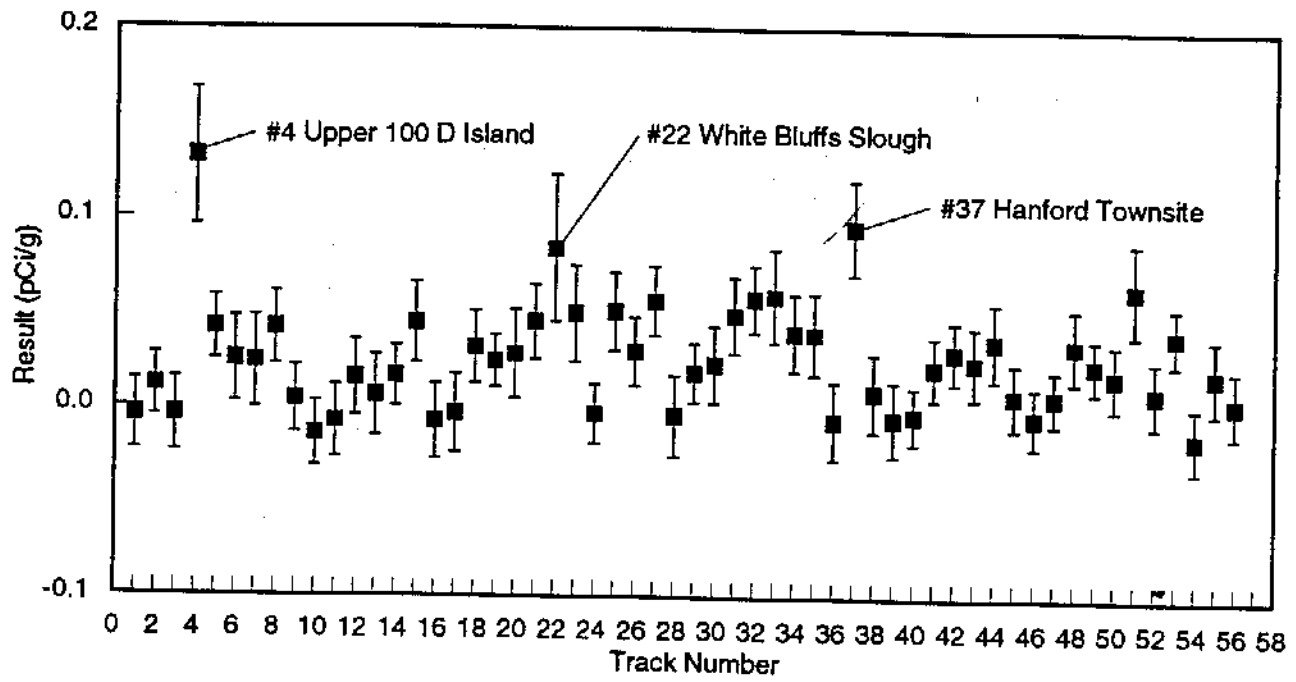


FIGURE 4.8. Sodium-22 ( $^{22}\text{Na}$ ) Concentrations in Soils

S9306049.3

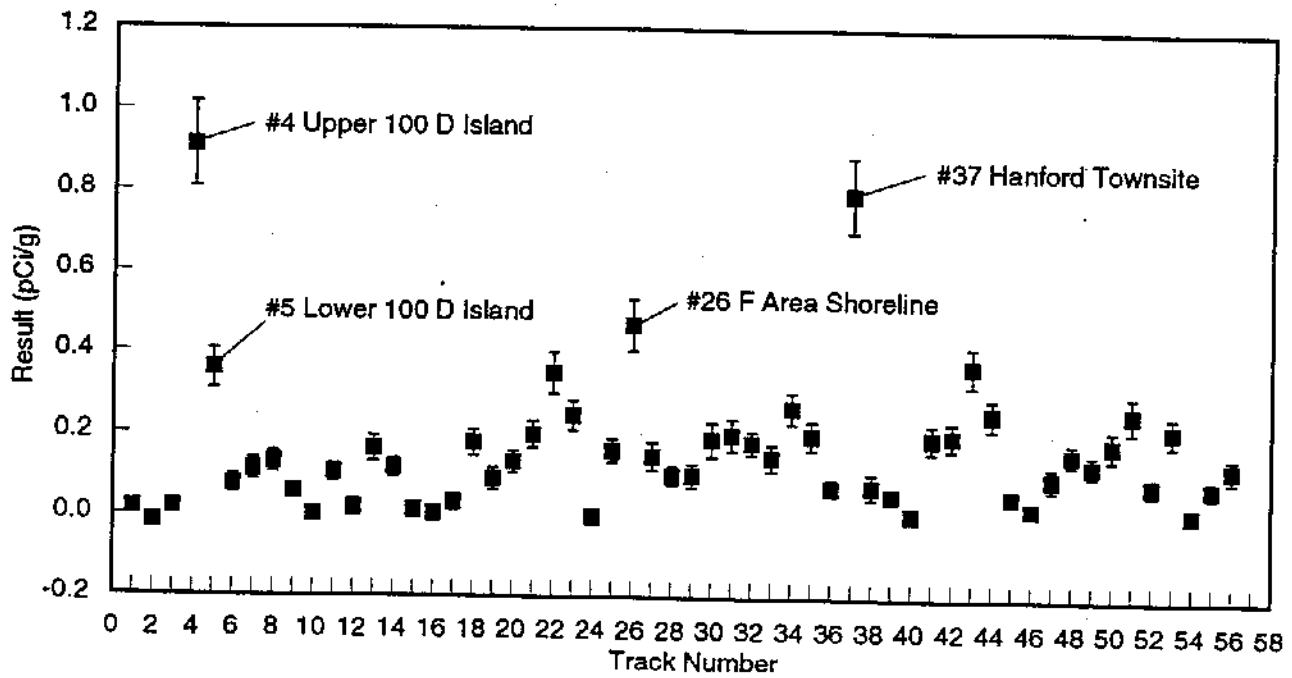


FIGURE 4.9. Cobalt-60 ( $^{60}\text{Co}$ ) Concentrations in Soils

S9306049.4

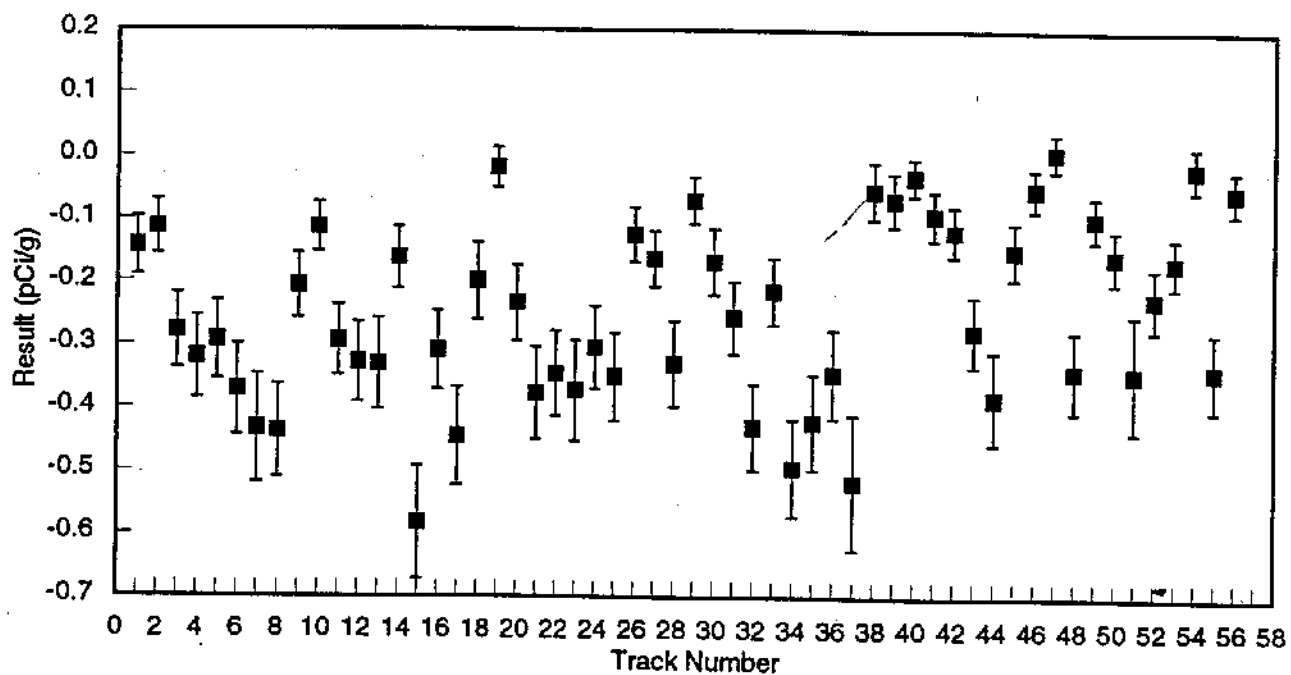


FIGURE 4.10. Zinc-65 ( $^{65}\text{Zn}$ ) Concentrations in Soils

S9306049.5

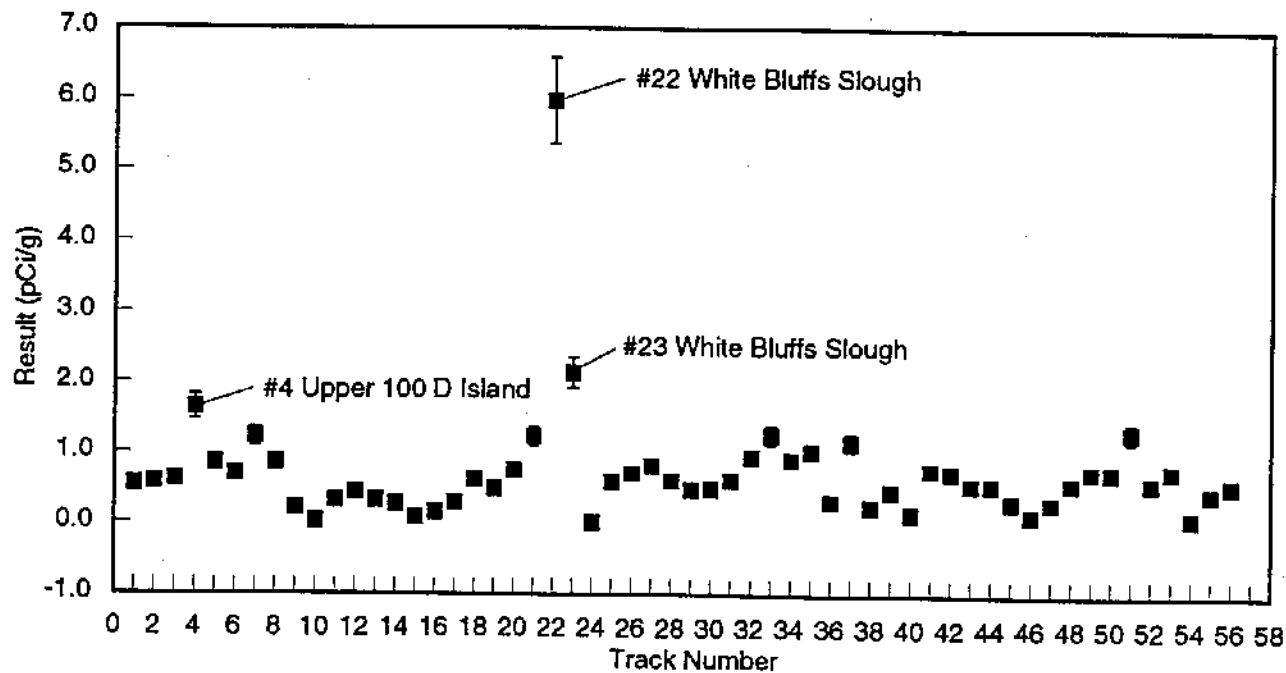
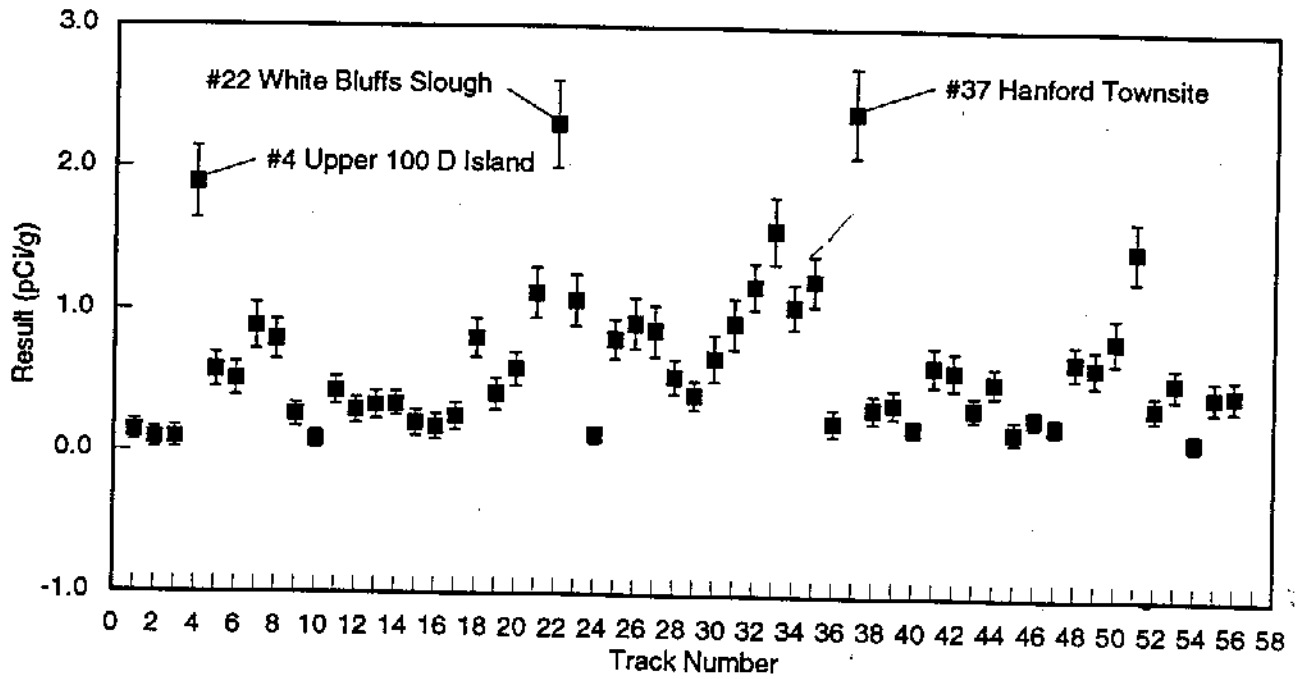


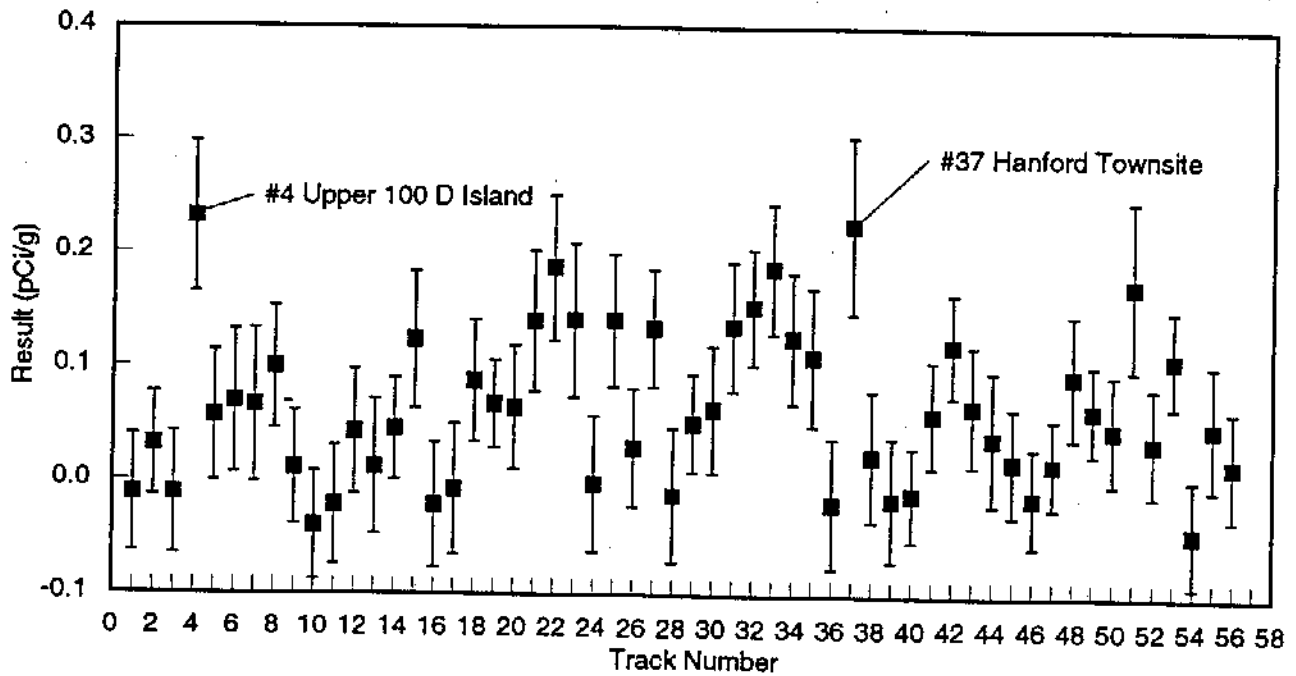
FIGURE 4.11. Cesium-137 ( $^{137}\text{Cs}$ ) Concentrations in Soils

S9306049.6



S9306049.7

FIGURE 4.12. Europium-152 ( $^{152}\text{Eu}$ ) Concentrations in Soils



S9306049.8

FIGURE 4.13. Europium-154 ( $^{154}\text{Eu}$ ) Concentrations in Soils

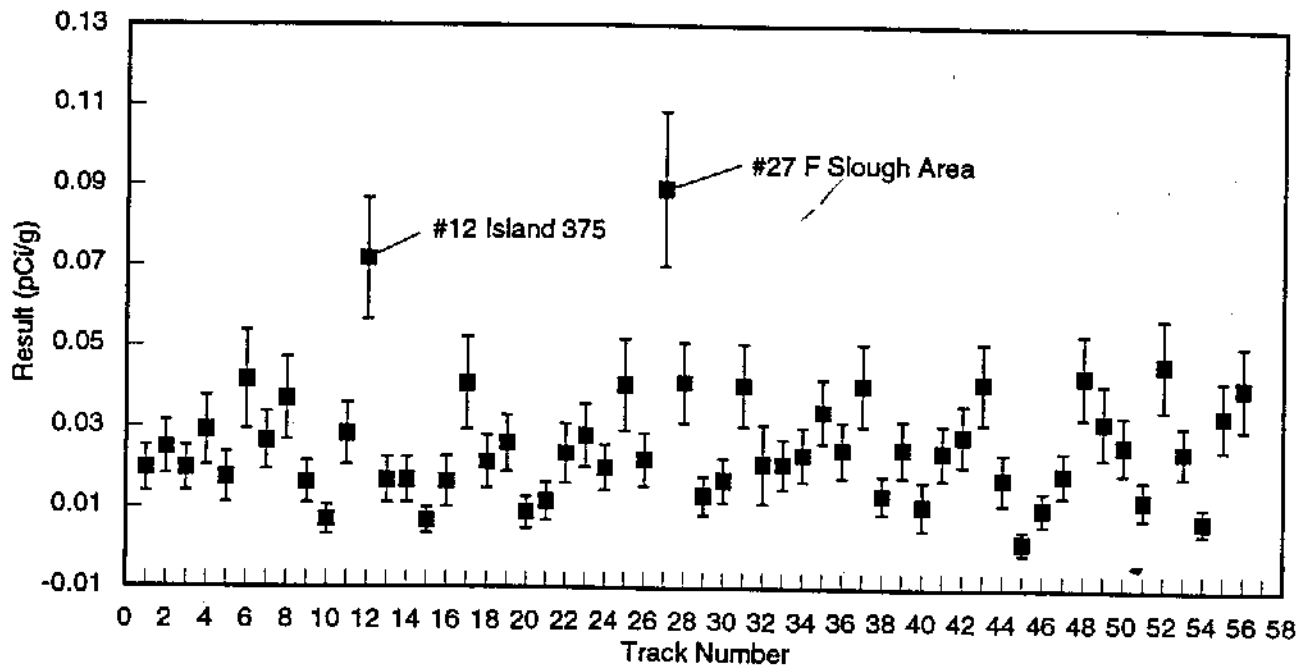


FIGURE 4.14. Strontium-90 ( $^{90}\text{Sr}$ ) Concentrations in Soils

S9306049.9

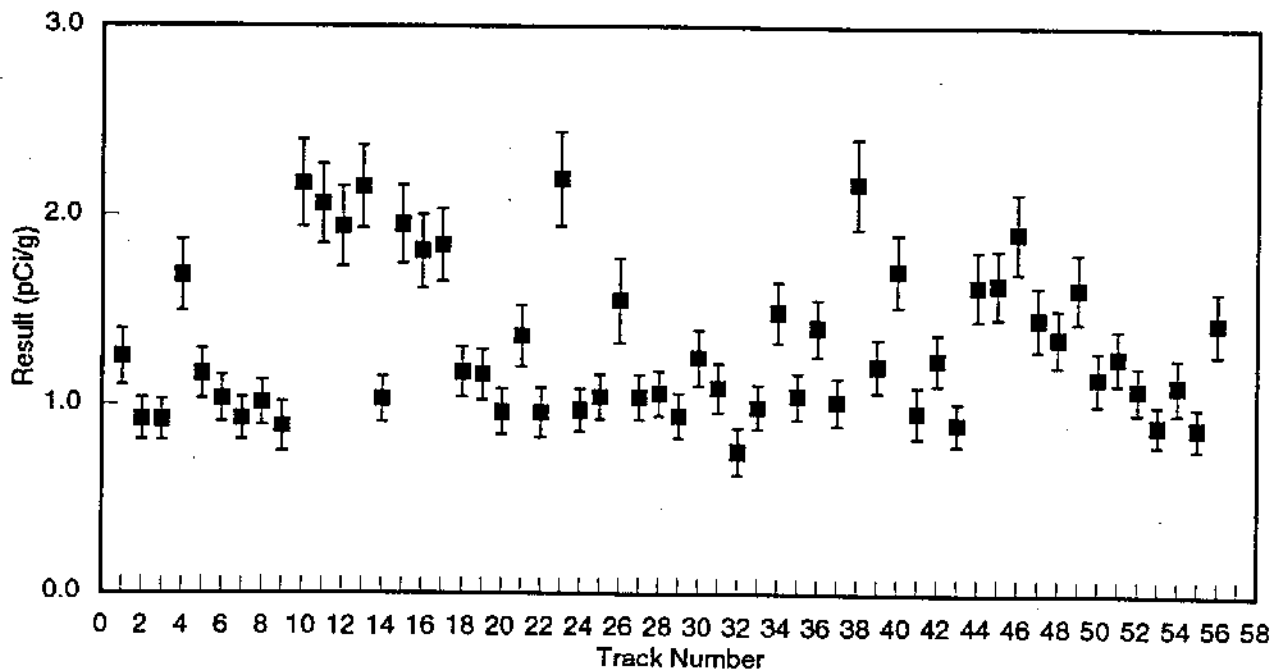
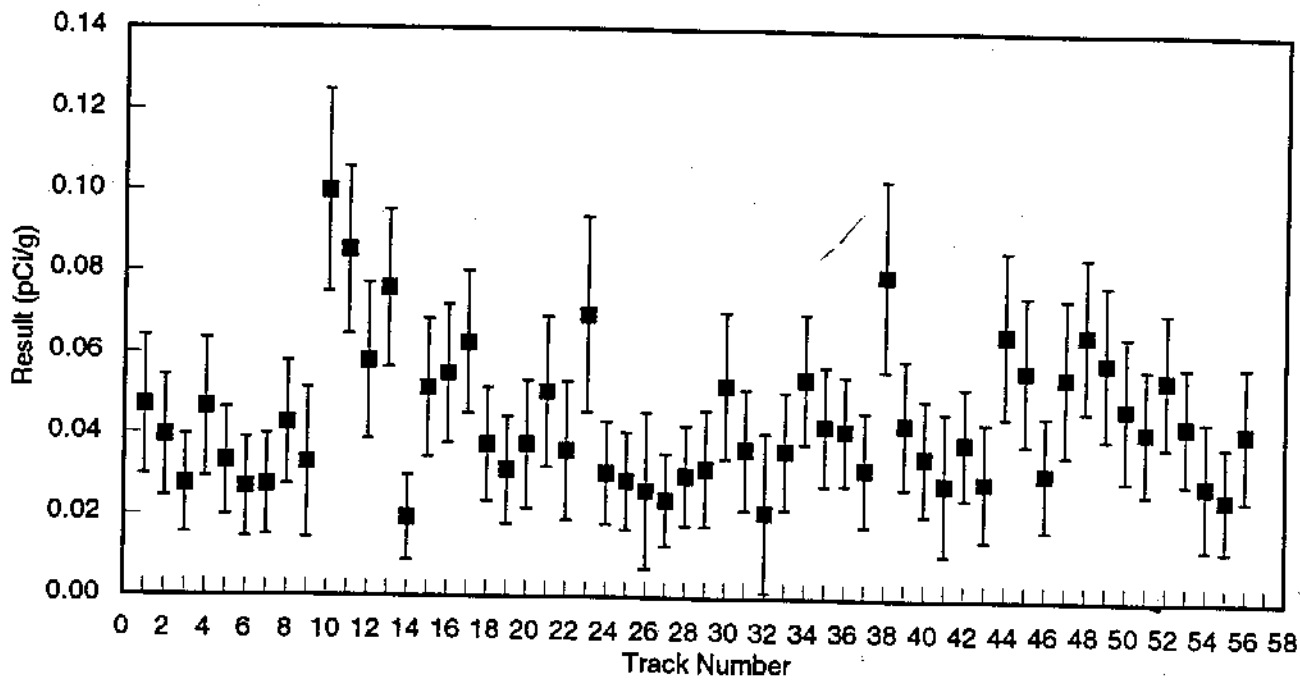


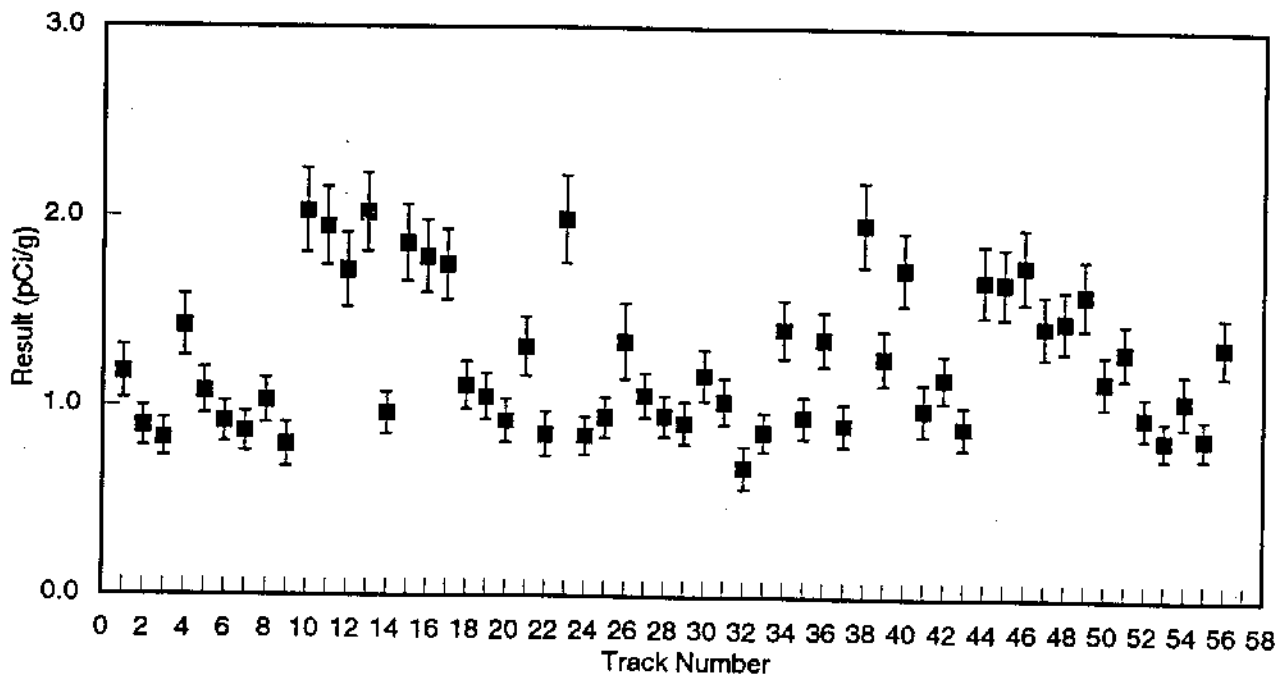
FIGURE 4.15. Uranium-234 ( $^{234}\text{U}$ ) Concentrations in Soils

S9306049.10



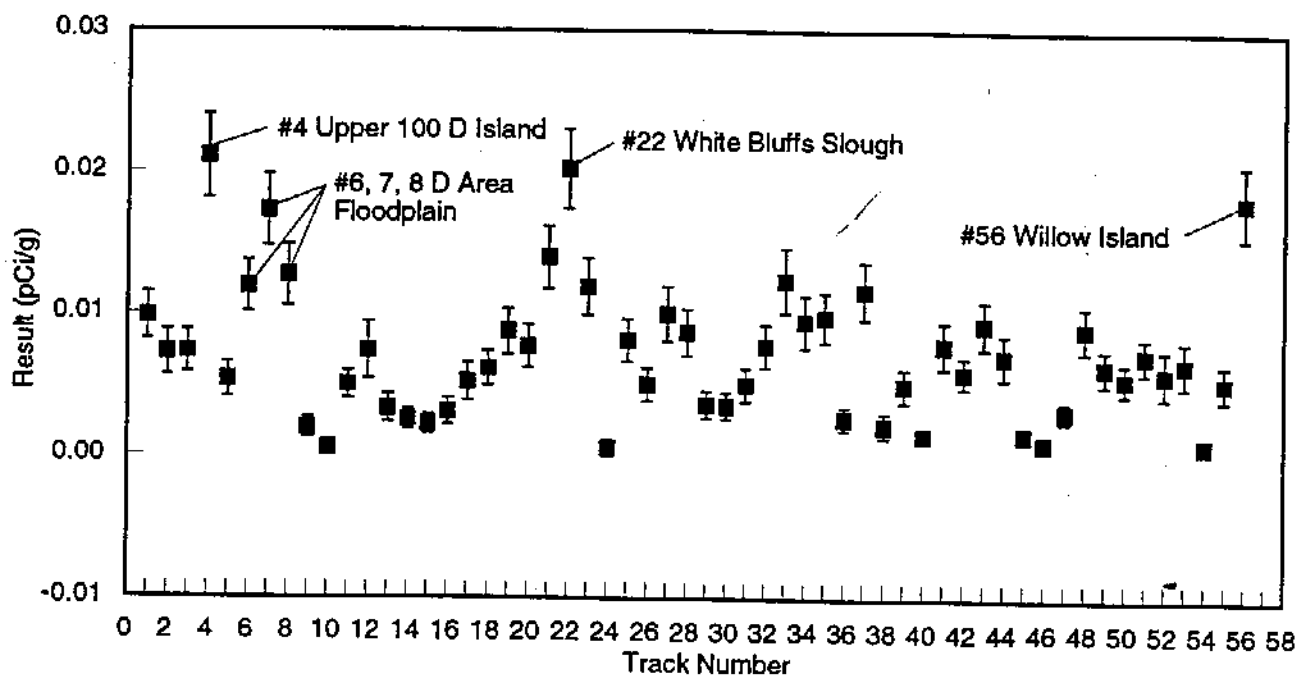
S9306049.11

FIGURE 4.16. Uranium-235 ( $^{235}\text{U}$ ) Concentrations in Soils



S9306049.12

FIGURE 4.17. Uranium-238 ( $^{238}\text{U}$ ) Concentrations in Soils



S9306049.13

FIGURE 4.18. Plutonium-239,240 ( $^{239,240}\text{Pu}$ ) Concentrations in Soils

the slough. The nonsoluble contaminants then settled out and became affixed to the soils before the next high water period.

Tracks 12, 27, 48, and 52 show elevated concentrations of  $^{90}\text{Sr}$  in soils. Tracks 10 through 17, 23, 40, 44 through 46, and 49 show elevations in  $^{234}\text{U}$  and  $^{238}\text{U}$  concentrations, and Tracks 10 and 11 indicate elevated levels of  $^{235}\text{U}$ . Tracks 4, 7, 21, 22, and 56 have elevated concentrations of  $^{239,240}\text{Pu}$ . Strontium-90 is likely the result of known discharges from the N Springs. The presence of elevated uranium may be due to reactor fuel rod failures; this is especially suggested in tracks 11 to 13, which are not only elevated in  $^{234}\text{U}$  and  $^{238}\text{U}$  concentrations, but also in those for  $^{235}\text{U}$ . Results for tracks farther downstream that are elevated in  $^{234}\text{U}$  and  $^{238}\text{U}$  concentrations, relative to the upstream background location concentrations, are difficult to interpret because of naturally elevated uranium in Franklin County soils adjacent to the river.

Table 4.2 shows the upstream background maximum, downstream maximum, and regional background maximum (nonshoreline) soil concentrations. The regional

**TABLE 4.2.** Comparison of Maximum Shoreline and Background Regional Soil Concentrations, pCi/g

Radio-nuclide	Shoreline Soils		Regional Soils
	Upstream	Downstream	Distant Locations <sup>(a)</sup>
<sup>22</sup> Na	0.01	0.13	NR <sup>(b)</sup>
<sup>60</sup> Co	0.02	0.91	0.01
<sup>90</sup> Sr	0.03	0.11	0.05
<sup>137</sup> Cs	0.62	5.97	0.45
<sup>152</sup> Eu	0.14	2.41	NR
<sup>154</sup> Eu	0.03	0.23	-0.01
<sup>234</sup> U	1.25	2.19	NR
<sup>235</sup> U	0.05	0.10	-0.04
<sup>238</sup> U	1.18	2.03	0.84
<sup>238</sup> Pu	3.24E-04	1.15E-03	6.51E-04
<sup>239,240</sup> Pu	9.82E-03	2.11E-02	7.76E-03

(a) Maximum value recorded in 1992 for either location (Yakima or Sunnyside).

(b) NR = not reported.

soil was collected from Yakima and Sunnyside (communities upwind from Hanford) in 1992. Sodium-22, <sup>152</sup>Eu, and <sup>234</sup>U were not reported (which implies they were not detected) for the distant locations. Distant locations show similar concentrations of <sup>65</sup>Zn, <sup>90</sup>Sr, and <sup>238</sup>Pu when compared to the upstream locations. The concentrations for the reported radionuclides in the downstream soils are higher than the upstream and the distant concentrations for each radionuclide except <sup>65</sup>Zn.

#### 4.4.1.1 External Dose Estimates From Gamma Emitters

Table 4.3 shows the external dose contribution from the maximum measured concentrations of the significant gamma emitters found in the soils along the Hanford Reach. The calculations assume an infinite plane of plane of soil

TABLE 4.3. External Dose Rates from Radionuclides in Soils

<u>Radionuclide</u>	<u>Maximum Concentration, pCi/g</u>	<u>Dose, mrem/y</u>
<sup>22</sup> Na	0.15	0.5
<sup>60</sup> Co	0.9	3.0
<sup>65</sup> Zn	0.008	0.007
<sup>137</sup> Cs	6	5.3
<sup>152</sup> Eu	2.5	4.2
<sup>154</sup> Eu	0.25	0.5

1 cm in depth containing the concentrations shown. If any one location along Hanford Reach had all of the soil concentrations shown in Table 4.3, the yearly dose (not including normal background) contribution from continuous occupancy would be approximately 14 mrem/yr. The public dose standard is 100 mrem/yr.

#### 4.4.2 Trace Metals

Chemicals containing several trace metals were known to have been used and discharged in past reactor and chemical processing operations, or have been identified as "contaminants of concern" as part of site restoration studies because it is suspected that they were used and disposed of in the environment. Figures 4.19 through 4.25 show the concentrations in the soil composites taken from each track for those trace metals analyzed that have been identified as "contaminants of concern" (barium, beryllium, cadmium, chromium, and lead) potentially entering the river or for which results were higher than at the upstream background locations (cobalt and manganese). Mercury has also been identified as a "contaminant of concern" and was analyzed for, but was not detected (<0.4 mg/kg) in any sample. (The data for all results and supplemental figures appear in Appendix C.) The concentration values are bounded by the estimated 2 sigma analytical error (i.e., the 95% confidence intervals). The analytical error for each type of trace metal analysis was calculated by analyzing multiple spiked samples and determining a coefficient of variation (standard deviation/mean) for each analysis type. Each analytical result was then multiplied by 2 times the coefficient of

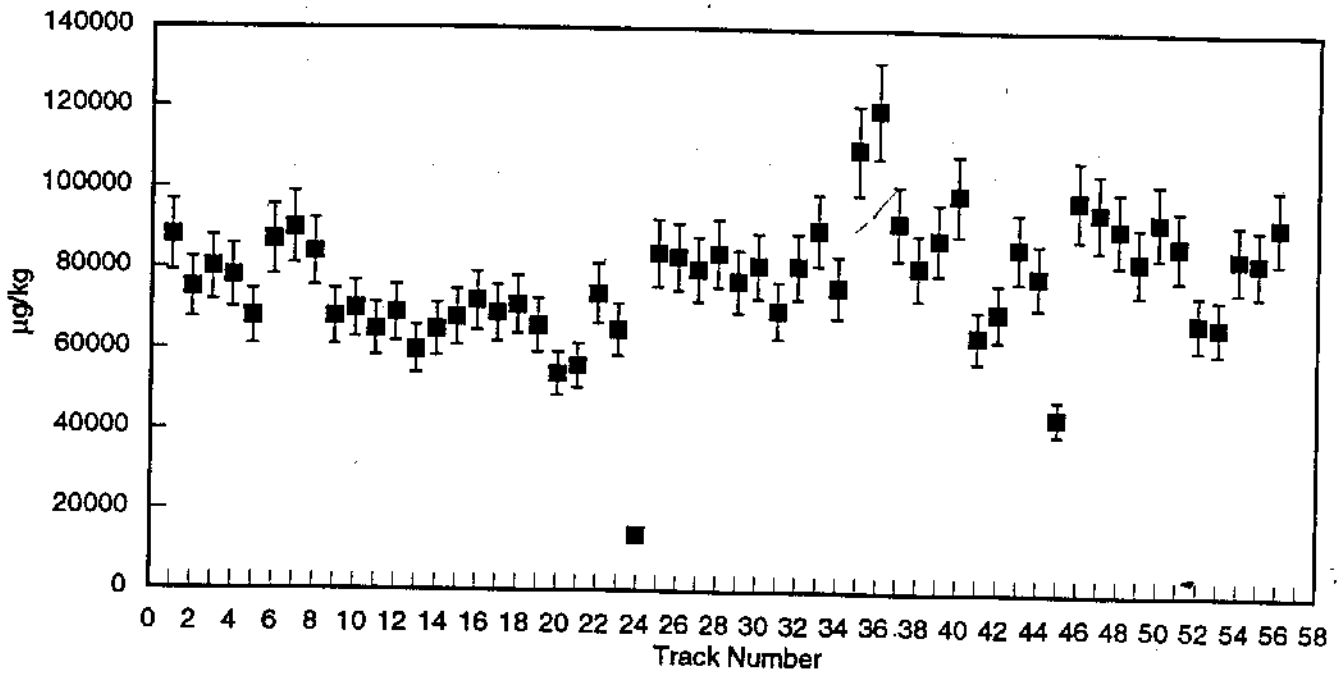


**FIGURE 4.19.** Barium Concentrations in Soils

S9306049.14

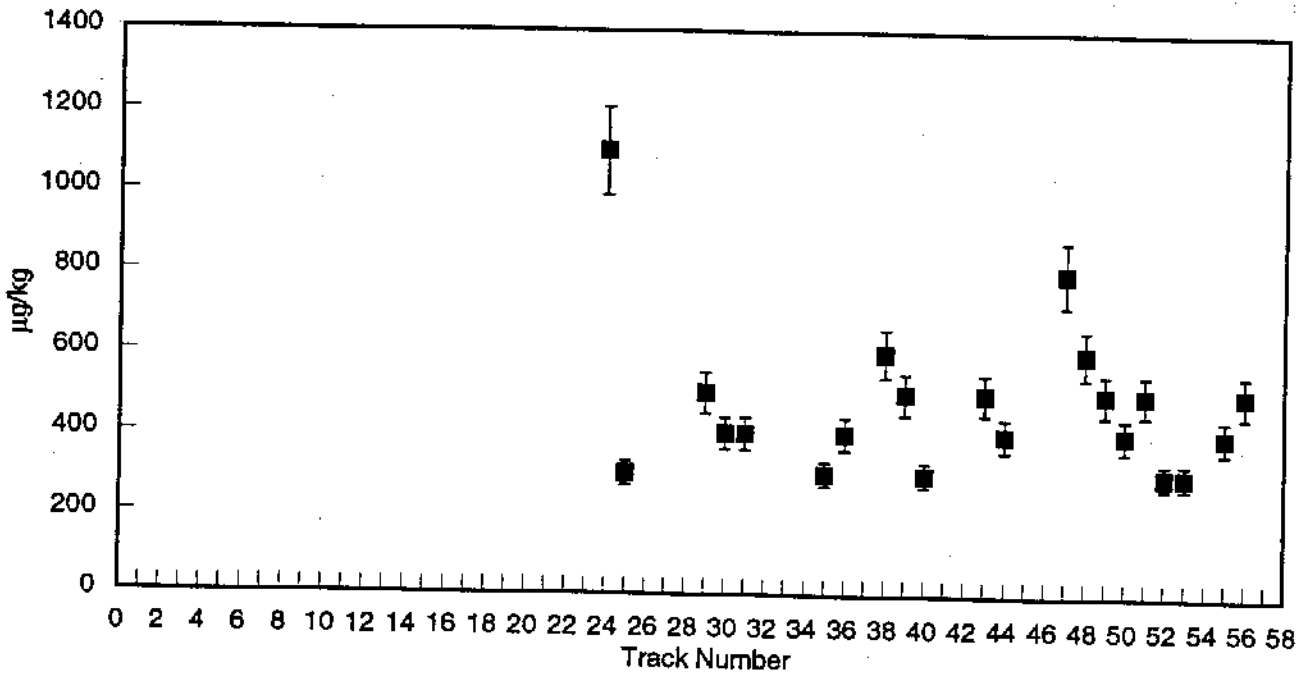


**FIGURE 4.20.** Beryllium Concentrations in Soils

S9306049.15

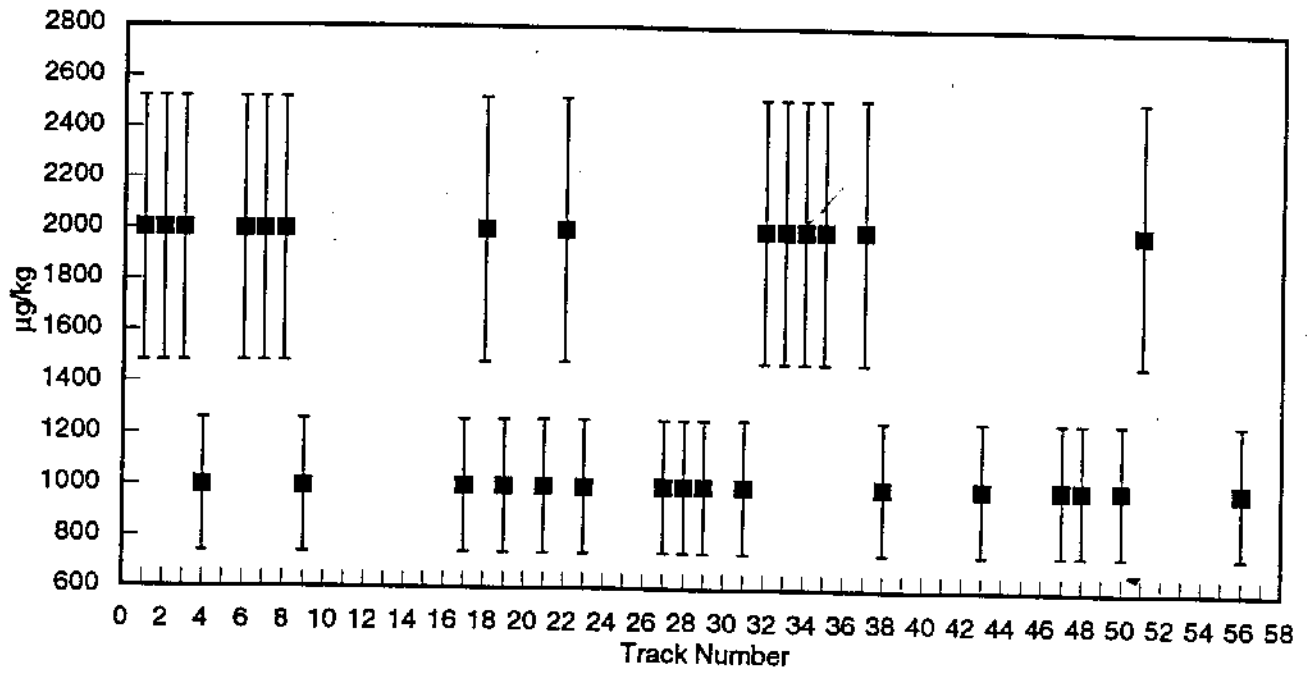


FIGURE 4.21. Cadmium Concentrations in Soils

S9306049.16

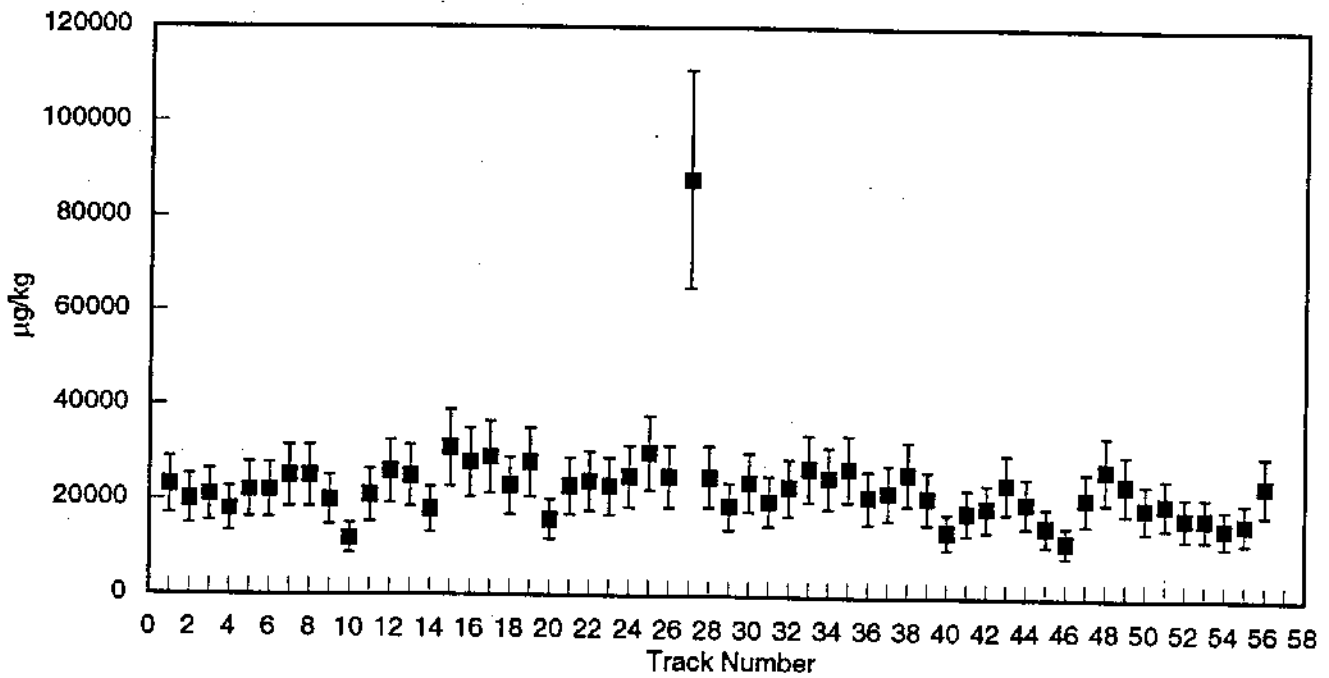


FIGURE 4.22. Chromium Concentrations in Soils

S9306049.17

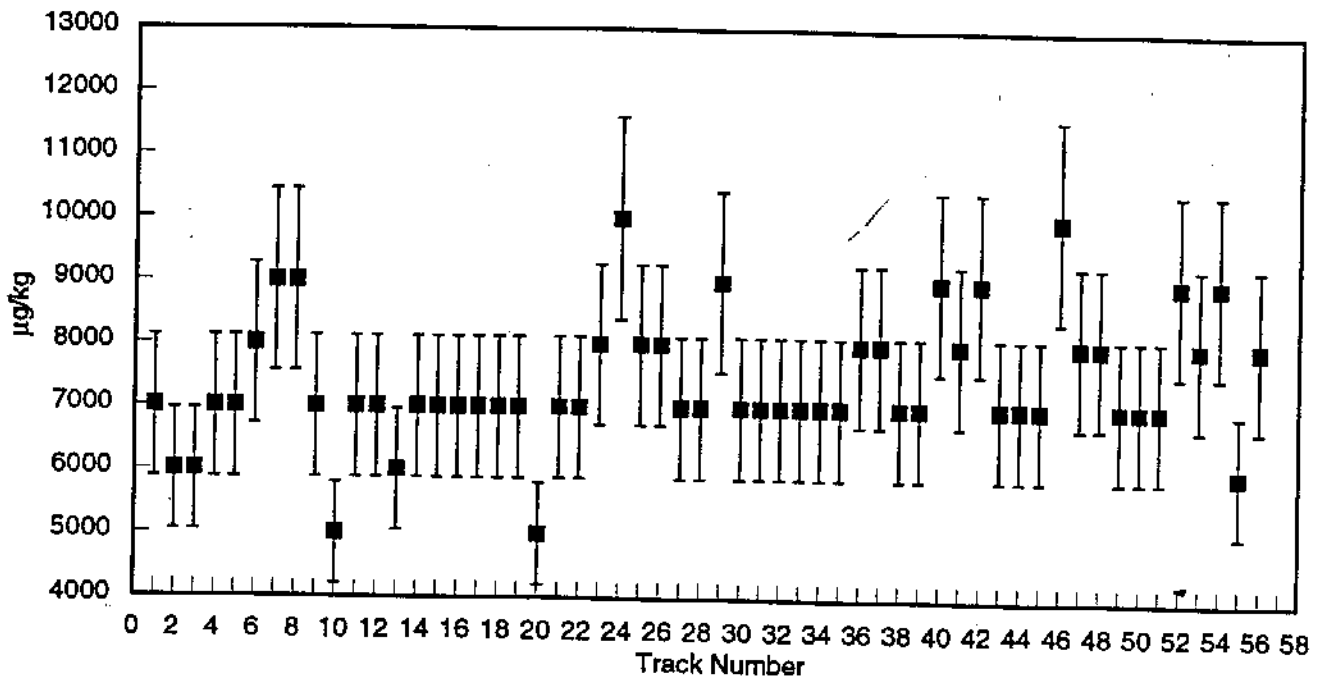


FIGURE 4.23. Cobalt Concentrations in Soils

S9306049.18

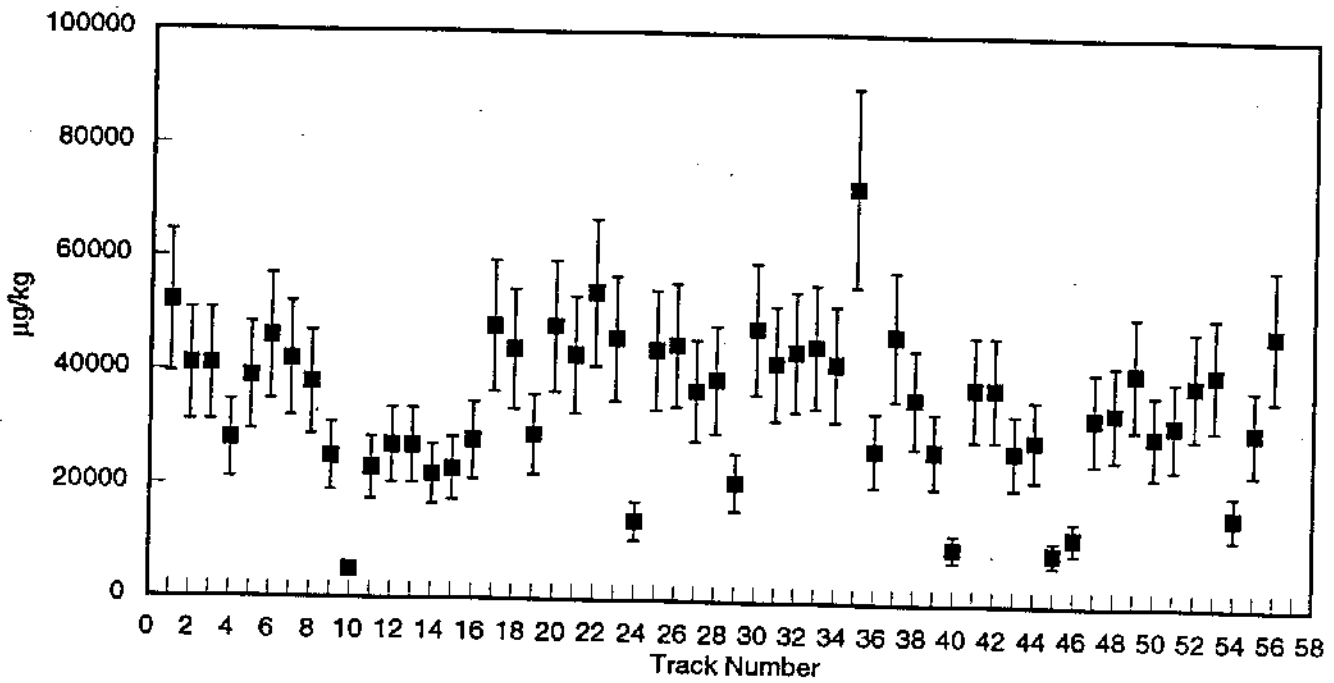


FIGURE 4.24. Lead Concentrations in Soils

S9306049.19

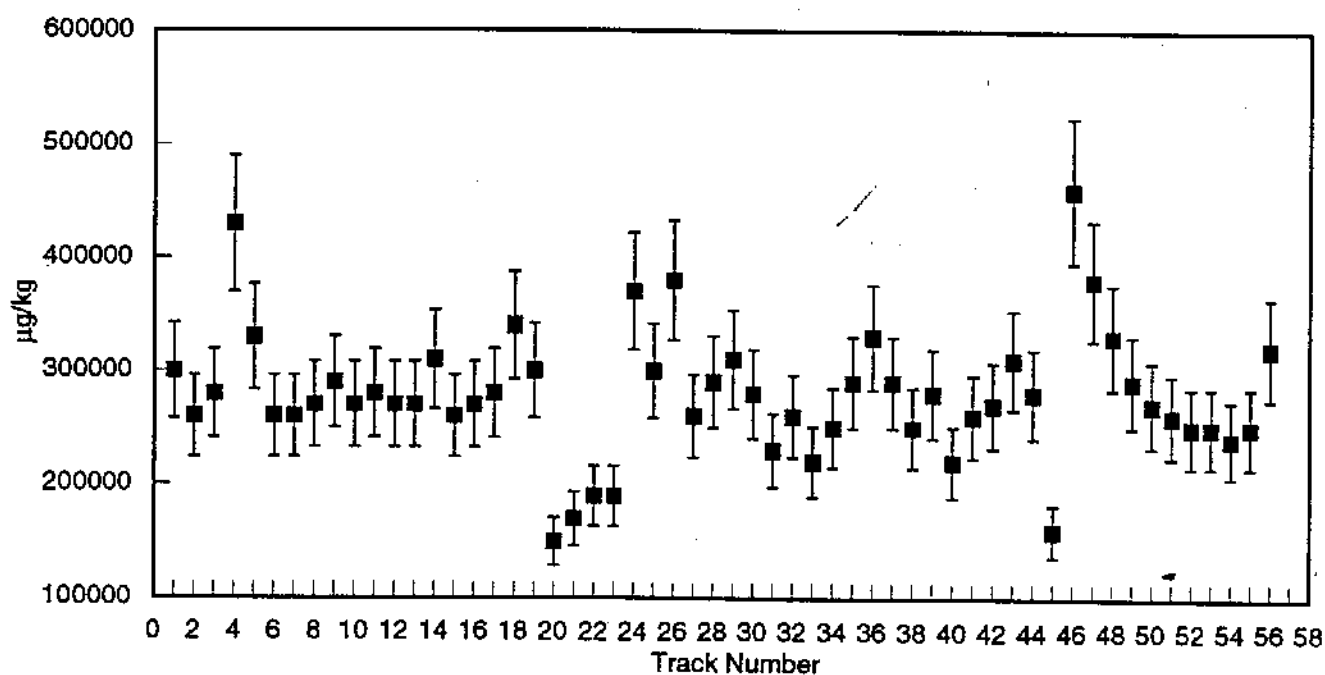


FIGURE 4.25. Manganese Concentrations in Soils

S9306049.20

variation of the appropriate analysis type to provide an estimate of the 2 sigma error about each analytical result.

Overall the trace metal results are very consistent and compare well with those from the upstream background locations. The only significantly elevated results were for barium on Tracks 35 and 36 (the Hanford Townsite Slough shoreline and the opposite shore, respectively), chromium concentrations along Track 27 (the 100-F Reactor floodplain area, see Figure 3.3), cobalt on Tracks 24 and 46, and manganese on Tracks 4 and 46. Most notable among these results is elevated chromium (88 mg/kg). Historically, elevated concentrations of chromium along the Hanford Reach have been attributed to the use of sodium dichromate, which was added to reactor cooling water to prevent corrosion. Tracks 25, 26, and 28 through 31 are also located at the 100-F floodplain area but show no chromium concentrations above the norm. Elevated chromium concentrations have previously been reported in N Springs area and associated sediments, the highest sediment concentration reported being 122 mg/kg (DOE/RL 1992).

Table 4.4 compares the concentrations of trace metals in Hanford Reach shoreline soils to Washington State marine sediment standards (WAC-173-204) established for the Puget Sound area and the concentrations established in the Hanford background soils study (Hoover 1993). Figure 4.26 shows that the maximum concentrations of trace metals in soils along the Hanford Reach are very similar to the maximum results reported in the Hanford Site background. Also, the concentrations of trace metals along the Hanford Reach fall well below the marine sediment standards established by Washington State (see Table 4.4). Standards for fresh water sediments have not yet been promulgated.

The major factor in choosing survey and soil sampling locations for this study was the EG&G exposure measurements, which identified areas with elevated levels of gamma-emitting radioactivity. This strategy assumes nongamma-emitting radionuclides and trace metals are deposited in the same locations as the gamma emitters. One of the objectives of this study was to test this assumption by examining the correlation between the concentrations of gamma-emitting radionuclides and nongamma-emitters and trace metals.

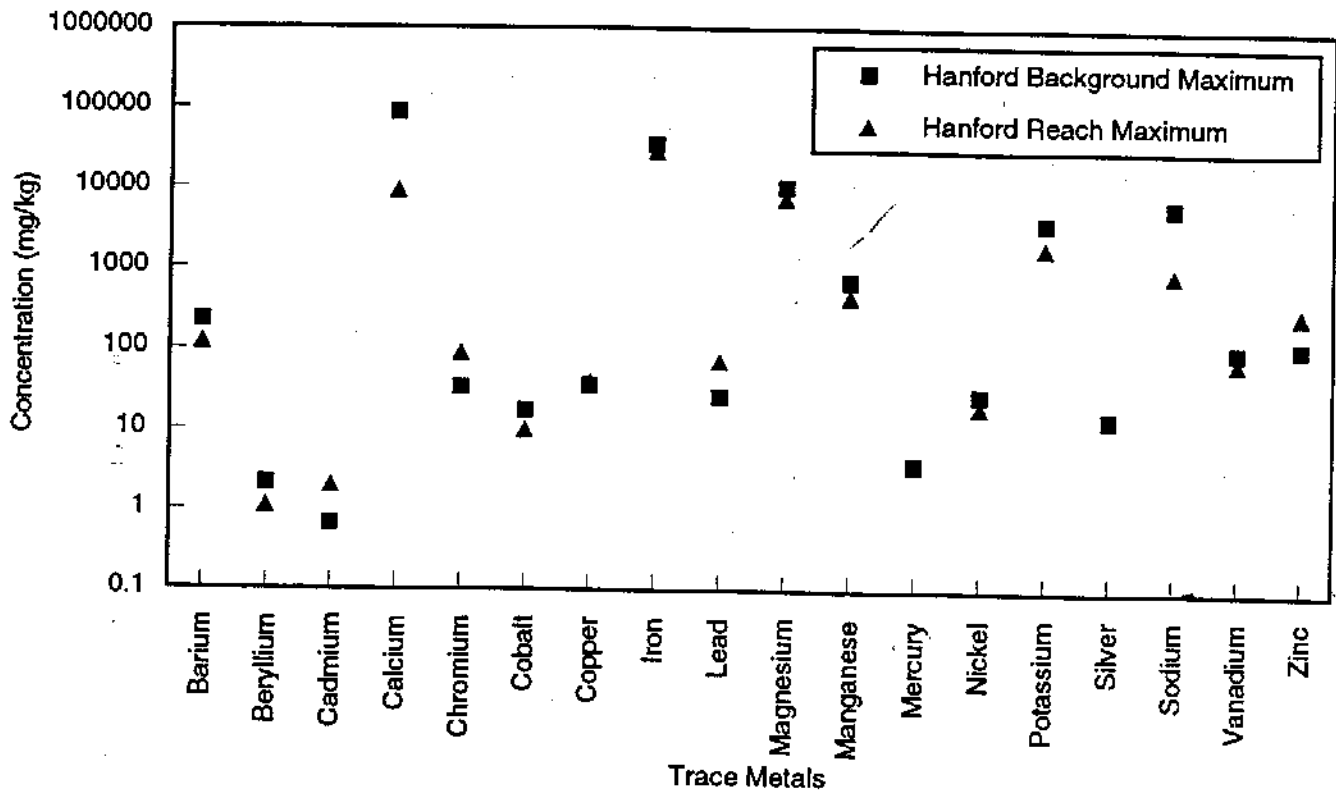
Because the analytes deposited along the Hanford Reach came from the same source streams, there should be some degree of correlation between analyte concentrations. Appendix D shows the Pearson correlation coefficient ( $r$ ) of paired (by location) sets of analytes for this survey. Good positive correlations ( $0.43 < r < 0.96$ ) exist between the major gamma emitters (i.e.,  $^{22}\text{Na}$ ,  $^{60}\text{Co}$ ,  $^{137}\text{Cs}$ ,  $^{152}\text{Eu}$ , and  $^{154}\text{Eu}$ ). Good positive correlations ( $0.52 < r < 0.68$ ) exist between  $^{239,240}\text{Pu}$  and  $^{22}\text{Na}$ ,  $^{60}\text{Co}$ ,  $^{137}\text{Cs}$ ,  $^{152}\text{Eu}$ , and  $^{154}\text{Eu}$ . A good correlation between  $^{239}\text{Pu}$  and gamma-emitter concentrations indicates that the presence of elevated concentrations of gamma emitters predicts the presence of  $^{239}\text{Pu}$ . Uranium, on the other hand, exhibits low correlations with the gamma emitters.

As shown in Appendix D, the trace metal concentrations show minimal correlation with radioactive analytes. Because the trace metal concentrations shown in Figures 4.19 through 4.25 and C.1 through C.9 are generally at background levels, one would not expect a correlation between trace metal and radioactive concentrations.

TABLE 4.4. Trace Metals Comparisons, mg/kg

	Hanford Background Soils		Hanford Reach Soils		Washington State Sediment Standards
	Maximum	Mean	Maximum	Mean	
Barium	221	94.5	120	77	
Beryllium	2.1	1.1	1.1	0.5	
Cadmium	0.66	0.7	2	1.5	6.7
Calcium	86,600	11,312	9,000	5,407	
Chromium	33.2	11.3	88	23	270
Cobalt	17.4	12	10	7	
Copper	36.1	15.8	40	26	390
Iron	35,100	24,585	29,000	21,285	
Lead	26.6	6.2	73	34	530
Magnesium	10,500	5,251	7,600	4,739	
Manganese	704	384	460	278	
Mercury	3.8	0.3	<4 <sup>(a)</sup>	<4 <sup>(a)</sup>	0.59
Nickel	28.4	13.2	20	15.8	
Potassium	3,780	1,415	1,900	1,245	
Silver	14.6	1.5	<2 <sup>(a)</sup>	<2 <sup>(a)</sup>	
Sodium	6,060	480.4	920	457	
Vanadium	105	58.3	77	53	
Zinc	119	52.6	300	212	960

(a) Less than the applicable detection limit.



S9306049.40

**FIGURE 4.26.** Comparison of Maximum Trace Metal Concentrations Between Soils Along the Hanford Reach and Soils from Background Areas Across the Hanford Site

## 5.0 REFERENCES

- Becker, C. D. 1990. "Aquatic Bioenvironmental Studies: The Hanford Experience 1944-84." Studies in Environmental Science 39, Elsevier, Amsterdam.
- Birchall, A., M. R. Bailey, and A. C. James. 1991. "LUDEP: A Lung Dose Evaluation Program." Radiation Protection Dosimetry 38:167-174.
- DOE/RL (U.S. Department of Energy, Richland Operations Office). 1992. Sampling and Analysis of 100 Areas Springs. DOE/RL-92-12, U.S. Department of Energy, Richland Operations Office, Richland, Washington.
- Durham, J. S. 1992. VARSKIN Mod 2 and SADDE Mod 2: Computer Codes for Assessing Skin Dose from Skin Contamination. NUREG/CR-5873, U.S. Nuclear Regulatory Commission, Washington, D.C.
- EG&G (EG&G Energy Measurements, The Remote Sensing Laboratory, Las Vegas, Nevada). 1990. An Aerial Radiological Survey of the Hanford Site and Surrounding Area, Richland, Washington. EGG-10617-1062, EG&G Energy Measurements, The Remote Sensing Laboratory, Las Vegas, Nevada.
- EPA (U.S. Environmental Protection Agency). 1982. Test Methods for Evaluating Solid Waste (SW-846). EPA-600/4-82-055, U.S. Environmental Protection Agency, Washington, D.C.
- Future Site Uses Working Group. 1992. The Future for Hanford: Uses and Cleanup. U.S. Department of Energy, Richland, Washington.
- Hahn, G. J., and W. Q. Meeker. 1991. Statistical Intervals, A Guide for Practitioners. John Wiley and Sons, Inc., New York.
- Havilcek, L. L., and R. D. Crane. 1988. Practical Statistics for the Physical Sciences. American Chemical Society, Washington, D.C.
- Hoover, J. D. 1993. Hanford Site Background: Part 1, Soil Background for Nonradioactive Analytes. DOE/RL-92-24, U.S. Department of Energy, Office of Environmental Restoration and Waste Management, Washington, D.C.
- NCRP (National Council on Radiation Protection and Measurements). 1989. Limit for Exposure to Hot Particles on the Skin. NCRP Report No. 106, National Council on Radiation Protection and Measurements, Bethesda, Maryland.
- Sula, M. J. 1980. Radiological Survey of Exposed Shorelines and Islands of the Columbia River Between Vernita and The Snake River Confluence. PNL-3127, Pacific Northwest Laboratory, Richland, Washington.
- WAC 173-204. "Sediment Management Standards." Washington State Department of Ecology. Washington Administrative Code.

Watson, E. V., M. G. Stabin, and W. E. Bolch. 1984. Documentation Package for MIRDOSE. Oak Ridge Associated Universities, Oak Ridge, Tennessee.

Woodruff, R. K., R. W. Hanf, and R. E. Lundgren. 1993. Hanford Site Environmental Report for Calendar Year 1992. PNL-8682, Pacific Northwest Laboratory, Richland, Washington.

APPENDIX A

EXPOSURE RATE DATA

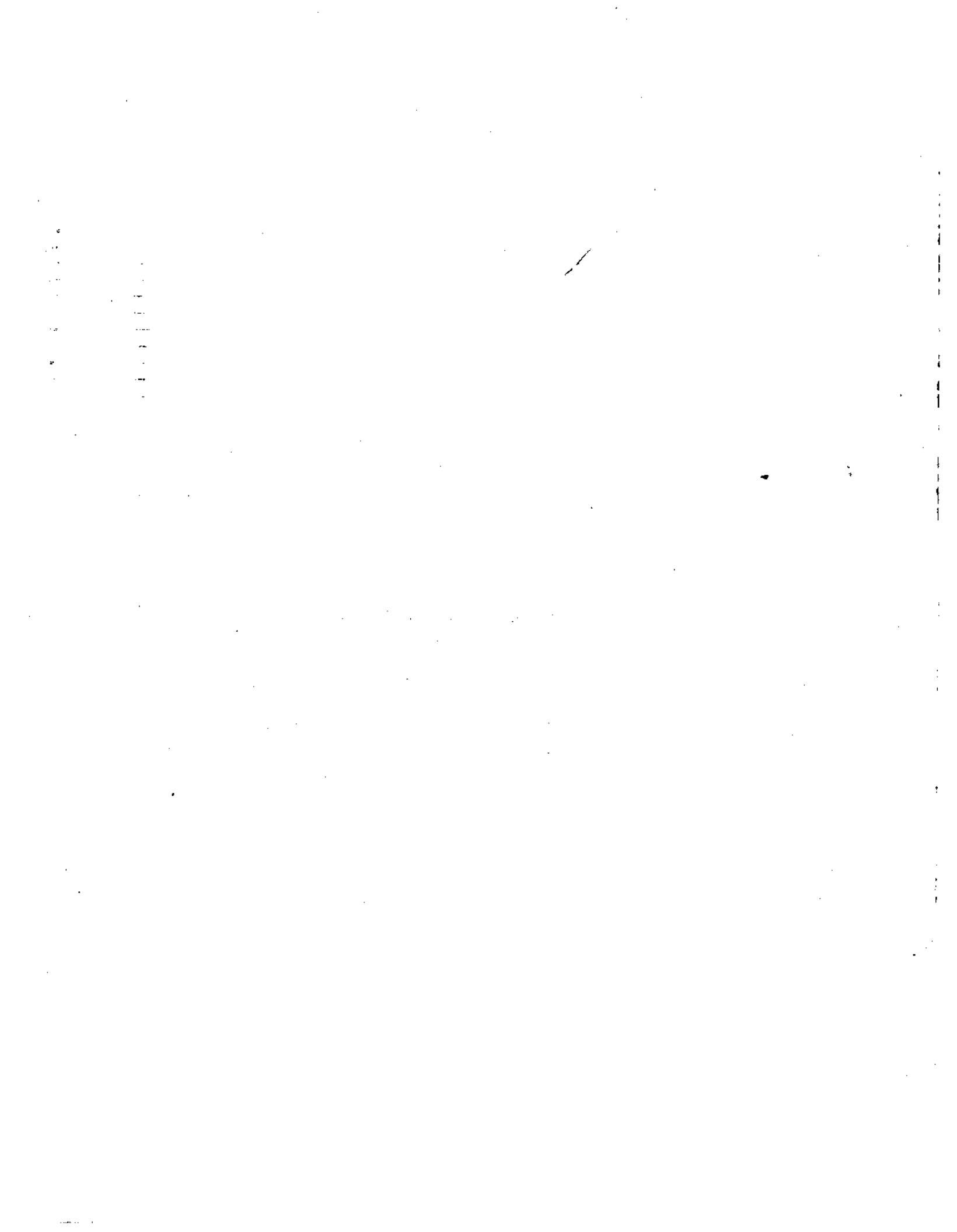
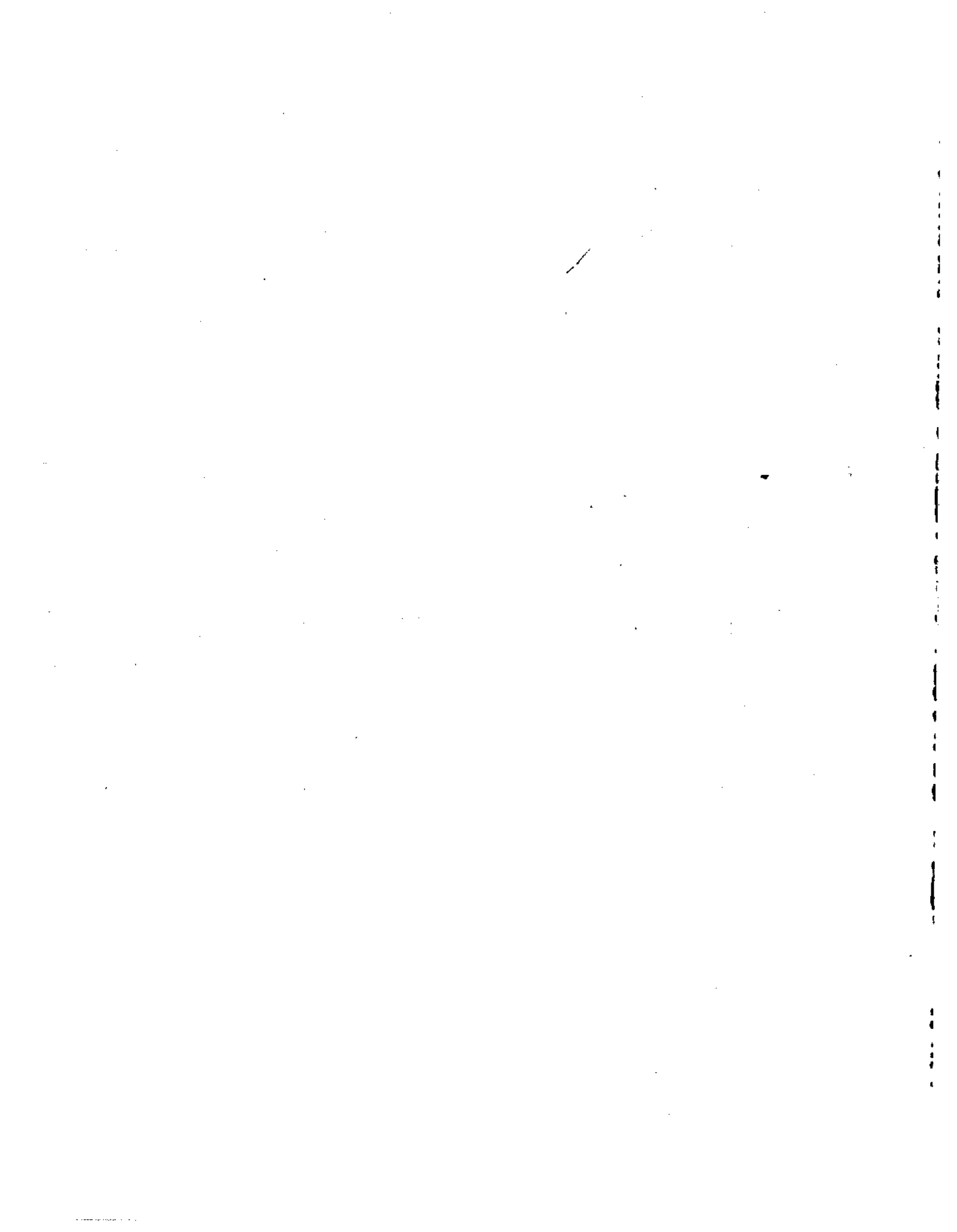


TABLE A.1. Exposure Rates Listed by Track

Survey Area	Track #	Number of Recorded Measurements*	Track Maximum uR/hr	Track Average uR/hr	Track Median uR/hr	2SD uR/hr	Particles
Vernita Shoreline	-	51	11.0	7.3	7.0	3.6	
Upper 100 D Island	4	8	10.0	10.0	10.0	0.0	8
Lower 100 D Island	5	7	11.0	10.1	10.0	0.8	3
D Floodplain	6	10	14.0	11.3	12.0	3.1	
D Floodplain	7	13	14.0	10.7	11.0	3.3	
D Floodplain	8	11	14.0	10.9	11.0	3.3	
Island 376	9	13	13.0	11.2	11.0	2.4	
White Bluffs Shoreline	10	9	12.0	9.8	10.0	3.3	
Island 375 Slough	11	11	13.0	10.9	10.0	2.3	
Island 375 Shoreline	12	10	11.0	10.2	10.0	1.3	
Island 373b	13	7	10.0	8.7	9.0	1.5	
Island 373a	14	5	10.0	9.2	10.0	2.2	
Lower Locke Island	15	11	15.0	13.2	13.0	2.8	
Mid Locke Island	16	9	15.0	12.4	12.0	2.8	
Upper Locke Island	17	12	14.0	12.2	12.0	2.1	
H Area Shoreline	18	14	16.0	11.3	11.0	3.4	
H Area Shoreline	19	12	12.0	11.4	12.0	1.8	
White Bluffs Slough	20	16	18.0	13.9	13.0	4.4	1
White Bluffs Slough	21	14	17.0	14.4	14.0	3.0	
White Bluffs Slough	22	13	28.0	20.8	22.0	11.6	
White Bluffs Slough	23	12	20.0	18.5	18.0	2.5	
East Bank Shoreline	24	10	12.0	11.7	12.0	1.3	
F Area Shoreline	25	11	11.0	10.6	11.0	1.0	
F Area Shoreline	26	11	14.0	12.9	13.0	2.3	
F Slough Area	27	12	17.0	13.6	13.5	3.4	
Island 367	28	10	13.0	12.1	13.0	2.6	
F Area Shoreline	29	9	14.0	12.7	12.5	1.7	
F Area Shoreline	30	12	14.5	12.8	13.0	2.7	
F Area Shoreline	31	8	16.0	14.4	14.5	2.4	
Hanford Townsite Peninsula	32	14	18.0	15.2	15.5	4.7	
Hanford Townsite Peninsula	33	13	20.0	16.2	16.0	4.3	
Hanford Townsite Peninsula	34	10	18.0	15.0	15.0	4.3	
Hanford Townsite Slough	35	15	18.0	13.7	14.0	4.5	
East Bank / Public Boat Launch	36	10	12.0	9.6	9.5	2.1	
Hanford Townsite Shoreline	37	10	18.0	14.2	15.0	7.6	
Savage Island Slough	38	8	18.0	16.5	16.5	2.1	
Savage Island Shoreline	39	10	16.5	15.2	15.5	1.9	
West Bank Shoreline	40	10	14.0	11.7	12.0	3.4	
Ringold Island	41	10	13.0	11.6	11.8	1.7	
Ringold Island	42	10	12.5	11.4	11.5	1.3	
Upper Island 353	43	10	12.5	11.4	11.5	1.7	
Lower Island 353	44	10	14.5	11.5	11.3	3.7	
West Bank Shoreline	45	9	14.0	12.2	12.0	1.9	
East Bank Shoreline	46	10	12.0	11.2	11.0	1.6	
Island 350	47	6	14.5	11.4	11.0	3.2	
Island 349	48	9	13.0	13.0	13.0	0.0	
Upper Wooded Island	49	10	15.0	14.3	14.8	2.0	
Lower Wooded Island	50	10	17.5	15.3	15.5	3.0	
West Bank Shoreline	51	10	12.0	10.6	10.0	1.9	
Lower Capp Island	52	11	14.5	13.5	13.5	1.9	
Upper Capp Island	53	10	16.0	15.1	15.3	1.4	
East Bank Shoreline	54	10	12.0	11.2	11.0	1.1	
Richland Pumphouse Shoreline	55	10	12.0	10.6	10.5	2.3	
Willow Island	56	10	18.0	13.7	14.0	3.9	

\* A measurement was recorded over 100 meter intervals



APPENDIX B

SOIL SAMPLE RADIONUCLIDE CONCENTRATION DATA  
AND SUPPLEMENTAL FIGURES

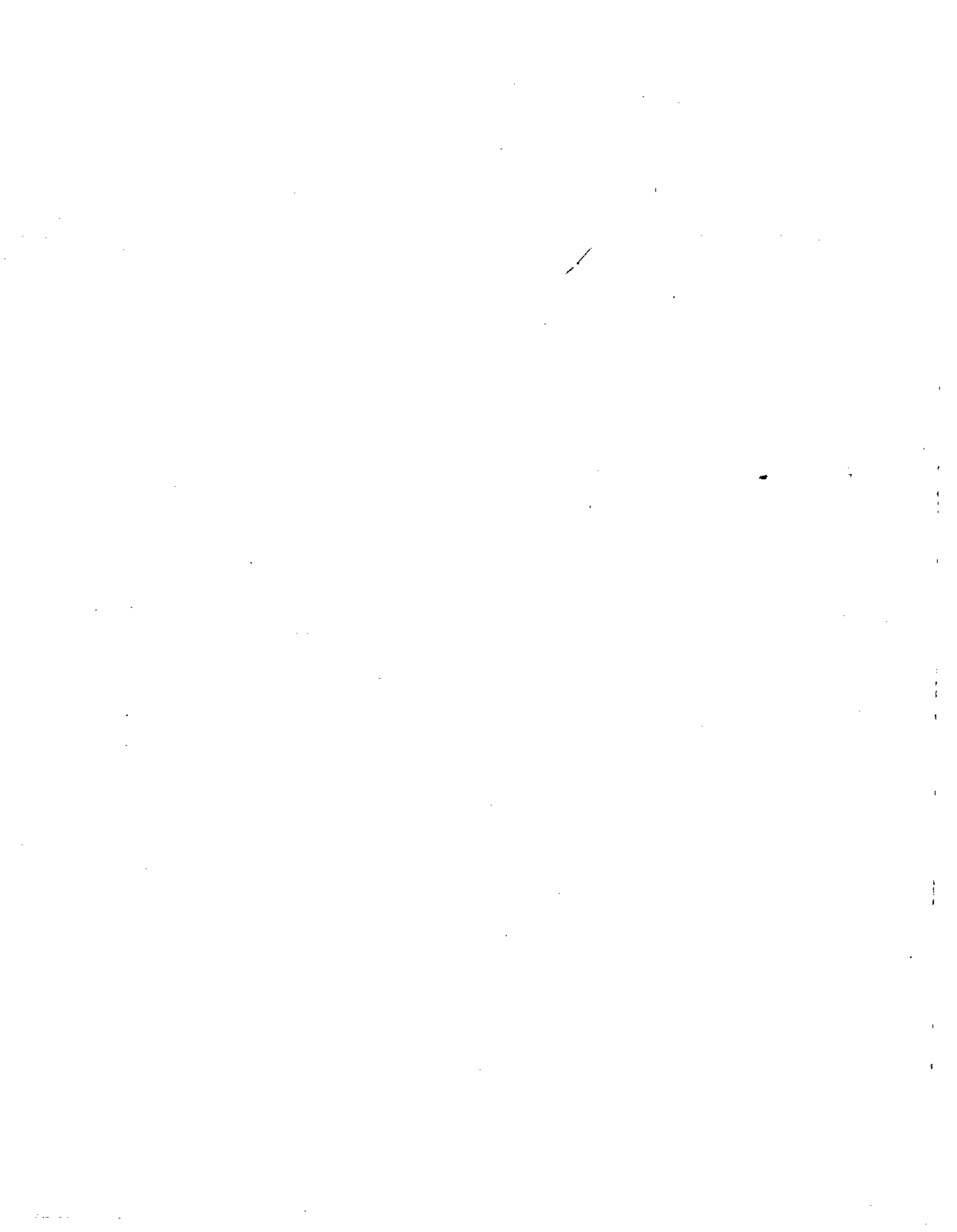


TABLE B.1. Gamma-Emitter Data

<u>Track #</u>	<u>Constituent</u>	<u>Result, pCi/g</u>	<u>Overall Error</u>
1	Be-7	6.26E-02	1.54E-01
2	Be-7	-1.27E-01	1.45E-01
3	Be-7	9.65E-02	1.63E-01
4	Be-7	3.86E-02	1.71E-01
5	Be-7	3.96E-02	1.60E-01
6	Be-7	6.49E-02	1.82E-01
7	Be-7	1.28E-02	2.17E-01
8	Be-7	-7.10E-02	1.80E-01
9	Be-7	-2.10E-02	1.40E-01
10	Be-7	2.52E-02	1.22E-01
11	Be-7	-2.89E-02	1.38E-01
12	Be-7	1.17E-01	1.58E-01
13	Be-7	4.98E-02	1.56E-01
14	Be-7	9.03E-02	1.31E-01
15	Be-7	1.04E-02	1.58E-01
16	Be-7	-2.27E-02	1.55E-01
17	Be-7	7.62E-02	1.56E-01
18	Be-7	-2.49E-02	1.68E-01
19	Be-7	-4.24E-02	1.23E-01
20	Be-7	-1.27E-01	1.71E-01
21	Be-7	2.24E-01	2.00E-01
22	Be-7	1.22E-01	2.39E-01
23	Be-7	-1.03E-01	2.26E-01
24	Be-7	1.68E-01	1.68E-01
25	Be-7	2.37E-01	1.75E-01
26	Be-7	6.37E-02	1.35E-01
27	Be-7	3.52E-02	1.34E-01
28	Be-7	-5.24E-02	1.67E-01
29	Be-7	1.04E-02	1.27E-01
30	Be-7	4.14E-02	1.68E-01
31	Be-7	-7.12E-02	1.53E-01
32	Be-7	9.92E-02	1.32E-01
33	Be-7	5.77E-02	1.47E-01
34	Be-7	-5.10E-03	1.60E-01
35	Be-7	-3.69E-02	1.55E-01
36	Be-7	7.26E-02	1.63E-01
37	Be-7	1.58E-01	2.35E-01
38	Be-7	2.56E-01	1.84E-01
39	Be-7	7.78E-02	1.60E-01
40	Be-7	7.43E-02	1.15E-01
41	Be-7	8.39E-02	1.13E-01
42	Be-7	7.44E-02	1.20E-01
43	Be-7	2.14E-01	1.36E-01
44	Be-7	-7.01E-02	1.48E-01
45	Be-7	6.76E-02	1.39E-01
46	Be-7	1.22E-01	1.04E-01
47	Be-7	1.09E-01	1.07E-01
48	Be-7	6.92E-02	1.46E-01
49	Be-7	4.29E-02	1.25E-01
50	Be-7	6.36E-02	1.15E-01
51	Be-7	7.56E-02	2.22E-01
52	Be-7	4.39E-02	1.23E-01
53	Be-7	7.77E-02	1.07E-01
54	Be-7	7.45E-02	1.02E-01
55	Be-7	4.03E-02	1.40E-01
56	Be-7	-9.22E-02	1.20E-01

TABLE B.1. (contd)

<u>Track #</u>	<u>Constituent</u>	<u>Result, pCi/g</u>	<u>Overall Error</u>
1	Na-22	-4.05E-03	1.85E-02
2	Na-22	1.16E-02	1.63E-02
3	Na-22	-4.00E-03	1.94E-02
4	Na-22	1.32E-01	3.57E-02
5	Na-22	4.19E-02	1.68E-02
6	Na-22	2.51E-02	2.27E-02
7	Na-22	2.40E-02	2.43E-02
8	Na-22	4.17E-02	1.93E-02
9	Na-22	4.09E-03	1.79E-02
10	Na-22	-1.42E-02	1.72E-02
11	Na-22	-7.57E-03	1.88E-02
12	Na-22	1.55E-02	1.97E-02
13	Na-22	6.04E-03	2.14E-02
14	Na-22	1.65E-02	1.60E-02
15	Na-22	0.04453	0.02138
16	Na-22	-7.56E-03	1.99E-02
17	Na-22	-3.46E-03	2.07E-02
18	Na-22	3.15E-02	1.91E-02
19	Na-22	2.42E-02	1.38E-02
20	Na-22	2.79E-02	2.35E-02
21	Na-22	4.51E-02	1.97E-02
22	Na-22	8.36E-02	3.87E-02
23	Na-22	4.95E-02	2.55E-02
24	Na-22	-3.54E-03	1.57E-02
25	Na-22	5.05E-02	2.09E-02
26	Na-22	2.95E-02	1.81E-02
27	Na-22	5.63E-02	1.82E-02
28	Na-22	-4.34E-03	2.12E-02
29	Na-22	1.84E-02	1.55E-02
30	Na-22	2.29E-02	2.01E-02
31	Na-22	4.88E-02	2.03E-02
32	Na-22	5.77E-02	1.76E-02
33	Na-22	5.93E-02	2.48E-02
34	Na-22	3.97E-02	2.05E-02
35	Na-22	3.93E-02	2.16E-02
36	Na-22	-6.56E-03	2.05E-02
37	Na-22	9.55E-02	2.48E-02
38	Na-22	8.43E-03	2.07E-02
39	Na-22	-5.43E-03	1.95E-02
40	Na-22	-3.69E-03	1.49E-02
41	Na-22	2.14E-02	1.66E-02
42	Na-22	2.96E-02	1.60E-02
43	Na-22	2.41E-02	1.88E-02
44	Na-22	3.54E-02	2.03E-02
45	Na-22	6.64E-03	1.69E-02
46	Na-22	-4.55E-03	1.55E-02
47	Na-22	6.08E-03	1.40E-02
48	Na-22	3.35E-02	1.93E-02
49	Na-22	2.30E-02	1.40E-02
50	Na-22	1.69E-02	1.72E-02
51	Na-22	6.32E-02	2.43E-02
52	Na-22	8.44E-03	1.72E-02
53	Na-22	3.89E-02	1.50E-02
54	Na-22	-1.56E-02	1.68E-02
55	Na-22	1.77E-02	1.95E-02
56	Na-22	3.58E-03	1.73E-02

TABLE B.1. (contd)

<u>Track #</u>	<u>Constituent</u>	<u>Result, pCi/g</u>	<u>Overall Error</u>
1	K-40	1.41E+01	1.52E+00
2	K-40	1.42E+01	1.53E+00
3	K-40	1.49E+01	1.60E+00
4	K-40	1.50E+01	1.61E+00
5	K-40	1.52E+01	1.62E+00
6	K-40	1.67E+01	1.78E+00
7	K-40	1.81E+01	1.73E+00
8	K-40	1.46E+01	1.56E+00
9	K-40	1.64E+01	1.72E+00
10	K-40	1.62E+01	1.71E+00
11	K-40	1.43E+01	1.52E+00
12	K-40	1.67E+01	1.76E+00
13	K-40	1.67E+01	1.77E+00
14	K-40	1.48E+01	1.57E+00
15	K-40	1.84E+01	1.94E+00
16	K-40	1.59E+01	1.69E+00
17	K-40	1.77E+01	1.87E+00
18	K-40	1.41E+01	1.52E+00
19	K-40	1.49E+01	1.59E+00
20	K-40	1.52E+01	1.62E+00
21	K-40	1.53E+01	1.63E+00
22	K-40	1.58E+01	1.72E+00
23	K-40	1.73E+01	1.83E+00
24	K-40	1.88E+01	1.99E+00
25	K-40	1.71E+01	1.80E+00
26	K-40	1.44E+01	1.54E+00
27	K-40	1.51E+01	1.62E+00
28	K-40	1.76E+01	1.86E+00
29	K-40	1.45E+01	1.56E+00
30	K-40	1.65E+01	1.80E+00
31	K-40	1.58E+01	1.72E+00
32	K-40	1.46E+01	1.55E+00
33	K-40	1.64E+01	1.76E+00
34	K-40	1.54E+01	1.64E+00
35	K-40	1.58E+01	1.68E+00
36	K-40	1.69E+01	1.78E+00
37	K-40	1.77E+01	1.89E+00
38	K-40	1.71E+01	1.86E+00
39	K-40	1.71E+01	1.85E+00
40	K-40	1.45E+01	1.54E+00
41	K-40	1.66E+01	1.76E+00
42	K-40	1.53E+01	1.63E+00
43	K-40	1.56E+01	1.65E+00
44	K-40	1.74E+01	1.82E+00
45	K-40	1.47E+01	1.56E+00
46	K-40	1.73E+01	1.83E+00
47	K-40	1.54E+01	1.63E+00
48	K-40	1.52E+01	1.62E+00
49	K-40	1.45E+01	1.54E+00
50	K-40	1.68E+01	1.78E+00
51	K-40	1.68E+01	1.81E+00
52	K-40	1.54E+01	1.63E+00
53	K-40	1.49E+01	1.58E+00
54	K-40	1.83E+01	1.94E+00
55	K-40	1.66E+01	1.76E+00
56	K-40	1.73E+01	1.84E+00

TABLE B.1. (contd)

<u>Track #</u>	<u>Constituent</u>	<u>Result, pCi/g</u>	<u>Overall Error</u>
1	Co-60	1.75E-02	1.61E-02
2	Co-60	-1.61E-02	1.48E-02
3	Co-60	1.90E-02	1.71E-02
4	Co-60	9.13E-01	1.05E-01
5	Co-60	3.57E-01	4.77E-02
6	Co-60	7.67E-02	2.18E-02
7	Co-60	1.12E-01	2.66E-02
8	Co-60	1.31E-01	2.58E-02
9	Co-60	5.75E-02	1.62E-02
10	Co-60	6.27E-04	1.34E-02
11	Co-60	1.05E-01	2.15E-02
12	Co-60	1.92E-02	2.01E-02
13	Co-60	1.64E-01	3.06E-02
14	Co-60	1.18E-01	2.30E-02
15	Co-60	1.31E-02	1.89E-02
16	Co-60	4.97E-03	1.93E-02
17	Co-60	3.22E-02	1.85E-02
18	Co-60	1.78E-01	3.10E-02
19	Co-60	8.94E-02	2.71E-02
20	Co-60	1.32E-01	2.68E-02
21	Co-60	1.98E-01	3.28E-02
22	Co-60	3.48E-01	5.10E-02
23	Co-60	2.45E-01	3.67E-02
24	Co-60	-2.01E-03	1.84E-02
25	Co-60	1.60E-01	2.89E-02
26	Co-60	4.68E-01	6.40E-02
27	Co-60	1.47E-01	3.39E-02
28	Co-60	1.00E-01	2.30E-02
29	Co-60	1.01E-01	2.92E-02
30	Co-60	1.89E-01	4.18E-02
31	Co-60	2.00E-01	3.80E-02
32	Co-60	1.81E-01	2.86E-02
33	Co-60	1.46E-01	3.12E-02
34	Co-60	2.67E-01	3.78E-02
35	Co-60	2.01E-01	3.48E-02
36	Co-60	7.32E-02	2.01E-02
37	Co-60	7.96E-01	9.21E-02
38	Co-60	7.64E-02	3.07E-02
39	Co-60	5.50E-02	1.84E-02
40	Co-60	7.19E-03	1.25E-02
41	Co-60	1.94E-01	3.37E-02
42	Co-60	2.01E-01	3.36E-02
43	Co-60	3.70E-01	4.73E-02
44	Co-60	2.55E-01	3.69E-02
45	Co-60	5.43E-02	1.64E-02
46	Co-60	2.51E-02	1.38E-02
47	Co-60	9.75E-02	2.72E-02
48	Co-60	1.59E-01	2.66E-02
49	Co-60	1.31E-01	2.68E-02
50	Co-60	1.82E-01	3.48E-02
51	Co-60	2.58E-01	4.30E-02
52	Co-60	8.29E-02	2.22E-02
53	Co-60	2.17E-01	3.47E-02
54	Co-60	1.42E-02	1.34E-02
55	Co-60	7.84E-02	1.98E-02
56	Co-60	1.25E-01	2.77E-02

TABLE B.1. (contd)

Track #	Constituent	Result, pCi/g	Overall Error
1	Zn-65	-1.44E-01	4.62E-02
2	Zn-65	-1.14E-01	4.39E-02
3	Zn-65	-2.79E-01	5.95E-02
4	Zn-65	-3.20E-01	6.50E-02
5	Zn-65	-2.94E-01	6.28E-02
6	Zn-65	-3.72E-01	7.21E-02
7	Zn-65	-4.34E-01	8.61E-02
8	Zn-65	-4.38E-01	7.35E-02
9	Zn-65	-2.08E-01	5.12E-02
10	Zn-65	-1.14E-01	3.98E-02
11	Zn-65	-2.94E-01	5.60E-02
12	Zn-65	-3.29E-01	6.39E-02
13	Zn-65	-3.32E-01	7.27E-02
14	Zn-65	-1.63E-01	4.95E-02
15	Zn-65	-5.83E-01	8.96E-02
16	Zn-65	-3.10E-01	6.24E-02
17	Zn-65	-4.46E-01	7.79E-02
18	Zn-65	-2.00E-01	6.14E-02
19	Zn-65	-1.84E-02	3.20E-02
20	Zn-65	-2.34E-01	6.00E-02
21	Zn-65	-3.78E-01	7.32E-02
22	Zn-65	-3.47E-01	6.77E-02
23	Zn-65	-3.73E-01	8.00E-02
24	Zn-65	-3.05E-01	6.61E-02
25	Zn-65	-3.51E-01	7.00E-02
26	Zn-65	-1.26E-01	4.36E-02
27	Zn-65	-1.64E-01	4.42E-02
28	Zn-65	-3.31E-01	6.86E-02
29	Zn-65	-7.05E-02	3.71E-02
30	Zn-65	-1.69E-01	5.25E-02
31	Zn-65	-2.57E-01	5.77E-02
32	Zn-65	-4.31E-01	6.89E-02
33	Zn-65	-2.15E-01	5.34E-02
34	Zn-65	-4.95E-01	7.77E-02
35	Zn-65	-4.23E-01	7.56E-02
36	Zn-65	-3.46E-01	7.07E-02
37	Zn-65	-5.18E-01	1.07E-01
38	Zn-65	-5.47E-02	4.51E-02
39	Zn-65	-6.90E-02	4.21E-02
40	Zn-65	-3.22E-02	2.91E-02
41	Zn-65	-9.34E-02	3.90E-02
42	Zn-65	-1.19E-01	3.96E-02
43	Zn-65	-2.78E-01	5.55E-02
44	Zn-65	-3.84E-01	7.38E-02
45	Zn-65	-1.50E-01	4.50E-02
46	Zn-65	-5.24E-02	3.31E-02
47	Zn-65	7.50E-03	2.89E-02
48	Zn-65	-3.42E-01	6.33E-02
49	Zn-65	-9.94E-02	3.50E-02
50	Zn-65	-1.60E-01	4.25E-02
51	Zn-65	-3.46E-01	9.21E-02
52	Zn-65	-2.27E-01	4.90E-02
53	Zn-65	-1.69E-01	3.91E-02
54	Zn-65	-1.92E-02	3.45E-02
55	Zn-65	-3.41E-01	6.15E-02
56	Zn-65	-5.52E-02	3.38E-02

TABLE B.1. (contd)

<u>Track #</u>	<u>Constituent</u>	<u>Result, pCi/g</u>	<u>Overall Error</u>
1	ZrNb-95	-5.36E-02	4.36E-02
2	ZrNb-95	-9.29E-02	4.20E-02
3	ZrNb-95	8.18E-02	4.50E-02
4	ZrNb-95	-1.26E-01	4.88E-02
5	ZrNb-95	3.80E-02	4.38E-02
6	ZrNb-95	1.56E-01	5.45E-02
7	ZrNb-95	7.71E-02	6.00E-02
8	ZrNb-95	-3.77E-03	4.98E-02
9	ZrNb-95	-3.07E-02	4.06E-02
10	ZrNb-95	5.20E-02	3.60E-02
11	ZrNb-95	-3.49E-02	4.05E-02
12	ZrNb-95	3.85E-02	4.69E-02
13	ZrNb-95	3.06E-02	4.86E-02
14	ZrNb-95	3.97E-02	3.84E-02
15	ZrNb-95	1.64E-01	5.14E-02
16	ZrNb-95	9.15E-02	4.59E-02
17	ZrNb-95	3.90E-02	4.61E-02
18	ZrNb-95	2.34E-03	4.78E-02
19	ZrNb-95	-9.19E-02	3.76E-02
20	ZrNb-95	-7.84E-02	4.43E-02
21	ZrNb-95	-2.18E-02	4.99E-02
22	ZrNb-95	-1.57E-01	5.48E-02
23	ZrNb-95	1.10E-01	5.64E-02
24	ZrNb-95	3.29E-02	4.75E-02
25	ZrNb-95	-3.95E-02	4.81E-02
26	ZrNb-95	-8.29E-02	3.98E-02
27	ZrNb-95	-1.15E-01	4.20E-02
28	ZrNb-95	7.80E-02	4.79E-02
29	ZrNb-95	-9.96E-02	3.95E-02
30	ZrNb-95	-1.29E-01	5.44E-02
31	ZrNb-95	-1.12E-01	4.70E-02
32	ZrNb-95	-1.33E-02	3.59E-02
33	ZrNb-95	-6.78E-02	4.11E-02
34	ZrNb-95	9.27E-02	4.53E-02
35	ZrNb-95	3.48E-02	4.28E-02
36	ZrNb-95	5.72E-02	4.58E-02
37	ZrNb-95	5.46E-02	6.85E-02
38	ZrNb-95	-3.30E-01	7.43E-02
39	ZrNb-95	-2.52E-01	6.10E-02
40	ZrNb-95	-1.46E-01	3.86E-02
41	ZrNb-95	-1.10E-01	3.79E-02
42	ZrNb-95	-1.24E-01	3.74E-02
43	ZrNb-95	2.58E-02	3.73E-02
44	ZrNb-95	1.18E-01	4.19E-02
45	ZrNb-95	-7.92E-02	3.89E-02
46	ZrNb-95	-1.37E-01	3.84E-02
47	ZrNb-95	8.90E-02	3.45E-02
48	ZrNb-95	-3.19E-02	4.17E-02
49	ZrNb-95	-1.66E-01	4.17E-02
50	ZrNb-95	-7.20E-02	3.42E-02
51	ZrNb-95	1.29E-01	6.06E-02
52	ZrNb-95	1.31E-03	3.47E-02
53	ZrNb-95	-1.26E-01	3.49E-02
54	ZrNb-95	-9.39E-02	3.35E-02
55	ZrNb-95	8.31E-04	3.74E-02
56	ZrNb-95	-9.77E-02	3.84E-02

TABLE B.1. (contd)

<u>Track #</u>	<u>Constituent</u>	<u>Result, pCi/g</u>	<u>Overall Error</u>
1	Ru-106 Da	-2.58E-02	1.20E-01
2	Ru-106 Da	-4.70E-03	1.18E-01
3	Ru-106 Da	-5.50E-02	1.30E-01
4	Ru-106 Da	1.72E-01	1.45E-01
5	Ru-106 Da	-4.51E-02	1.35E-01
6	Ru-106 Da	4.42E-02	1.43E-01
7	Ru-106 Da	-3.03E-02	1.59E-01
8	Ru-106 Da	6.16E-02	1.32E-01
9	Ru-106 Da	-1.16E-02	1.22E-01
10	Ru-106 Da	2.09E-02	1.01E-01
11	Ru-106 Da	-3.41E-02	1.27E-01
12	Ru-106 Da	7.07E-02	1.38E-01
13	Ru-106 Da	1.47E-01	1.43E-01
14	Ru-106 Da	3.59E-04	1.01E-01
15	Ru-106 Da	1.04E-02	1.51E-01
16	Ru-106 Da	-3.87E-02	1.39E-01
17	Ru-106 Da	-2.04E-01	1.46E-01
18	Ru-106 Da	-3.56E-02	1.35E-01
19	Ru-106 Da	-1.67E-02	1.08E-01
20	Ru-106 Da	4.13E-02	1.21E-01
21	Ru-106 Da	3.24E-02	1.43E-01
22	Ru-106 Da	-1.70E-01	1.88E-01
23	Ru-106 Da	6.08E-02	1.66E-01
24	Ru-106 Da	-1.00E-02	1.44E-01
25	Ru-106 Da	-2.12E-02	1.50E-01
26	Ru-106 Da	1.05E-02	1.27E-01
27	Ru-106 Da	5.43E-02	1.19E-01
28	Ru-106 Da	-6.06E-02	1.42E-01
29	Ru-106 Da	4.76E-02	1.08E-01
30	Ru-106 Da	-5.07E-03	1.33E-01
31	Ru-106 Da	-5.70E-02	1.30E-01
32	Ru-106 Da	-4.20E-02	1.11E-01
33	Ru-106 Da	5.94E-02	1.26E-01
34	Ru-106 Da	-1.47E-02	1.40E-01
35	Ru-106 Da	6.11E-02	1.35E-01
36	Ru-106 Da	7.06E-02	1.33E-01
37	Ru-106 Da	9.58E-02	1.88E-01
38	Ru-106 Da	-1.16E-01	1.61E-01
39	Ru-106 Da	1.18E-01	1.41E-01
40	Ru-106 Da	-6.77E-02	9.89E-02
41	Ru-106 Da	1.15E-02	9.85E-02
42	Ru-106 Da	1.10E-01	1.15E-01
43	Ru-106 Da	7.54E-02	1.16E-01
44	Ru-106 Da	-1.76E-02	1.30E-01
45	Ru-106 Da	-7.74E-02	1.14E-01
46	Ru-106 Da	7.09E-03	9.86E-02
47	Ru-106 Da	5.14E-02	1.06E-01
48	Ru-106 Da	-1.34E-01	1.34E-01
49	Ru-106 Da	-9.41E-02	1.13E-01
50	Ru-106 Da	-5.13E-02	1.02E-01
51	Ru-106 Da	1.01E-01	1.73E-01
52	Ru-106 Da	-3.14E-02	1.11E-01
53	Ru-106 Da	-8.60E-03	9.80E-02
54	Ru-106 Da	1.22E-01	9.48E-02
55	Ru-106 Da	3.21E-02	1.19E-01
56	Ru-106 Da	-1.51E-01	1.18E-01

TABLE B.1. (contd)

Track #	Constituent	Result, pCi/g	Overall Error
1	Sb-125	-1.92E-02	3.72E-02
2	Sb-125	-1.41E-02	3.53E-02
3	Sb-125	5.95E-02	4.20E-02
4	Sb-125	-1.06E-02	4.40E-02
5	Sb-125	-5.85E-03	4.26E-02
6	Sb-125	-5.14E-02	4.63E-02
7	Sb-125	1.63E-02	5.33E-02
8	Sb-125	-1.90E-02	4.27E-02
9	Sb-125	-2.27E-02	3.43E-02
10	Sb-125	3.63E-03	2.97E-02
11	Sb-125	3.27E-02	4.04E-02
12	Sb-125	4.44E-04	4.36E-02
13	Sb-125	5.38E-03	4.41E-02
14	Sb-125	2.06E-02	3.24E-02
15	Sb-125	-1.59E-02	4.63E-02
16	Sb-125	3.28E-02	4.28E-02
17	Sb-125	-1.87E-02	4.47E-02
18	Sb-125	-7.45E-04	4.14E-02
19	Sb-125	-1.16E-02	3.19E-02
20	Sb-125	2.31E-03	4.12E-02
21	Sb-125	3.50E-02	4.73E-02
22	Sb-125	-3.61E-02	5.72E-02
23	Sb-125	-2.35E-02	5.43E-02
24	Sb-125	-8.42E-03	4.15E-02
25	Sb-125	2.95E-02	4.26E-02
26	Sb-125	1.47E-02	3.52E-02
27	Sb-125	-2.22E-02	3.57E-02
28	Sb-125	-2.44E-02	4.47E-02
29	Sb-125	-4.21E-02	3.14E-02
30	Sb-125	-5.62E-02	4.15E-02
31	Sb-125	6.84E-04	3.57E-02
32	Sb-125	1.39E-02	3.60E-02
33	Sb-125	3.07E-02	3.97E-02
34	Sb-125	4.01E-03	4.44E-02
35	Sb-125	-1.42E-02	4.29E-02
36	Sb-125	6.09E-03	4.28E-02
37	Sb-125	-4.31E-03	5.78E-02
38	Sb-125	1.67E-02	4.53E-02
39	Sb-125	2.51E-02	3.84E-02
40	Sb-125	7.61E-03	2.69E-02
41	Sb-125	-3.21E-03	3.25E-02
42	Sb-125	-2.78E-02	3.35E-02
43	Sb-125	4.43E-03	3.45E-02
44	Sb-125	9.03E-03	3.94E-02
45	Sb-125	-7.41E-03	3.33E-02
46	Sb-125	-3.47E-03	2.80E-02
47	Sb-125	2.17E-03	2.91E-02
48	Sb-125	-9.88E-03	3.65E-02
49	Sb-125	2.10E-02	3.26E-02
50	Sb-125	-1.57E-02	3.29E-02
51	Sb-125	1.09E-01	5.58E-02
52	Sb-125	-3.94E-03	3.52E-02
53	Sb-125	1.72E-02	3.03E-02
54	Sb-125	-1.22E-02	2.99E-02
55	Sb-125	-1.45E-03	3.33E-02
56	Sb-125	9.51E-03	3.16E-02

TABLE B.1. (contd)

<u>Track #</u>	<u>Constituent</u>	<u>Result, pCi/g</u>	<u>Overall Error</u>
1	Cs-134	-8.35E-02	1.75E-02
2	Cs-134	-8.63E-02	1.75E-02
3	Cs-134	-2.55E-01	3.43E-02
4	Cs-134	1.31E-03	1.46E-02
5	Cs-134	-1.17E-01	2.11E-02
6	Cs-134	-3.28E-01	4.13E-02
7	Cs-134	-3.15E-01	4.11E-02
8	Cs-134	-8.95E-02	1.87E-02
9	Cs-134	-2.24E-01	2.96E-02
10	Cs-134	-6.69E-02	1.45E-02
11	Cs-134	-1.28E-01	2.12E-02
12	Cs-134	-3.28E-01	4.00E-02
13	Cs-134	-3.03E-01	3.86E-02
14	Cs-134	-4.39E-02	1.35E-02
15	Cs-134	-4.59E-01	5.29E-02
16	Cs-134	-1.83E-01	2.68E-02
17	Cs-134	-3.74E-01	4.45E-02
18	Cs-134	-6.17E-02	1.71E-02
19	Cs-134	-8.45E-03	1.09E-02
20	Cs-134	-7.23E-02	1.66E-02
21	Cs-134	-1.02E-01	2.03E-02
22	Cs-134	7.15E-03	1.66E-02
23	Cs-134	-3.43E-01	4.31E-02
24	Cs-134	-3.16E-01	3.98E-02
25	Cs-134	-3.44E-01	4.20E-02
26	Cs-134	3.62E-03	1.25E-02
27	Cs-134	-8.21E-05	1.21E-02
28	Cs-134	-2.76E-01	3.53E-02
29	Cs-134	8.42E-03	1.09E-02
30	Cs-134	2.16E-03	1.35E-02
31	Cs-134	3.52E-03	1.26E-02
32	Cs-134	-7.90E-02	1.59E-02
33	Cs-134	5.96E-03	1.33E-02
34	Cs-134	-1.41E-01	2.29E-02
35	Cs-134	-6.81E-02	1.73E-02
36	Cs-134	-2.89E-01	3.67E-02
37	Cs-134	-3.07E-01	4.11E-02
38	Cs-134	2.26E-03	1.61E-02
39	Cs-134	3.14E-03	1.39E-02
40	Cs-134	-5.31E-03	9.75E-03
41	Cs-134	-1.18E-02	1.16E-02
42	Cs-134	-6.59E-04	1.08E-02
43	Cs-134	-1.31E-01	2.10E-02
44	Cs-134	-2.79E-01	3.53E-02
45	Cs-134	-4.38E-02	1.35E-02
46	Cs-134	-4.18E-03	1.01E-02
47	Cs-134	1.44E-02	1.03E-02
48	Cs-134	-1.50E-01	2.33E-02
49	Cs-134	-9.56E-03	1.10E-02
50	Cs-134	-3.58E-03	1.12E-02
51	Cs-134	-2.79E-01	3.86E-02
52	Cs-134	-4.66E-02	1.38E-02
53	Cs-134	-8.03E-03	9.95E-03
54	Cs-134	1.60E-03	9.64E-03
55	Cs-134	-1.19E-01	2.04E-02
56	Cs-134	3.78E-03	1.08E-02

TABLE B.1. (contd)

<u>Track #</u>	<u>Constituent</u>	<u>Result, pCi/g</u>	<u>Overall Error</u>
1	Cs-137 Da	5.49E-01	6.24E-02
2	Cs-137 Da	5.72E-01	6.48E-02
3	Cs-137 Da	6.20E-01	7.10E-02
4	Cs-137 Da	1.64E+00	1.73E-01
5	Cs-137 Da	6.47E-01	9.21E-02
6	Cs-137 Da	7.02E-01	7.85E-02
7	Cs-137 Da	1.23E+00	1.32E-01
8	Cs-137 Da	8.57E-01	9.32E-02
9	Cs-137 Da	2.12E-01	3.04E-02
10	Cs-137 Da	2.74E-02	1.35E-02
11	Cs-137 Da	3.12E-01	3.95E-02
12	Cs-137 Da	4.36E-01	5.30E-02
13	Cs-137 Da	3.14E-01	4.19E-02
14	Cs-137 Da	2.67E-01	3.41E-02
15	Cs-137 Da	7.48E-02	2.36E-02
16	Cs-137 Da	1.46E-01	2.56E-02
17	Cs-137 Da	2.82E-01	3.84E-02
18	Cs-137 Da	6.13E-01	6.98E-02
19	Cs-137 Da	4.84E-01	5.77E-02
20	Cs-137 Da	7.55E-01	8.34E-02
21	Cs-137 Da	1.23E+00	1.30E-01
22	Cs-137 Da	5.97E+00	6.05E-01
23	Cs-137 Da	2.13E+00	2.20E-01
24	Cs-137 Da	2.49E-03	1.79E-02
25	Cs-137 Da	5.84E-01	6.58E-02
26	Cs-137 Da	7.08E-01	8.06E-02
27	Cs-137 Da	8.15E-01	9.11E-02
28	Cs-137 Da	6.02E-01	6.82E-02
29	Cs-137 Da	4.80E-01	5.83E-02
30	Cs-137 Da	4.85E-01	6.35E-02
31	Cs-137 Da	6.08E-01	7.19E-02
32	Cs-137 Da	9.51E-01	1.01E-01
33	Cs-137 Da	1.26E+00	1.36E-01
34	Cs-137 Da	9.10E-01	9.85E-02
35	Cs-137 Da	1.03E+00	1.11E-01
36	Cs-137 Da	3.17E-01	4.05E-02
37	Cs-137 Da	1.16E+00	1.25E-01
38	Cs-137 Da	2.34E-01	4.13E-02
39	Cs-137 Da	4.60E-01	6.24E-02
40	Cs-137 Da	1.43E-01	2.54E-02
41	Cs-137 Da	7.66E-01	8.48E-02
42	Cs-137 Da	7.36E-01	8.29E-02
43	Cs-137 Da	5.56E-01	6.28E-02
44	Cs-137 Da	5.52E-01	6.36E-02
45	Cs-137 Da	3.20E-01	3.93E-02
46	Cs-137 Da	1.19E-01	2.60E-02
47	Cs-137 Da	2.96E-01	4.03E-02
48	Cs-137 Da	5.72E-01	6.46E-02
49	Cs-137 Da	7.39E-01	8.31E-02
50	Cs-137 Da	7.23E-01	8.03E-02
51	Cs-137 Da	1.31E+00	1.39E-01
52	Cs-137 Da	5.70E-01	6.38E-02
53	Cs-137 Da	7.61E-01	8.35E-02
54	Cs-137 Da	8.60E-02	2.18E-02
55	Cs-137 Da	4.39E-01	5.24E-02
56	Cs-137 Da	5.61E-01	6.70E-02

TABLE B.1. (contd)

<u>Track #</u>	<u>Constituent</u>	<u>Result, pCi/g</u>	<u>Overall Error</u>
1	CePr-144	-1.51E-01	1.74E-01
2	CePr-144	7.14E-02	1.62E-01
3	CePr-144	-8.13E-03	1.79E-01
4	CePr-144	-9.92E-02	1.74E-01
5	CePr-144	-8.18E-02	1.71E-01
6	CePr-144	-9.54E-02	1.95E-01
7	CePr-144	-1.20E-01	2.09E-01
8	CePr-144	6.94E-02	1.74E-01
9	CePr-144	1.41E-03	1.64E-01
10	CePr-144	8.97E-03	1.38E-01
11	CePr-144	-1.71E-01	1.82E-01
12	CePr-144	-4.25E-02	2.03E-01
13	CePr-144	-1.22E-01	1.92E-01
14	CePr-144	-9.95E-02	1.46E-01
15	CePr-144	7.45E-04	2.15E-01
16	CePr-144	-6.49E-02	1.97E-01
17	CePr-144	-1.43E-01	2.03E-01
18	CePr-144	2.72E-02	1.77E-01
19	CePr-144	4.40E-02	1.43E-01
20	CePr-144	1.76E-03	1.68E-01
21	CePr-144	-9.71E-02	1.95E-01
22	CePr-144	-5.18E-03	2.02E-01
23	CePr-144	-3.05E-01	2.22E-01
24	CePr-144	-5.97E-01	2.28E-01
25	CePr-144	-6.61E-03	2.04E-01
26	CePr-144	-1.46E-01	1.57E-01
27	CePr-144	-1.20E-02	1.54E-01
28	CePr-144	-1.95E-01	1.88E-01
29	CePr-144	9.09E-02	1.36E-01
30	CePr-144	1.18E-02	1.73E-01
31	CePr-144	1.14E-01	1.61E-01
32	CePr-144	-7.71E-02	1.50E-01
33	CePr-144	-1.49E-01	1.62E-01
34	CePr-144	-5.59E-02	1.80E-01
35	CePr-144	1.16E-01	1.70E-01
36	CePr-144	-1.38E-01	1.88E-01
37	CePr-144	-8.00E-02	2.20E-01
38	CePr-144	1.81E-01	2.19E-01
39	CePr-144	4.94E-02	1.78E-01
40	CePr-144	3.79E-02	1.30E-01
41	CePr-144	-2.43E-02	1.37E-01
42	CePr-144	-3.01E-02	1.36E-01
43	CePr-144	6.62E-02	1.58E-01
44	CePr-144	-2.08E-01	1.98E-01
45	CePr-144	-5.74E-02	1.57E-01
46	CePr-144	-5.58E-02	1.39E-01
47	CePr-144	2.95E-02	1.24E-01
48	CePr-144	-4.45E-03	1.78E-01
49	CePr-144	-6.61E-02	1.43E-01
50	CePr-144	-1.95E-01	1.40E-01
51	CePr-144	-4.24E-01	2.44E-01
52	CePr-144	-3.44E-02	1.49E-01
53	CePr-144	1.14E-02	1.26E-01
54	CePr-144	-2.54E-02	1.33E-01
55	CePr-144	5.41E-02	1.59E-01
56	CePr-144	6.30E-02	1.48E-01

TABLE B.1. (contd)

<u>Track #</u>	<u>Constituent</u>	<u>Result, pCi/g</u>	<u>Overall Error</u>
1	Eu-152	1.43E-01	7.53E-02
2	Eu-152	9.10E-02	7.31E-02
3	Eu-152	9.84E-02	8.12E-02
4	Eu-152	1.89E+00	2.55E-01
5	Eu-152	5.76E-01	1.23E-01
6	Eu-152	5.15E-01	1.17E-01
7	Eu-152	8.88E-01	1.63E-01
8	Eu-152	7.94E-01	1.38E-01
9	Eu-152	2.64E-01	8.53E-02
10	Eu-152	8.93E-02	6.40E-02
11	Eu-152	4.35E-01	9.96E-02
12	Eu-152	2.95E-01	9.48E-02
13	Eu-152	3.33E-01	9.87E-02
14	Eu-152	3.43E-01	8.50E-02
15	Eu-152	2.06E-01	9.21E-02
16	Eu-152	1.81E-01	9.04E-02
17	Eu-152	2.53E-01	9.42E-02
18	Eu-152	8.09E-01	1.35E-01
19	Eu-152	4.16E-01	1.15E-01
20	Eu-152	5.93E-01	1.17E-01
21	Eu-152	1.13E+00	1.77E-01
22	Eu-152	2.31E+00	3.09E-01
23	Eu-152	1.08E+00	1.80E-01
24	Eu-152	1.29E-01	6.09E-02
25	Eu-152	8.08E-01	1.38E-01
26	Eu-152	9.21E-01	1.77E-01
27	Eu-152	8.68E-01	1.78E-01
28	Eu-152	5.45E-01	1.21E-01
29	Eu-152	4.17E-01	1.01E-01
30	Eu-152	6.79E-01	1.61E-01
31	Eu-152	9.27E-01	1.78E-01
32	Eu-152	1.19E+00	1.64E-01
33	Eu-152	1.58E+00	2.32E-01
34	Eu-152	1.05E+00	1.57E-01
35	Eu-152	1.23E+00	1.76E-01
36	Eu-152	2.34E-01	9.72E-02
37	Eu-152	2.41E+00	3.16E-01
38	Eu-152	3.31E-01	9.79E-02
39	Eu-152	3.68E-01	9.98E-02
40	Eu-152	1.99E-01	6.19E-02
41	Eu-152	6.40E-01	1.41E-01
42	Eu-152	6.08E-01	1.33E-01
43	Eu-152	3.40E-01	8.68E-02
44	Eu-152	5.33E-01	1.04E-01
45	Eu-152	1.78E-01	7.93E-02
46	Eu-152	2.73E-01	6.38E-02
47	Eu-152	2.21E-01	6.34E-02
48	Eu-152	6.80E-01	1.19E-01
49	Eu-152	6.40E-01	1.27E-01
50	Eu-152	8.32E-01	1.59E-01
51	Eu-152	1.46E+00	2.08E-01
52	Eu-152	3.60E-01	8.57E-02
53	Eu-152	5.39E-01	1.13E-01
54	Eu-152	1.22E-01	6.56E-02
55	Eu-152	4.49E-01	1.12E-01
56	Eu-152	4.62E-01	1.14E-01

TABLE B.1. (contd)

<u>Track #</u>	<u>Constituent</u>	<u>Result, pCi/g</u>	<u>Overall Error</u>
1	Eu-154	-1.12E-02	5.15E-02
2	Eu-154	3.21E-02	4.53E-02
3	Eu-154	-1.11E-02	5.38E-02
4	Eu-154	2.32E-01	6.69E-02
5	Eu-154	5.69E-02	5.72E-02
6	Eu-154	6.96E-02	6.29E-02
7	Eu-154	6.64E-02	6.73E-02
8	Eu-154	9.96E-02	5.31E-02
9	Eu-154	1.14E-02	4.98E-02
10	Eu-154	-3.95E-02	4.78E-02
11	Eu-154	-2.11E-02	5.24E-02
12	Eu-154	4.33E-02	5.48E-02
13	Eu-154	1.27E-02	5.92E-02
14	Eu-154	4.59E-02	4.45E-02
15	Eu-154	1.24E-01	5.97E-02
16	Eu-154	-2.11E-02	5.54E-02
17	Eu-154	-7.48E-03	5.76E-02
18	Eu-154	8.76E-02	5.29E-02
19	Eu-154	6.74E-02	3.82E-02
20	Eu-154	6.42E-02	5.41E-02
21	Eu-154	1.40E-01	6.17E-02
22	Eu-154	1.87E-01	6.39E-02
23	Eu-154	1.41E-01	6.76E-02
24	Eu-154	-2.59E-03	5.97E-02
25	Eu-154	1.41E-01	5.80E-02
26	Eu-154	2.93E-02	5.21E-02
27	Eu-154	1.34E-01	5.16E-02
28	Eu-154	-1.21E-02	5.88E-02
29	Eu-154	5.12E-02	4.29E-02
30	Eu-154	6.35E-02	5.58E-02
31	Eu-154	1.36E-01	5.63E-02
32	Eu-154	1.53E-01	5.09E-02
33	Eu-154	1.87E-01	5.73E-02
34	Eu-154	1.26E-01	5.75E-02
35	Eu-154	1.10E-01	6.04E-02
36	Eu-154	-1.83E-02	5.69E-02
37	Eu-154	2.26E-01	7.83E-02
38	Eu-154	2.34E-02	5.73E-02
39	Eu-154	-1.51E-02	5.42E-02
40	Eu-154	-1.02E-02	4.14E-02
41	Eu-154	5.97E-02	4.65E-02
42	Eu-154	1.20E-01	4.44E-02
43	Eu-154	6.73E-02	5.24E-02
44	Eu-154	3.91E-02	5.84E-02
45	Eu-154	1.85E-02	4.72E-02
46	Eu-154	-1.27E-02	4.33E-02
47	Eu-154	1.70E-02	3.91E-02
48	Eu-154	9.35E-02	5.38E-02
49	Eu-154	6.42E-02	3.90E-02
50	Eu-154	4.70E-02	4.80E-02
51	Eu-154	1.73E-01	7.41E-02
52	Eu-154	3.62E-02	4.71E-02
53	Eu-154	1.09E-01	4.18E-02
54	Eu-154	-4.37E-02	4.69E-02
55	Eu-154	4.92E-02	5.42E-02
56	Eu-154	1.64E-02	4.73E-02

TABLE B.I. (contd)

<u>Track #</u>	<u>Constituent</u>	<u>Result, pCi/g</u>	<u>Overall Error</u>
1	Mn-54	2.63E-02	1.22E-02
11	Mn-54	1.86E-02	1.31E-02
16	Mn-54	3.46E-02	1.52E-02
21	Mn-54	1.93E-02	1.39E-02
55	Mn-54	1.94E-02	1.18E-02

TABLE B.1. (contd)

<u>Track #</u>	<u>Constituent</u>	<u>Result, pCi/g</u>	<u>Overall Error</u>
1	Eu-155	5.08E-02	5.32E-02
2	Eu-155	1.24E-02	4.99E-02
3	Eu-155	8.88E-02	5.49E-02
4	Eu-155	4.94E-02	4.95E-02
5	Eu-155	6.22E-02	5.59E-02
6	Eu-155	3.17E-02	5.81E-02
7	Eu-155	4.89E-02	6.25E-02
8	Eu-155	7.29E-02	5.61E-02
9	Eu-155	7.79E-02	5.08E-02
10	Eu-155	4.91E-02	4.23E-02
11	Eu-155	1.04E-01	5.97E-02
12	Eu-155	1.07E-01	6.29E-02
13	Eu-155	1.04E-01	6.02E-02
14	Eu-155	2.50E-02	4.61E-02
15	Eu-155	1.15E-01	6.65E-02
16	Eu-155	1.43E-01	6.37E-02
17	Eu-155	9.87E-02	6.12E-02
18	Eu-155	6.24E-02	5.61E-02
19	Eu-155	8.03E-02	4.23E-02
20	Eu-155	7.64E-02	5.32E-02
21	Eu-155	8.70E-02	6.21E-02
22	Eu-155	6.03E-02	6.08E-02
23	Eu-155	2.61E-02	6.80E-02
24	Eu-155	6.03E-02	5.76E-02
25	Eu-155	9.78E-02	6.29E-02
26	Eu-155	8.07E-02	4.27E-02
27	Eu-155	8.45E-02	4.18E-02
28	Eu-155	1.13E-01	5.74E-02
29	Eu-155	5.63E-02	3.75E-02
30	Eu-155	1.07E-01	5.18E-02
31	Eu-155	8.86E-02	4.92E-02
32	Eu-155	1.70E-02	4.97E-02
33	Eu-155	8.07E-02	4.53E-02
34	Eu-155	4.57E-02	5.91E-02
35	Eu-155	2.80E-02	5.78E-02
36	Eu-155	1.34E-01	5.76E-02
37	Eu-155	4.83E-02	7.24E-02
38	Eu-155	1.86E-01	6.43E-02
39	Eu-155	7.51E-02	5.14E-02
40	Eu-155	8.86E-02	3.85E-02
41	Eu-155	4.99E-02	3.87E-02
42	Eu-155	9.09E-02	3.96E-02
43	Eu-155	1.74E-02	5.05E-02
44	Eu-155	1.73E-02	6.14E-02
45	Eu-155	6.62E-02	5.09E-02
46	Eu-155	6.54E-02	4.07E-02
47	Eu-155	6.42E-02	3.58E-02
48	Eu-155	9.29E-02	5.86E-02
49	Eu-155	1.07E-01	3.84E-02
50	Eu-155	6.12E-02	4.15E-02
51	Eu-155	8.89E-02	7.74E-02
52	Eu-155	6.01E-02	4.77E-02
53	Eu-155	6.71E-02	3.24E-02
54	Eu-155	6.58E-02	3.81E-02
55	Eu-155	3.40E-03	5.16E-02
56	Eu-155	8.97E-02	4.46E-02

TABLE B.2. Strontium-90, Plutonium, and Uranium

<u>Track #</u>	<u>Constituent</u>	<u>Result, pCi/g</u>	<u>Overall Error</u>
1	Sr-90	1.98E-02	5.68E-03
2	Sr-90	2.48E-02	6.64E-03
3	Sr-90	1.96E-02	5.62E-03
4	Sr 90	2.90E-02	8.73E-03
5	Sr 90	1.74E-02	6.15E-03
6	Sr 90	4.16E-02	1.21E-02
7	Sr 90	2.64E-02	7.20E-03
8	Sr 90	3.69E-02	1.01E-02
9	Sr 90	1.61E-02	5.28E-03
10	Sr 90	6.90E-03	3.72E-03
11	Sr 90	2.82E-02	7.68E-03
12	Sr 90	7.16E-02	1.51E-02
13	Sr 90	1.67E-02	5.66E-03
14	Sr 90	1.68E-02	5.62E-03
15	Sr 90	6.71E-03	3.21E-03
16	Sr 90	1.64E-02	6.30E-03
17	Sr 90	4.08E-02	1.14E-02
18	Sr 90	2.14E-02	6.57E-03
19	Sr 90	2.60E-02	7.03E-03
20	Sr 90	8.86E-03	3.89E-03
21	Sr 90	1.16E-02	4.80E-03
22	Sr 90	2.35E-02	7.45E-03
23	Sr 90	2.80E-02	7.89E-03
24	Sr 90	2.00E-02	5.61E-03
25	Sr 90	4.05E-02	1.19E-02
26	Sr 90	2.20E-02	6.69E-03
27	Sr 90	8.91E-02	1.94E-02
28	Sr 90	4.11E-02	9.88E-03
29	Sr 90	1.31E-02	4.74E-03
30	Sr 90	1.70E-02	5.41E-03
31	Sr 90	4.05E-02	1.02E-02
32	Sr 90	2.10E-02	9.86E-03
33	Sr 90	2.10E-02	6.25E-03
34	Sr 90	2.34E-02	6.76E-03
35	Sr 90	3.41E-02	7.81E-03
36	Sr 90	2.46E-02	6.92E-03
37	Sr 90	4.07E-02	1.02E-02
38	Sr 90	1.34E-02	4.67E-03
39	Sr 90	2.50E-02	6.99E-03
40	Sr 90	1.08E-02	6.05E-03
41	Sr 90	2.41E-02	6.79E-03
42	Sr 90	2.83E-02	7.58E-03
43	Sr 90	4.12E-02	9.88E-03
44	Sr 90	1.76E-02	6.39E-03
45	Sr 90	1.94E-03	3.00E-03
46	Sr 90	1.03E-02	4.14E-03
47	Sr 90	1.88E-02	5.56E-03
48	Sr 90	4.31E-02	1.02E-02
49	Sr 90	3.19E-02	9.14E-03
50	Sr 90	2.61E-02	7.19E-03
51	Sr 90	1.26E-02	4.70E-03
52	Sr 90	4.61E-02	1.12E-02
53	Sr 90	2.46E-02	6.36E-03
54	Sr 90	7.39E-03	3.29E-03
55	Sr 90	3.36E-02	8.52E-03
56	Sr 90	4.06E-02	1.02E-02

TABLE B.2. (contd)

<u>Track #</u>	<u>Constituent</u>	<u>Result, pCi/g</u>	<u>Overall Error</u>
1	U 234	1.25E+00	1.46E-01
2	U 234	9.22E-01	1.10E-01
3	U 234	9.17E-01	1.08E-01
4	U 234	1.68E+00	1.88E-01
5	U 234	1.16E+00	1.31E-01
6	U 234	1.03E+00	1.22E-01
7	U 234	9.26E-01	1.11E-01
8	U 234	1.01E+00	1.18E-01
9	U 234	8.87E-01	1.30E-01
10	U 234	2.17E+00	2.32E-01
11	U 234	2.06E+00	2.13E-01
12	U 234	1.94E+00	2.14E-01
13	U 234	2.15E+00	2.21E-01
14	U 234	1.03E+00	1.20E-01
15	U 234	1.95E+00	2.08E-01
16	U 234	1.81E+00	1.94E-01
17	U 234	1.84E+00	1.92E-01
18	U 234	1.17E+00	1.32E-01
19	U 234	1.16E+00	1.34E-01
20	U 234	9.61E-01	1.20E-01
21	U 234	1.36E+00	1.62E-01
22	U 234	9.58E-01	1.28E-01
23	U 234	2.19E+00	2.52E-01
24	U 234	9.71E-01	1.13E-01
25	U 234	1.04E+00	1.19E-01
26	U 234	1.55E+00	2.23E-01
27	U 234	1.04E+00	1.19E-01
28	U 234	1.06E+00	1.19E-01
29	U 234	9.43E-01	1.18E-01
30	U 234	1.25E+00	1.46E-01
31	U 234	1.09E+00	1.29E-01
32	U 234	7.59E-01	1.25E-01
33	U 234	9.92E-01	1.16E-01
34	U 234	1.49E+00	1.59E-01
35	U 234	1.05E+00	1.20E-01
36	U 234	1.41E+00	1.50E-01
37	U 234	1.02E+00	1.23E-01
38	U 234	2.17E+00	2.40E-01
39	U 234	1.21E+00	1.40E-01
40	U 234	1.71E+00	1.89E-01
41	U 234	9.64E-01	1.35E-01
42	U 234	1.24E+00	1.35E-01
43	U 234	9.03E-01	1.14E-01
44	U 234	1.63E+00	1.82E-01
45	U 234	1.64E+00	1.80E-01
46	U 234	1.91E+00	2.11E-01
47	U 234	1.46E+00	1.69E-01
48	U 234	1.36E+00	1.52E-01
49	U 234	1.62E+00	1.81E-01
50	U 234	1.15E+00	1.40E-01
51	U 234	1.26E+00	1.44E-01
52	U 234	1.09E+00	1.24E-01
53	U 234	9.02E-01	1.05E-01
54	U 234	1.11E+00	1.48E-01
55	U 234	8.87E-01	1.10E-01
56	U 234	1.44E+00	1.66E-01

TABLE B.2. (contd)

<u>Track #</u>	<u>Constituent</u>	<u>Result, pCi/g</u>	<u>Overall Error</u>
1	U 235	4.69E-02	1.71E-02
2	U 235	3.94E-02	1.49E-02
3	U 235	2.75E-02	1.21E-02
4	U 235	4.64E-02	1.71E-02
5	U 235	3.32E-02	1.32E-02
6	U 235	2.68E-02	1.23E-02
7	U 235	2.75E-02	1.25E-02
8	U 235	4.28E-02	1.53E-02
9	U 235	3.30E-02	1.86E-02
10	U 235	1.00E-01	2.50E-02
11	U 235	8.53E-02	2.07E-02
12	U 235	5.81E-02	1.93E-02
13	U 235	7.60E-02	1.94E-02
14	U 235	1.94E-02	1.05E-02
15	U 235	5.14E-02	1.71E-02
16	U 235	5.50E-02	1.71E-02
17	U 235	6.27E-02	1.76E-02
18	U 235	3.75E-02	1.40E-02
19	U 235	3.12E-02	1.33E-02
20	U 235	3.76E-02	1.58E-02
21	U 235	5.06E-02	1.86E-02
22	U 235	3.61E-02	1.72E-02
23	U 235	6.97E-02	2.41E-02
24	U 235	3.06E-02	1.27E-02
25	U 235	2.87E-02	1.20E-02
26	U 235	2.63E-02	1.93E-02
27	U 235	2.40E-02	1.13E-02
28	U 235	3.00E-02	1.23E-02
29	U 235	3.19E-02	1.44E-02
30	U 235	5.24E-02	1.81E-02
31	U 235	3.66E-02	1.49E-02
32	U 235	2.11E-02	1.96E-02
33	U 235	3.64E-02	1.45E-02
34	U 235	5.42E-02	1.60E-02
35	U 235	4.26E-02	1.47E-02
36	U 235	4.15E-02	1.35E-02
37	U 235	3.20E-02	1.41E-02
38	U 235	7.98E-02	2.35E-02
39	U 235	4.32E-02	1.60E-02
40	U 235	3.50E-02	1.43E-02
41	U 235	2.85E-02	1.76E-02
42	U 235	3.87E-02	1.37E-02
43	U 235	2.91E-02	1.45E-02
44	U 235	6.56E-02	2.04E-02
45	U 235	5.67E-02	1.83E-02
46	U 235	3.13E-02	1.41E-02
47	U 235	5.52E-02	1.94E-02
48	U 235	6.57E-02	1.90E-02
49	U 235	5.89E-02	1.90E-02
50	U 235	4.76E-02	1.80E-02
51	U 235	4.19E-02	1.55E-02
52	U 235	5.48E-02	1.67E-02
53	U 235	4.35E-02	1.45E-02
54	U 235	2.88E-02	1.58E-02
55	U 235	2.55E-02	1.29E-02
56	U 235	4.18E-02	1.66E-02

TABLE B.2. (contd)

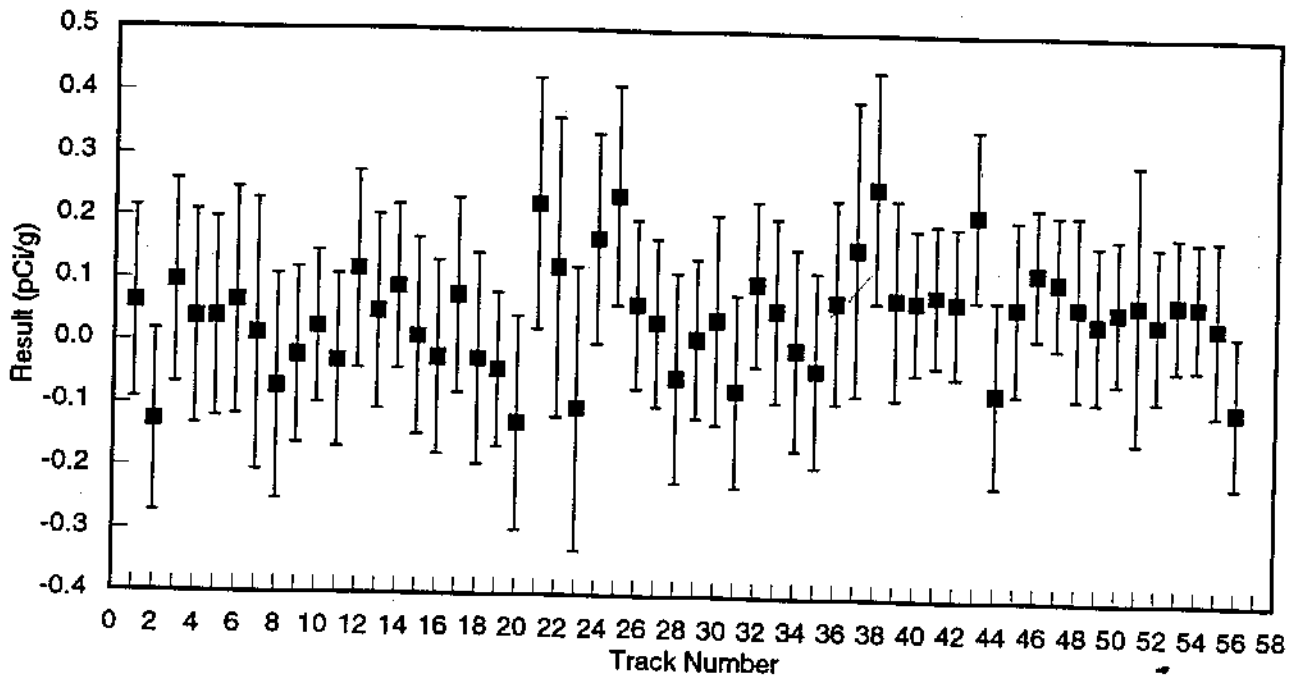
<u>Track #</u>	<u>Constituent</u>	<u>Result, pCi/g</u>	<u>Overall Error</u>
1	Pu 238	2.70E-04	2.19E-04
2	Pu 238	3.24E-04	3.04E-04
3	Pu 238	1.93E-04	2.11E-04
4	Pu 238	8.83E-04	3.96E-04
5	Pu 238	1.94E-04	2.12E-04
6	Pu 238	4.21E-04	2.56E-04
7	Pu 238	4.09E-04	2.73E-04
8	Pu 238	3.14E-04	2.81E-04
9	Pu 238	1.86E-04	2.30E-04
10	Pu 238	-1.60E-05	1.89E-04
11	Pu 238	2.15E-04	1.89E-04
12	Pu 238	1.81E-04	2.81E-04
13	Pu 238	1.07E-03	5.39E-04
14	Pu 238	5.84E-05	1.07E-04
15	Pu 238	1.69E-04	1.87E-04
16	Pu 238	4.57E-04	3.57E-04
17	Pu 238	2.27E-04	2.77E-04
18	Pu 238	5.48E-04	3.08E-04
19	Pu 238	6.53E-04	3.65E-04
20	Pu 238	3.37E-04	2.70E-04
21	Pu 238	6.74E-04	3.65E-04
22	Pu 238	1.01E-03	4.33E-04
23	Pu 238	7.18E-04	3.86E-04
24	Pu 238	5.52E-04	5.75E-04
25	Pu 238	7.29E-04	3.81E-04
26	Pu 238	7.27E-04	4.07E-04
27	Pu 238	1.15E-03	5.50E-04
28	Pu 238	2.23E-04	2.16E-04
29	Pu 238	1.84E-04	2.47E-04
30	Pu 238	3.84E-04	3.49E-04
31	Pu 238	8.18E-05	1.96E-04
32	Pu 238	1.82E-04	2.00E-04
33	Pu 238	9.09E-04	4.89E-04
34	Pu 238	3.64E-04	3.11E-04
35	Pu 238	8.40E-04	4.15E-04
36	Pu 238	8.75E-05	1.48E-04
37	Pu 238	3.27E-04	2.62E-04
38	Pu 238	1.31E-04	2.09E-04
39	Pu 238	5.15E-04	3.53E-04
40	Pu 238	7.66E-05	1.28E-04
41	Pu 238	3.36E-04	2.91E-04
42	Pu 238	5.35E-04	2.73E-04
43	Pu 238	2.16E-04	2.10E-04
44	Pu 238	4.21E-05	1.17E-04
45	Pu 238	2.62E-04	2.13E-04
46	Pu 238	1.30E-04	2.01E-04
47	Pu 238	1.56E-04	1.63E-04
48	Pu 238	1.11E-04	1.90E-04
49	Pu 238	1.01E-04	1.76E-04
50	Pu 238	1.37E-04	1.89E-04
51	Pu 238	1.15E-03	4.19E-04
52	Pu 238	2.53E-04	3.13E-04
53	Pu 238	4.76E-04	3.77E-04
54	Pu 238	4.98E-05	1.22E-04
55	Pu 238	3.23E-04	2.59E-04
58	Pu 238	4.92E-04	3.27E-04

TABLE B.2. (contd)

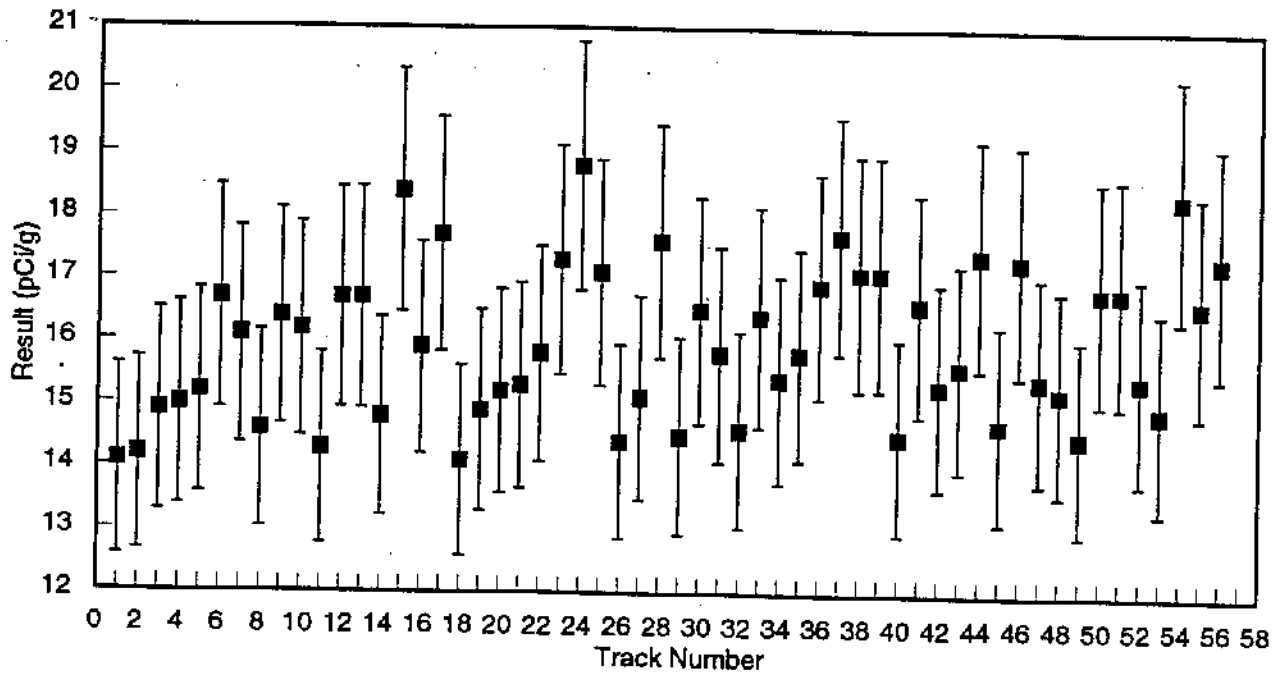
<u>Track #</u>	<u>Constituent</u>	<u>Result, pCi/g</u>	<u>Overall Error</u>
1	U 238	1.18E+00	1.39E-01
2	U 238	8.92E-01	1.07E-01
3	U 238	8.30E-01	9.94E-02
4	U 238	1.43E+00	1.64E-01
5	U 238	1.08E+00	1.23E-01
6	U 238	9.17E-01	1.10E-01
7	U 238	8.65E-01	1.05E-01
8	U 238	1.03E+00	1.19E-01
9	U 238	7.96E-01	1.19E-01
10	U 238	2.03E+00	2.19E-01
11	U 238	1.95E+00	2.03E-01
12	U 238	1.72E+00	1.93E-01
13	U 238	2.02E+00	2.08E-01
14	U 238	9.62E-01	1.12E-01
15	U 238	1.86E+00	1.99E-01
16	U 238	1.79E+00	1.91E-01
17	U 238	1.75E+00	1.83E-01
18	U 238	1.11E+00	1.26E-01
19	U 238	1.05E+00	1.22E-01
20	U 238	9.23E-01	1.16E-01
21	U 238	1.32E+00	1.57E-01
22	U 238	8.53E-01	1.17E-01
23	U 238	1.99E+00	2.31E-01
24	U 238	8.45E-01	1.01E-01
25	U 238	9.42E-01	1.09E-01
26	U 238	1.35E+00	1.99E-01
27	U 238	1.06E+00	1.21E-01
28	U 238	9.48E-01	1.08E-01
29	U 238	9.13E-01	1.14E-01
30	U 238	1.17E+00	1.38E-01
31	U 238	1.03E+00	1.23E-01
32	U 238	6.80E-01	1.14E-01
33	U 238	8.67E-01	1.04E-01
34	U 238	1.42E+00	1.52E-01
35	U 238	9.48E-01	1.10E-01
36	U 238	1.37E+00	1.45E-01
37	U 238	9.07E-01	1.12E-01
38	U 238	1.97E+00	2.20E-01
39	U 238	1.27E+00	1.45E-01
40	U 238	1.74E+00	1.91E-01
41	U 238	9.92E-01	1.37E-01
42	U 238	1.16E+00	1.27E-01
43	U 238	8.98E-01	1.13E-01
44	U 238	1.68E+00	1.86E-01
45	U 238	1.67E+00	1.83E-01
46	U 238	1.76E+00	1.96E-01
47	U 238	1.44E+00	1.67E-01
48	U 238	1.47E+00	1.62E-01
49	U 238	1.61E+00	1.80E-01
50	U 238	1.15E+00	1.39E-01
51	U 238	1.31E+00	1.48E-01
52	U 238	9.59E-01	1.11E-01
53	U 238	8.38E-01	9.81E-02
54	U 238	1.05E+00	1.39E-01
55	U 238	8.48E-01	1.05E-01
56	U 238	1.34E+00	1.55E-01

TABLE B.2. (contd)

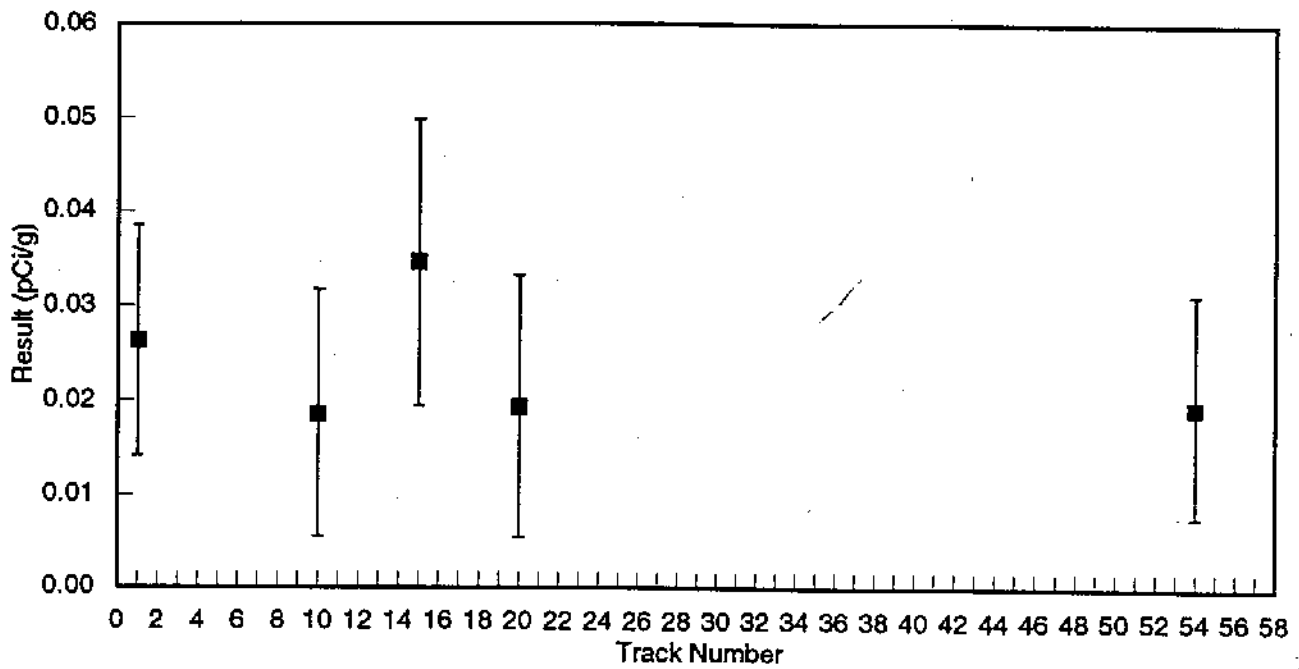
<u>Track #</u>	<u>Constituent</u>	<u>Result, pCi/g</u>	<u>Overall Error</u>
1	Pu 239,240	9.82E-03	1.66E-03
2	Pu 239,240	7.25E-03	1.59E-03
3	Pu 239,240	7.33E-03	1.50E-03
4	Pu 239,240	2.11E-02	2.95E-03
5	Pu 239,240	5.32E-03	1.22E-03
6	Pu 239,240	1.19E-02	1.80E-03
7	Pu 239,240	1.73E-02	2.55E-03
8	Pu 239,240	1.27E-02	2.14E-03
9	Pu 239,240	1.91E-03	7.02E-04
10	Pu 239,240	5.38E-04	4.12E-04
11	Pu 239,240	4.98E-03	9.99E-04
12	Pu 239,240	7.38E-03	1.99E-03
13	Pu 239,240	3.30E-03	9.73E-04
14	Pu 239,240	2.58E-03	6.87E-04
15	Pu 239,240	2.21E-03	6.97E-04
16	Pu 239,240	3.06E-03	9.34E-04
17	Pu 239,240	5.21E-03	1.35E-03
18	Pu 239,240	6.13E-03	1.20E-03
19	Pu 239,240	8.73E-03	1.60E-03
20	Pu 239,240	7.70E-03	1.53E-03
21	Pu 239,240	1.40E-02	2.21E-03
22	Pu 239,240	2.02E-02	2.83E-03
23	Pu 239,240	1.19E-02	1.99E-03
24	Pu 239,240	5.43E-04	5.74E-04
25	Pu 239,240	8.12E-03	1.51E-03
26	Pu 239,240	5.01E-03	1.19E-03
27	Pu 239,240	1.00E-02	1.95E-03
28	Pu 239,240	8.72E-03	1.63E-03
29	Pu 239,240	3.58E-03	9.43E-04
30	Pu 239,240	3.52E-03	9.44E-04
31	Pu 239,240	5.01E-03	1.16E-03
32	Pu 239,240	7.75E-03	1.52E-03
33	Pu 239,240	1.24E-02	2.26E-03
34	Pu 239,240	9.49E-03	1.86E-03
35	Pu 239,240	9.81E-03	1.74E-03
36	Pu 239,240	2.67E-03	8.07E-04
37	Pu 239,240	1.17E-02	2.01E-03
38	Pu 239,240	2.18E-03	8.52E-04
39	Pu 239,240	4.99E-03	1.15E-03
40	Pu 239,240	1.48E-03	4.95E-04
41	Pu 239,240	7.87E-03	1.65E-03
42	Pu 239,240	5.90E-03	1.07E-03
43	Pu 239,240	9.31E-03	1.68E-03
44	Pu 239,240	7.06E-03	1.54E-03
45	Pu 239,240	1.59E-03	5.38E-04
46	Pu 239,240	9.62E-04	4.92E-04
47	Pu 239,240	3.15E-03	6.83E-04
48	Pu 239,240	8.99E-03	1.59E-03
49	Pu 239,240	6.35E-03	1.23E-03
50	Pu 239,240	5.49E-03	1.09E-03
51	Pu 239,240	7.19E-03	1.23E-03
52	Pu 239,240	5.86E-03	1.66E-03
53	Pu 239,240	6.58E-03	1.59E-03
54	Pu 239,240	8.63E-04	3.99E-04
55	Pu 239,240	5.30E-03	1.18E-03
56	Pu 239,240	1.81E-02	2.57E-03



**FIGURE B.1.** Beryllium-7 (<sup>7</sup>Be) Concentrations in Soils S9306049.21

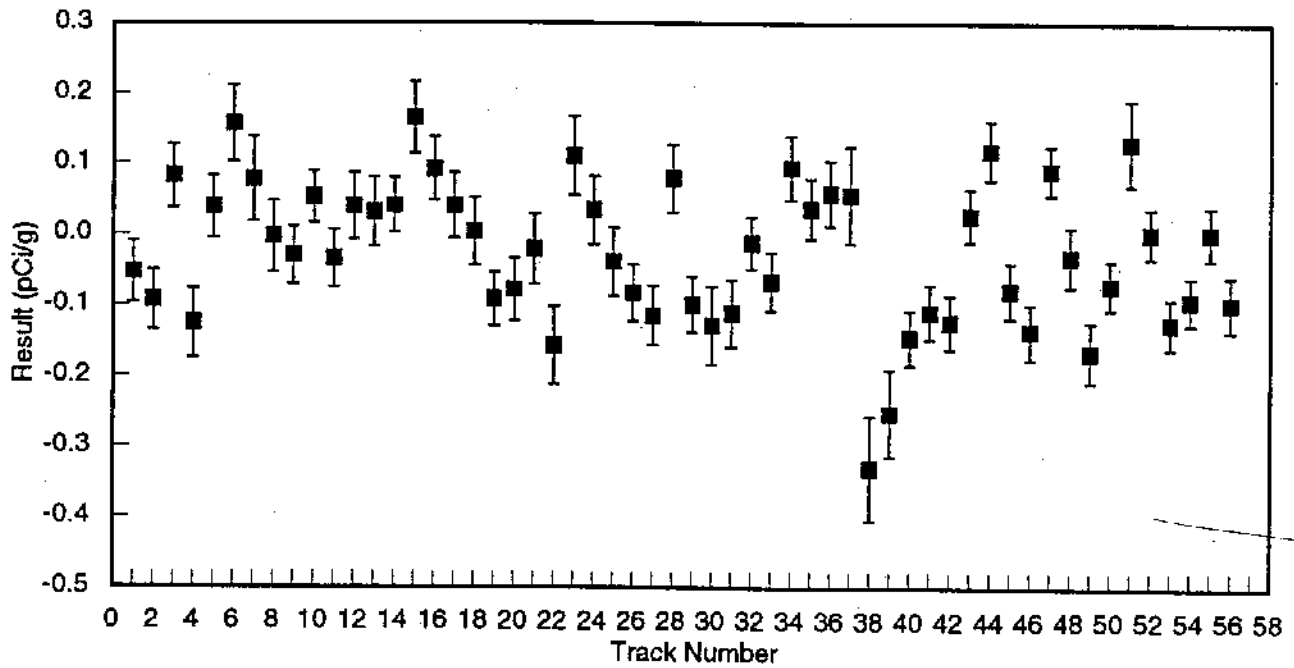


**FIGURE B.2.** Potassium-40 (<sup>40</sup>K) Concentrations in Soils S9306049.22



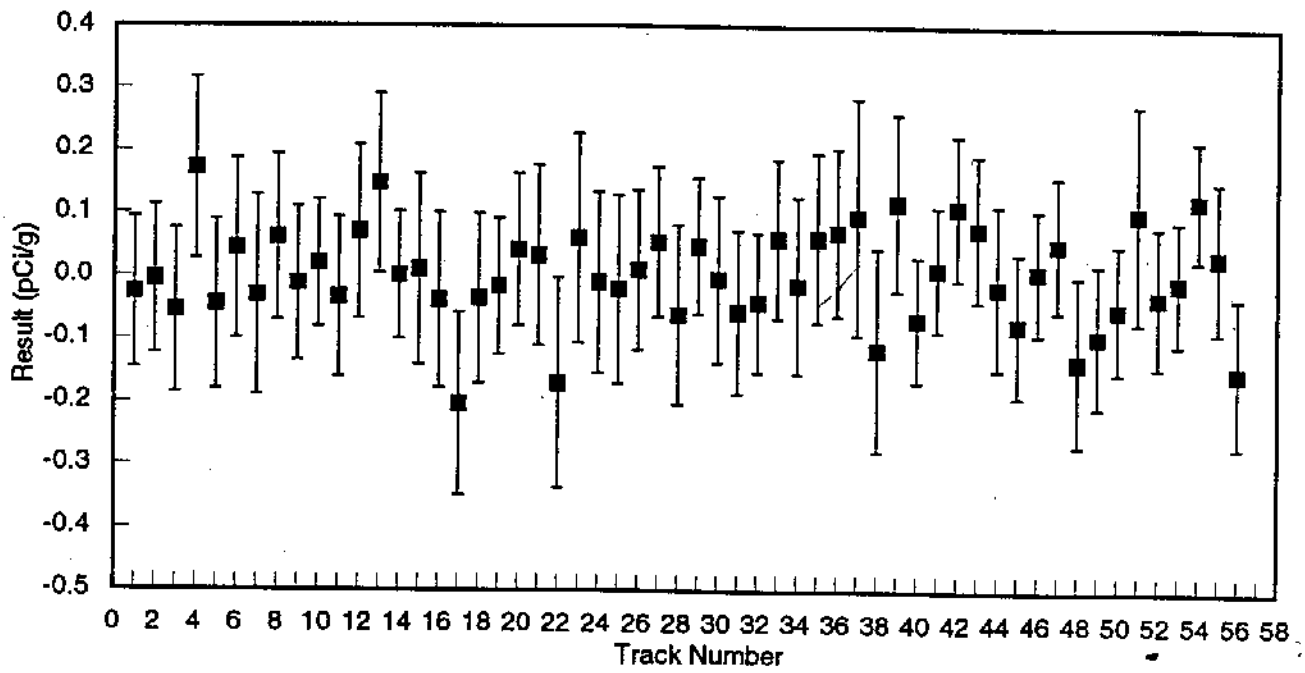
S9306049.23

FIGURE B.3. Manganese-54 ( $^{54}\text{Mn}$ ) Concentrations in Soils



S9306049.24

FIGURE B.4. Zirconium/Niobium-95 ( $^{95}\text{ZrNb}$ ) Concentrations in Soils



**FIGURE B.5.** Ruthenium-106 (<sup>106</sup>Ru) Concentrations in Soils S9306049.25

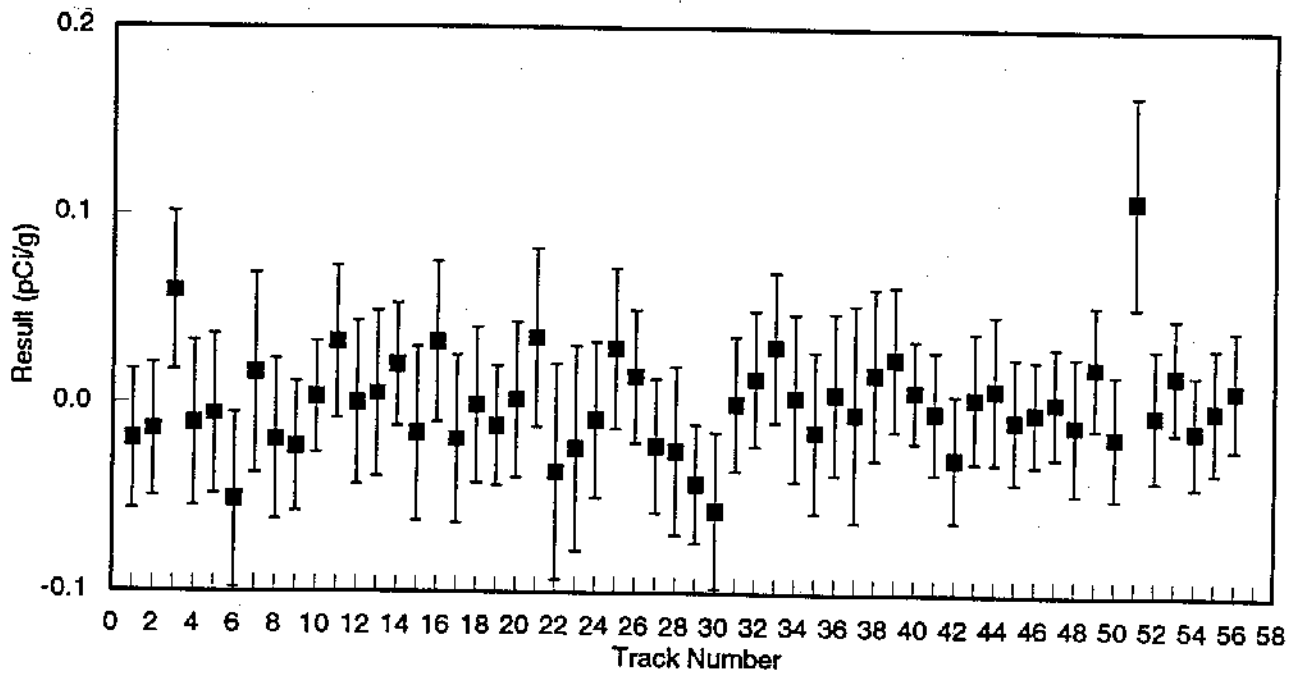


**FIGURE B.6.** Antimony-125 (<sup>125</sup>Sb) Concentrations in Soils S9306049.26

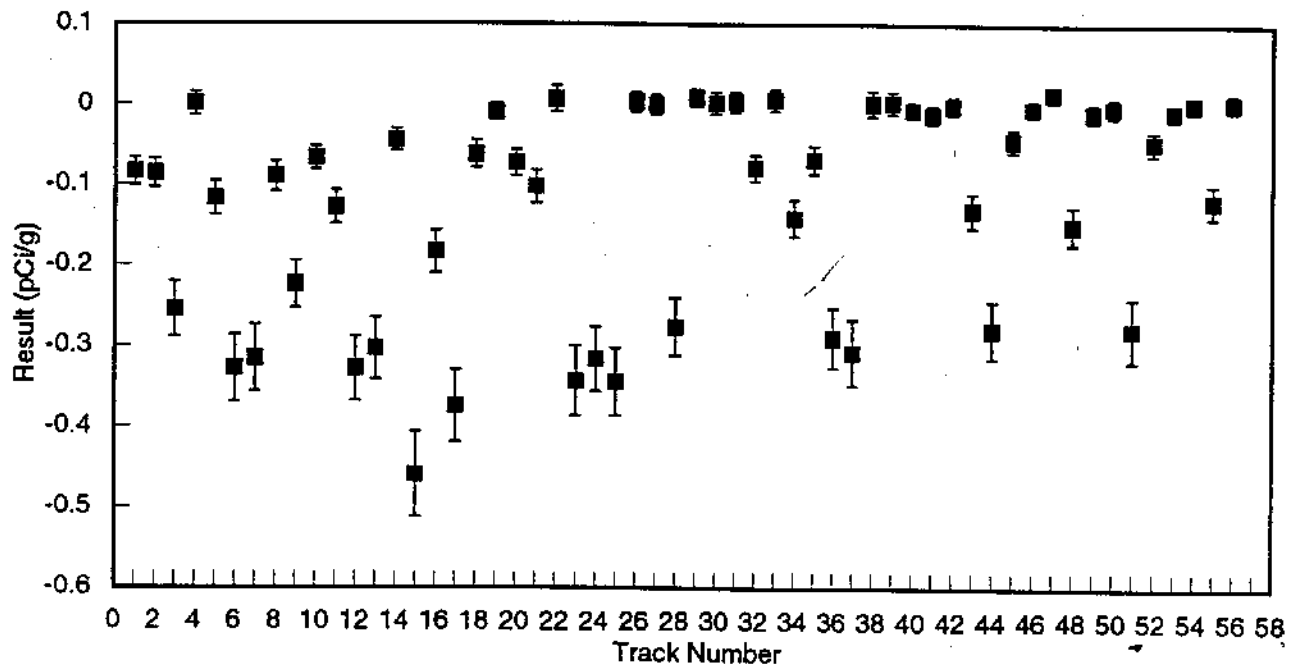


FIGURE B.7. Cesium-134 ( $^{134}\text{Cs}$ ) Concentrations in Soils

S9306049.27

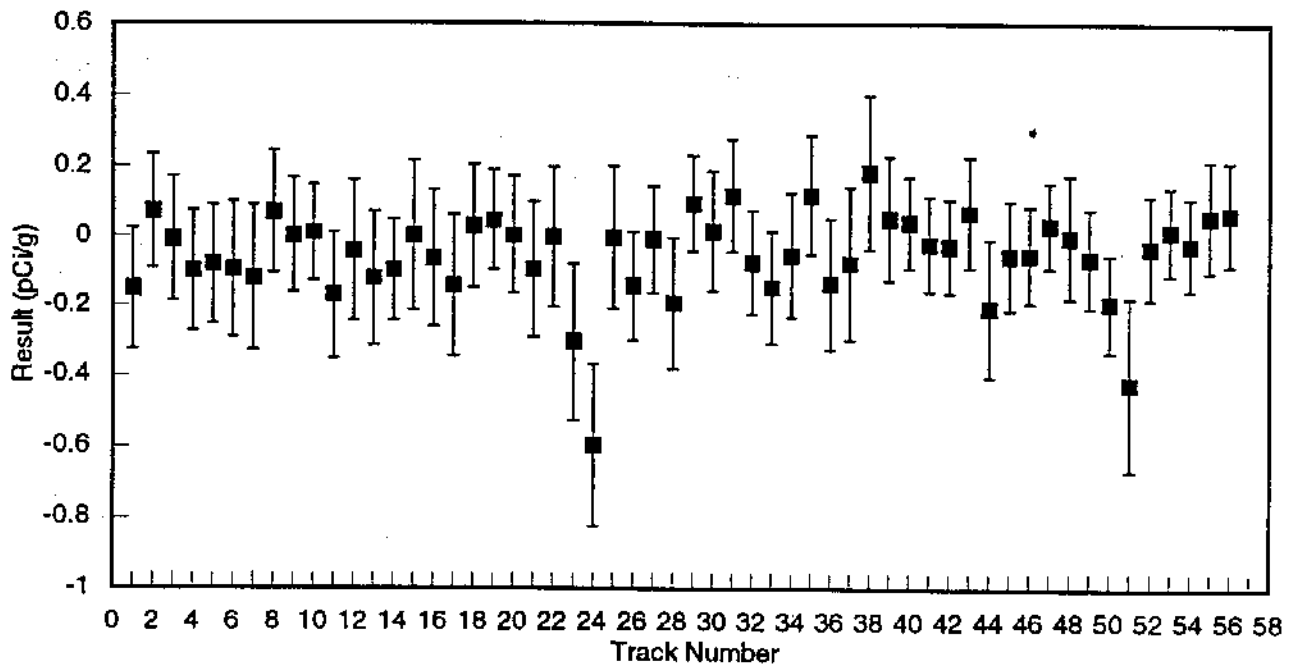


FIGURE B.8. Cerium/Praseodymium-144 ( $^{144}\text{CePr}$ ) Concentrations in Soils

S9306049.28

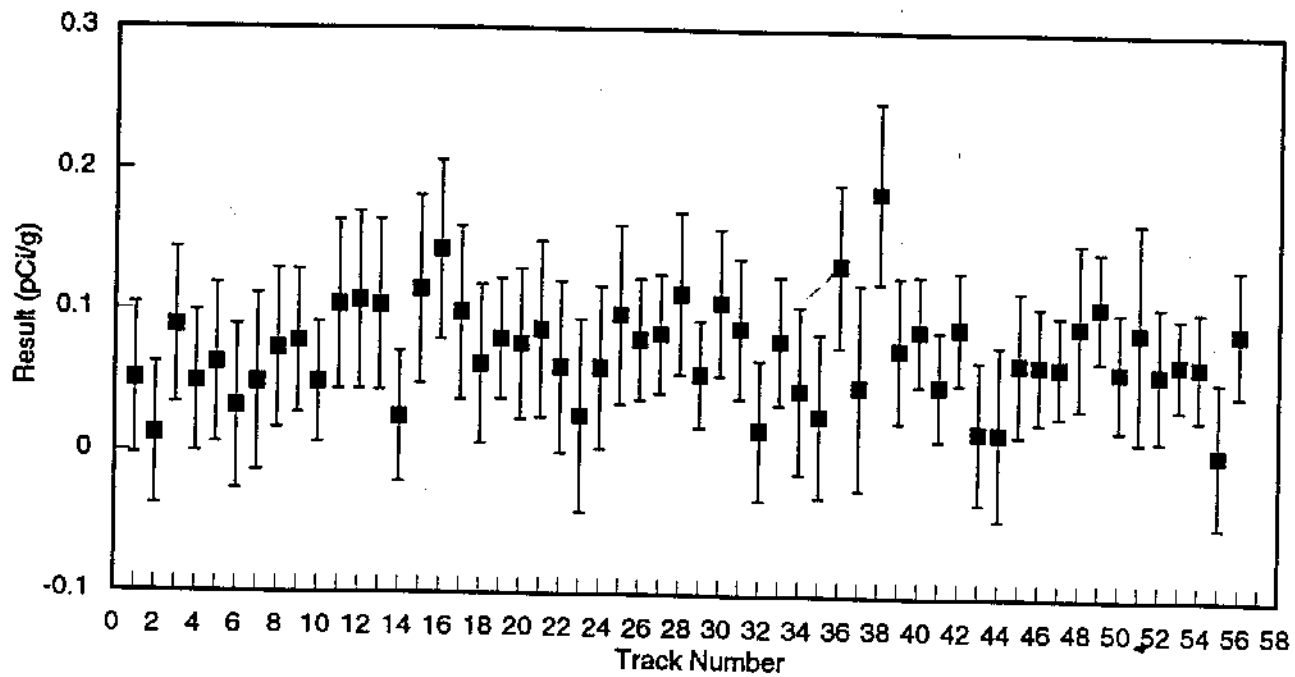


FIGURE B.9. Europium-155 ( $^{155}\text{Eu}$ ) Concentrations in Soils S9306049.29

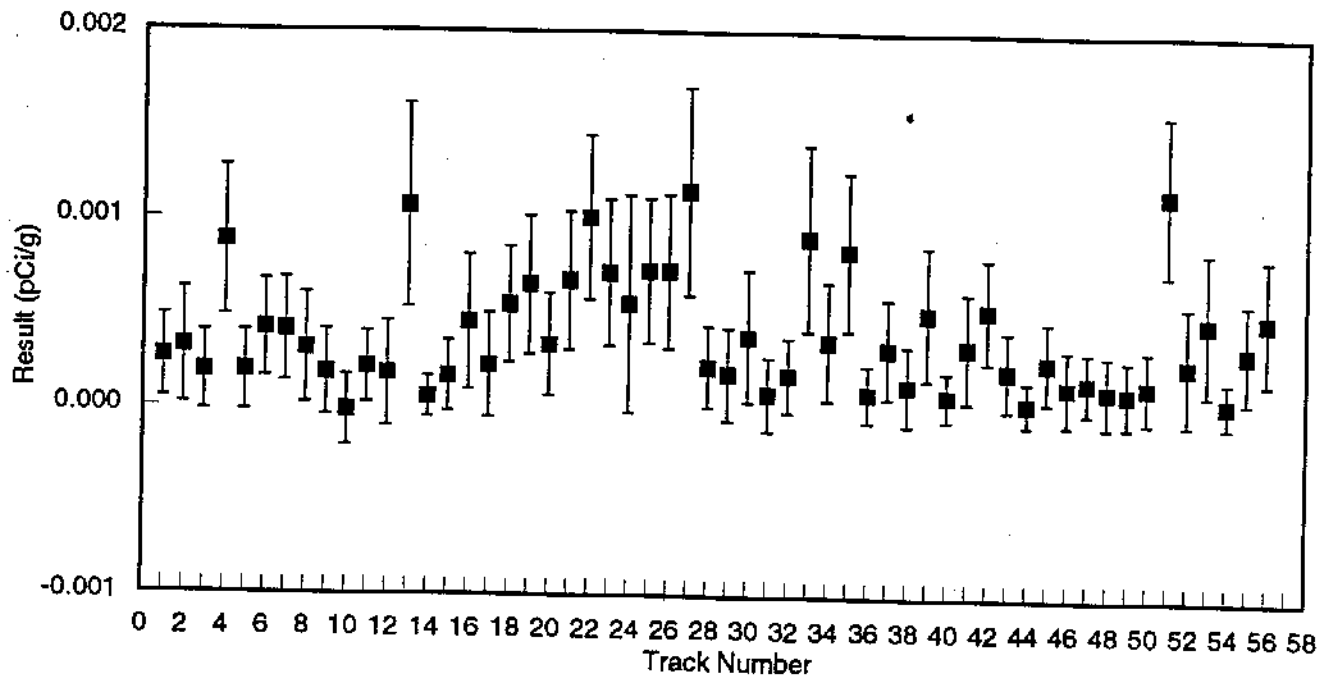


FIGURE B.10. Plutonium-238 ( $^{238}\text{Pu}$ ) Concentrations in Soils S9306049.30

APPENDIX C

SOIL SAMPLE TRACE METAL CONCENTRATION DATA  
AND SUPPLEMENTAL FIGURES

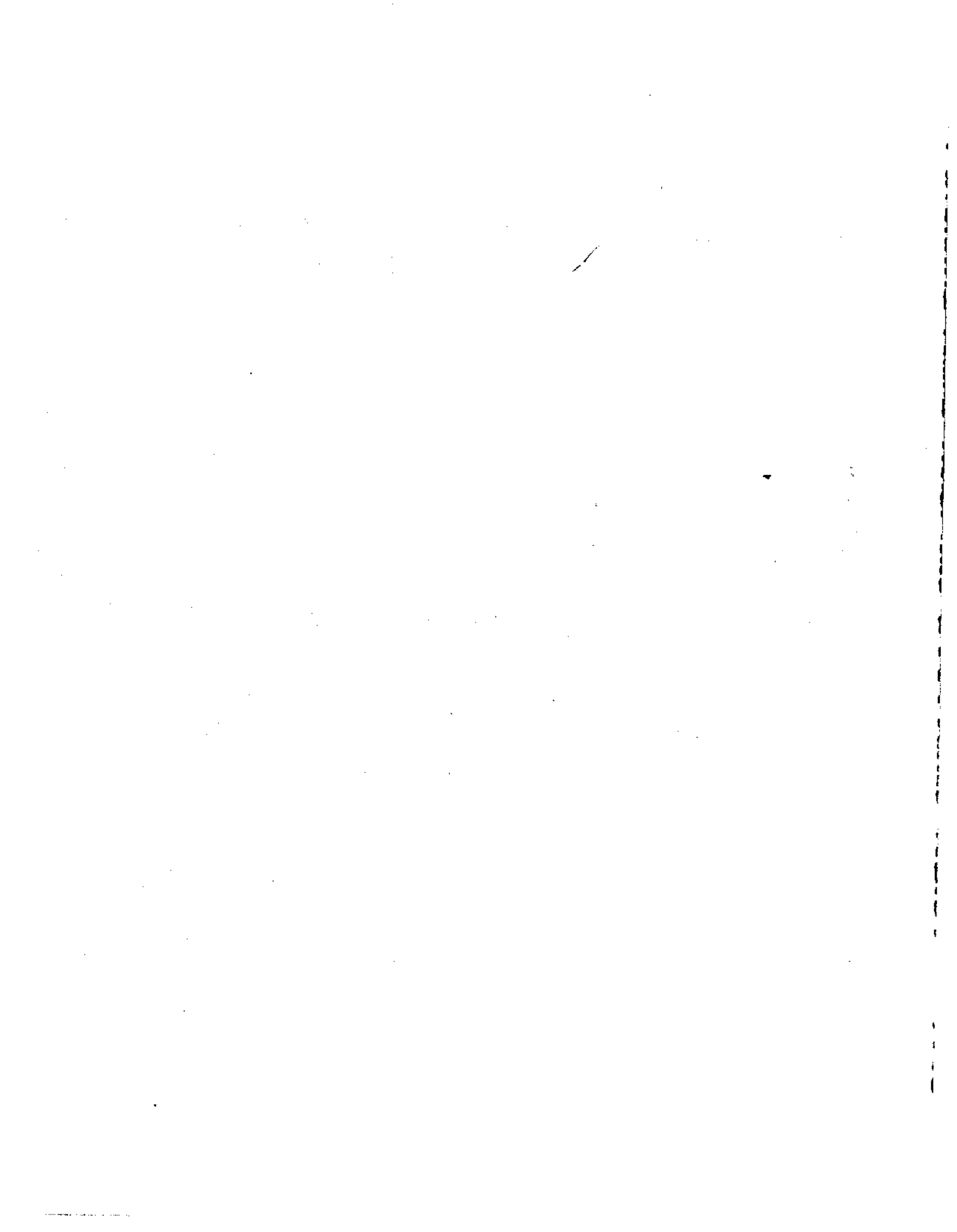


TABLE C.1. Trace Metals in Soils ( $\mu\text{g}/\text{kg}$ )

<u>Track #</u>	<u>Lead</u> <u>DL = 500</u>	<u>2 SD</u>	<u>Mercury</u> <u>400</u>	<u>2SD</u>	<u>Antimony</u> <u>20000</u>	<u>2SD</u>
1	52000	12468	ND		ND	
2	41000	9830	ND		ND	
3	41000	9830	ND		ND	
4	28000	6713	ND		ND	
5	39000	9351	ND		ND	
6	46000	11029	ND		ND	
7	42000	10070	ND		ND	
8	38000	9111	ND		ND	
9	25000	5994	ND		ND	
10	5000	1199	ND		ND	
11	23000	5514	ND		ND	
12	27000	6474	ND		ND	
13	27000	6474	ND		ND	
14	22000	5275	ND		ND	
15	23000	5514	ND		ND	
16	28000	6713	ND		ND	
17	48000	11508	ND		ND	
18	44000	10549	ND		ND	
19	29000	6953	ND		ND	
20	48000	11508	ND		ND	
21	43000	10310	ND		ND	
22	54000	12947	ND		ND	
23	46000	11029	ND		ND	
24	14000	3357	ND		ND	
25	44000	10549	ND		ND	
26	45000	10789	ND		ND	
27	37000	8871	ND		ND	
28	39000	9351	ND		ND	
29	21000	5035	ND		ND	
30	48000	11508	ND		ND	
31	42000	10070	ND		ND	
32	44000	10549	ND		ND	
33	45000	10789	ND		ND	
34	42000	10070	ND		ND	
35	73000	17502	ND		ND	
36	27000	6474	ND		ND	
37	47000	11269	ND		ND	
38	36000	8631	ND		ND	
39	27000	6474	ND		ND	
40	10000	2398	ND		ND	
41	38000	9111	ND		ND	
42	38000	9111	ND		ND	
43	27000	6474	ND		ND	
44	29000	6953	ND		ND	
45	9200	2206	ND		ND	
46	12000	2877	ND		ND	
47	33000	7912	ND		ND	
48	34000	8152	ND		ND	
49	41000	9830	ND		ND	
50	30000	7193	ND		ND	
51	32000	7672	ND		ND	
52	39000	9351	ND		ND	
53	41000	9830	ND		ND	
54	16000	3836	ND		ND	
55	31000	7433	ND		ND	
56	48000	11508	ND		ND	

TABLE C.1. (contd)

Track #	Barium 2000	2 SD	Beryllium 300	2 SD	Cadmium 1000	2 SD
1	88000	8791	ND			
2	80000	7493	ND		2000	519
3	75000	7992	ND		2000	519
4	78000	7792	ND		2000	519
5	68000	6793	ND		1000	260
6	87000	8691	ND		ND	
7	90000	8991	ND		2000	519
8	84000	8392	ND		2000	519
9	68000	6793	ND		2000	519
10	70000	6993	ND		1000	260
11	85000	8494	ND		ND	
12	69000	6893	ND		ND	
13	60000	5994	ND		ND	
14	65000	6494	ND		ND	
15	68000	6793	ND		ND	
16	72000	7193	ND		ND	
17	69000	6893	ND		ND	
18	71000	7093	ND		1000	260
19	66000	6593	ND		2000	519
20	54000	5395	ND		1000	260
21	56000	5594	ND		ND	
22	74000	7393	ND		1000	260
23	65000	6494	ND		2000	519
24	14000	1399	ND		1000	260
25	84000	8392	1100	110	ND	
26	83000	8292	300	30	ND	
27	80000	7992	ND		ND	
28	84000	8392	ND		1000	260
29	77000	7692	ND		1000	260
30	81000	8092	500	50	1000	260
31	70000	6993	400	40	ND	
32	81000	8092	400	40	1000	260
33	90000	8991	ND		2000	519
34	76000	7592	ND		2000	519
35	110000	10989	ND		2000	519
36	120000	11988	300	30	2000	519
37	92000	9191	400	40	ND	
38	81000	8092	ND		2000	519
39	88000	8791	500	60	1000	260
40	99000	9890	500	50	ND	
41	64000	6394	300	30	ND	
42	70000	6993	ND		ND	
43	86000	8591	ND		ND	
44	79000	7892	500	50	1000	260
45	44000	4396	400	40	ND	
46	98000	9790	ND		ND	
47	95000	9491	ND		ND	
48	91000	9091	800	80	1000	260
49	83000	8292	600	60	1000	260
50	93000	9291	500	50	ND	
51	87000	8691	400	40	1000	260
52	68000	6793	500	50	2000	519
53	67000	6693	300	30	ND	
54	84000	8392	300	30	ND	
55	83000	8292	ND		ND	
56	92000	9191	400	40	ND	
			500	50	1000	260

TABLE C.1. (contd)

Track #	Calcium 10000	2 SD	Chromium 2000	2 SD	Cobalt 2000	2 SD
1	5900000	943056	23000	5974	7000	1119
2	5600000	815184	21000	5195	6000	959
3	5100000	895104	20000	5455	8000	959
4	5400000	863136	18000	4675	7000	1119
5	5800000	927072	22000	5714	7000	1119
6	4900000	783216	22000	5714	8000	1279
7	5000000	799200	25000	6494	9000	1439
8	4700000	751248	25000	6494	9000	1439
9	6300000	1006992	20000	5195	7000	1119
10	4900000	783216	12000	3117	5000	799
11	5300000	847152	21000	5455	7000	1119
12	5200000	831168	26000	6753	7000	1119
13	4700000	751248	25000	6494	6000	959
14	6300000	1006992	18000	4675	7000	1119
15	4600000	735264	31000	8052	7000	1119
16	4700000	751248	28000	7273	7000	1119
17	5000000	799200	29000	7532	7000	1119
18	5400000	863136	23000	5974	7000	1119
19	4900000	783216	28000	7273	7000	1119
20	3800000	607392	16000	4156	5000	799
21	4200000	671328	23000	5974	7000	1119
22	4600000	735264	24000	6234	7000	1119
23	4400000	703296	23000	5974	8000	1279
24	9000000	1438560	25000	6494	10000	1598
25	5600000	895104	30000	7792	8000	1279
26	5800000	927072	25000	6494	8000	1279
27	5700000	911088	88000	22857	7000	1119
28	5900000	943056	25000	6494	7000	1119
29	5900000	943056	19000	4935	9000	1439
30	5600000	895104	24000	6234	7000	1119
31	4800000	767232	20000	5195	7000	1119
32	5500000	879120	23000	5974	7000	1119
33	5400000	863136	27000	7013	7000	1119
34	5700000	911088	25000	6494	7000	1119
35	6200000	991008	27000	7013	7000	1119
36	5900000	943056	21000	5455	8000	1279
37	4900000	783216	22000	5714	8000	1279
38	5200000	831168	26000	6753	7000	1119
39	5100000	815184	21000	5455	7000	1119
40	3700000	591408	14000	3636	9000	1439
41	4500000	719280	18000	4675	8000	1279
42	4500000	719280	19000	4935	9000	1439
43	6500000	1038960	24000	6234	7000	1119
44	6800000	1086912	20000	5195	7000	1119
45	2900000	463536	15000	3896	7000	1119
46	4000000	639360	12000	3117	10000	1598
47	6100000	975024	21000	5455	8000	1279
48	7600000	1214784	27000	7013	8000	1279
49	6800000	1086912	24000	6234	7000	1119
50	6100000	975024	19000	4935	7000	1119
51	6100000	975024	20000	5195	7000	1119
52	4900000	783216	17000	4416	9000	1439
53	4900000	783216	17000	4416	8000	1279
54	4900000	783216	15000	3896	9000	1439
55	6400000	1022976	16000	4156	6000	959
56	7200000	1150848	24000	6234	8000	1279

TABLE C.1. (contd)

Track #	Copper 2000	2 SD	Iron 2000	2 SD	Magnesium 10000	2 SD
1	31000	9910	23000000	9650340	4900000	5678316
2	25000	7353	20000000	7972020	4700000	4867128
3	23000	7992	19000000	8391600	4200000	5446548
4	32000	10230	20000000	8391600	4600000	5330664
5	38000	12148	21000000	8811180	4900000	5678316
6	22000	7033	19000000	7972020	4800000	5562432
7	23000	7353	19000000	7972020	5000000	5794200
8	21000	6713	18000000	7552440	4700000	5446548
9	39000	12468	22000000	9230760	4700000	5446548
10	15000	4795	18000000	7552440	4200000	4867128
11	34000	10869	22000000	9230760	4600000	5330664
12	31000	9910	24000000	10069920	4800000	5562432
13	27000	8631	23000000	9650340	4400000	5098896
14	40000	12787	21000000	8811180	4700000	5446548
15	23000	7353	29000000	12167820	4500000	5214780
16	25000	7992	26000000	10909080	4400000	5098896
17	31000	9910	28000000	11748240	4700000	5446548
18	31000	9910	22000000	9230760	4600000	5330664
19	28000	8951	27000000	11328660	4900000	5678316
20	21000	6713	13000000	5454540	3300000	3824172
21	27000	8631	17000000	7132860	3900000	4519476
22	23000	7353	16000000	6713280	4400000	5098896
23	30000	9590	18000000	7552440	4200000	4867128
24	23000	7353	26000000	10909080	7600000	8807184
25	32000	10230	25000000	10489500	4900000	5678316
26	35000	11189	23000000	9650340	4900000	5678316
27	25000	7992	23000000	9650340	4700000	5446548
28	34000	10869	24000000	10069920	5300000	6141852
29	19000	6074	26000000	10909080	5200000	6025968
30	28000	8951	21000000	8811180	5300000	6141852
31	27000	8631	19000000	7972020	4800000	5562432
32	30000	9590	21000000	8811180	5000000	5794200
33	30000	9590	20000000	8391600	5200000	6025968
34	29000	9271	25000000	10489500	5000000	5794200
35	29000	9271	21000000	8811180	5600000	6489504
36	25000	7992	23000000	9650340	5000000	5794200
37	20000	6394	19000000	7972020	4800000	5562432
38	28000	8951	26000000	10909080	4500000	5214780
39	19000	6074	20000000	8391600	5100000	5910084
40	10000	3197	22000000	9230760	3500000	4055940
41	26000	8312	19000000	7972020	4300000	4983012
42	25000	7992	20000000	8391600	4300000	4983012
43	25000	7992	21000000	8811180	5100000	5910084
44	31000	9910	21000000	8811180	4900000	5678316
45	9000	2877	18000000	7552440	3400000	3940056
46	14000	4476	19000000	7972020	3500000	4055940
47	28000	8951	23000000	9650340	5100000	5910084
48	31000	9910	25000000	10489500	5500000	6373620
49	30000	9590	25000000	10489500	4800000	5562432
50	23000	7353	18000000	7552440	5000000	5794200
51	15000	4795	20000000	8391600	5800000	6721272
52	30000	9590	17000000	7132860	4600000	5330664
53	32000	10230	18000000	7552440	4300000	4983012
54	18000	5754	17000000	7132860	4500000	5214780
55	18000	5754	18000000	7552440	4700000	5446548
56	28000	8951	24000000	10069920	5100000	5910084

TABLE C.I. (contd)

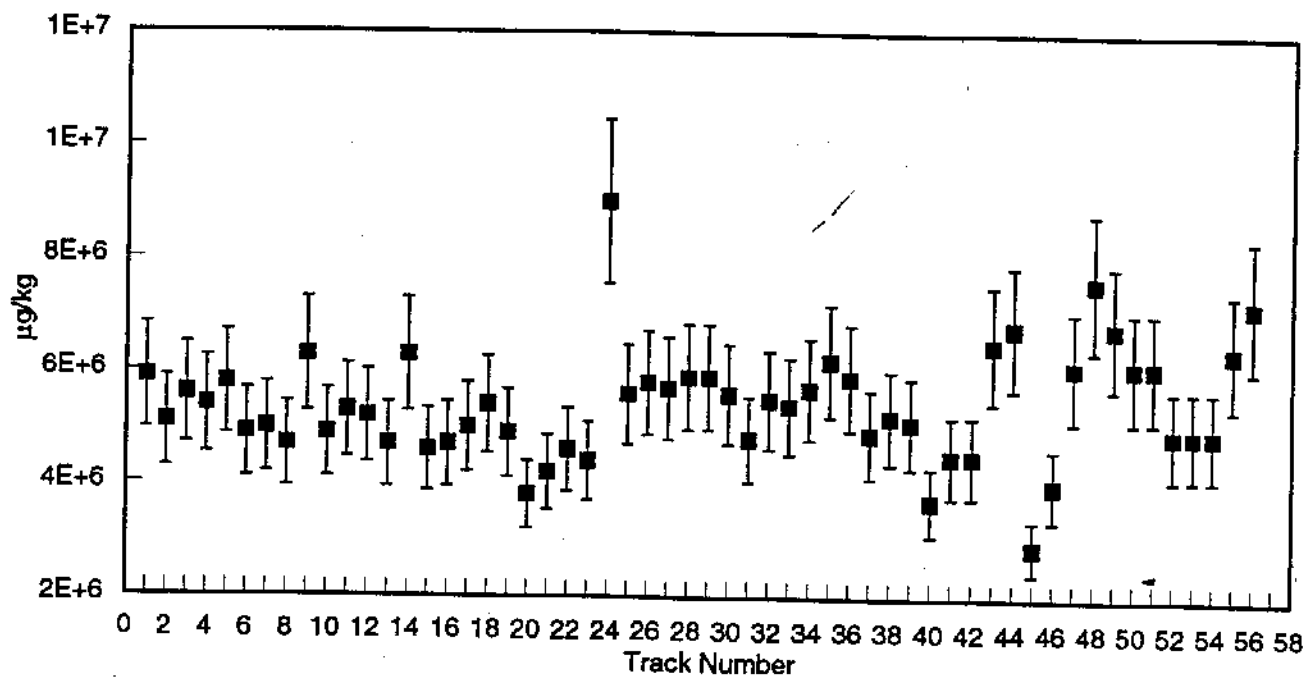
Track #	Manganese 1000	2 SD	Nickel 3000	2 SD	Potassium 30000	2 SD
1	300000	41958	17000	4416	1600000	671328
2	280000	36364	18000	4156	1700000	587412
3	260000	39161	16000	4675	1400000	713286
4	430000	60140	18000	4675	1000000	419580
5	330000	46154	18000	4675	1100000	461538
6	260000	36364	18000	4675	1200000	503496
7	260000	36364	18000	4675	1200000	503496
8	270000	37762	17000	4416	1300000	545454
9	290000	40559	15000	3896	1200000	503496
10	270000	37762	12000	3117	810000	339860
11	280000	39161	17000	4416	1000000	419580
12	270000	37762	20000	5195	1200000	503496
13	270000	37762	16000	4156	890000	373426
14	310000	43357	17000	4416	1000000	419580
15	260000	36364	19000	4935	1000000	419580
16	270000	37762	18000	4675	1200000	503496
17	280000	39161	16000	4156	1300000	545454
18	340000	47552	17000	4416	1200000	503496
19	300000	41958	18000	4675	1100000	461538
20	150000	20979	11000	2857	710000	297902
21	170000	23776	14000	3636	840000	352447
22	190000	26573	15000	3896	1100000	461538
23	190000	26573	15000	3896	950000	398601
24	370000	51748	18000	4675	1300000	545454
25	300000	41958	17000	4416	1500000	629370
26	380000	53147	17000	4416	1200000	503496
27	260000	36364	13000	3377	1400000	587412
28	290000	40559	18000	4675	1500000	629370
29	310000	43357	15000	3896	1100000	461538
30	280000	39161	17000	4416	1400000	587412
31	230000	32168	15000	3896	1100000	461538
32	260000	36364	17000	4416	1300000	545454
33	220000	30769	18000	4675	1400000	587412
34	250000	34965	17000	4416	1400000	587412
35	290000	40559	18000	4675	1900000	797202
36	330000	46154	14000	3636	1600000	671328
37	290000	40559	16000	4156	1300000	545454
38	250000	34965	15000	3896	1000000	419580
39	280000	39161	18000	4675	1200000	503496
40	220000	30769	9000	2338	620000	260140
41	260000	36364	14000	3636	1300000	545454
42	270000	37762	15000	3896	1200000	503496
43	310000	43357	16000	4156	1600000	671328
44	280000	39161	15000	3896	1400000	587412
45	160000	22378	12000	3117	690000	289510
46	460000	64336	11000	2857	850000	356643
47	380000	53147	16000	4156	1500000	629370
48	330000	46154	18000	4675	1700000	713286
49	290000	40559	14000	3636	1500000	629370
50	270000	37762	14000	3636	1500000	629370
51	260000	36364	15000	3896	1400000	587412
52	250000	34965	16000	4156	1400000	587412
53	250000	34965	16000	4156	1200000	503496
54	240000	33566	14000	3636	1100000	461538
55	250000	34965	11000	2857	1600000	671328
56	320000	44755	16000	4156	1600000	671328

TABLE C.1. (contd)

Track #	Silver 2000	2 SD	Sodium 30000	2 SD	Tin 10000	2 SD
1	ND		460000	137862	ND	
2	ND		510000	143856	ND	
3	ND		480000	152847	ND	
4	ND		410000	122877	ND	
5	ND		540000	161838	ND	
6	ND		390000	116883	ND	
7	ND		440000	131868	ND	
8	ND		400000	119880	ND	
9	ND		570000	170829	ND	
10	ND		240000	71928	ND	
11	ND		420000	125874	ND	
12	ND		380000	113886	ND	
13	ND		390000	116883	ND	
14	ND		540000	161838	ND	
15	ND		260000	77922	ND	
16	ND		350000	104895	ND	
17	ND		330000	98901	ND	
18	ND		520000	155844	ND	
19	ND		370000	110889	ND	
20	ND		320000	95904	ND	
21	ND		330000	98901	ND	
22	ND		330000	98901	ND	
23	ND		320000	95904	ND	
24	ND		860000	257742	ND	
25	ND		400000	119880	ND	
26	ND		500000	149850	ND	
27	ND		490000	146853	ND	
28	ND		400000	119880	ND	
29	ND		640000	191808	ND	
30	ND		390000	116883	ND	
31	ND		360000	107892	ND	
32	ND		440000	131868	ND	
33	ND		410000	122877	ND	
34	ND		460000	137862	ND	
35	ND		450000	134865	ND	
36	ND		300000	89910	ND	
37	ND		320000	95904	ND	
38	ND		320000	95904	ND	
39	ND		290000	86913	ND	
40	ND		240000	71928	ND	
41	ND		340000	101898	ND	
42	ND		320000	95904	ND	
43	ND		780000	233766	ND	
44	ND		760000	227772	ND	
45	ND		170000	50949	ND	
46	ND		200000	59940	ND	
47	ND		540000	161838	ND	
48	ND		840000	251748	ND	
49	ND		810000	242757	ND	
50	ND		820000	245754	ND	
51	ND		830000	248751	ND	
52	ND		320000	95904	ND	
53	ND		360000	107892	ND	
54	ND		260000	77922	ND	
55	ND		920000	275724	ND	
56	ND		770000	230769	ND	

TABLE C.1. (contd)

Track #	Vanadium 3000	2 SD	Zinc 1000	2 SD
1	56000	8951	300000	89910
2	47000	7672	270000	71928
3	48000	7512	240000	80919
4	48000	7672	220000	65934
5	53000	8472	270000	80919
6	46000	7353	260000	77922
7	43000	6873	250000	74925
8	43000	6873	240000	71928
9	55000	8791	170000	50949
10	44000	7033	63000	18881
11	56000	8951	160000	47952
12	61000	9750	160000	47952
13	61000	9750	150000	44955
14	53000	8472	170000	50949
15	75000	11988	130000	38961
16	69000	11029	150000	44955
17	69000	11029	230000	68931
18	58000	9271	260000	77922
19	69000	11029	190000	56943
20	30000	4795	280000	83916
21	41000	6553	240000	71928
22	36000	5754	300000	89910
23	43000	6873	250000	74925
24	48000	7672	50000	14985
25	64000	10230	230000	68931
26	59000	9431	250000	74925
27	61000	9750	200000	59940
28	55000	8791	240000	71928
29	77000	12308	180000	53946
30	50000	7992	270000	80919
31	44000	7033	270000	80919
32	50000	7992	260000	77922
33	48000	7672	290000	86913
34	65000	10390	260000	77922
35	51000	8152	260000	77922
36	52000	8312	180000	53946
37	41000	6553	260000	77922
38	67000	10709	230000	68931
39	48000	7672	170000	50949
40	70000	11189	96000	28771
41	42000	6713	220000	65934
42	47000	7512	240000	71928
43	55000	8791	190000	56943
44	54000	8631	200000	59940
45	46000	7353	100000	29970
46	49000	7832	110000	32967
47	57000	9111	220000	65934
48	70000	11189	240000	71928
49	67000	10709	270000	80919
50	44000	7033	200000	59940
51	54000	8631	220000	65934
52	37000	5914	240000	71928
53	42000	6713	260000	77922
54	35000	5594	110000	32967
55	48000	7672	150000	44955
56	66000	10549	280000	83916



**FIGURE C.1.** Calcium Concentrations in Soils

S9306049.31

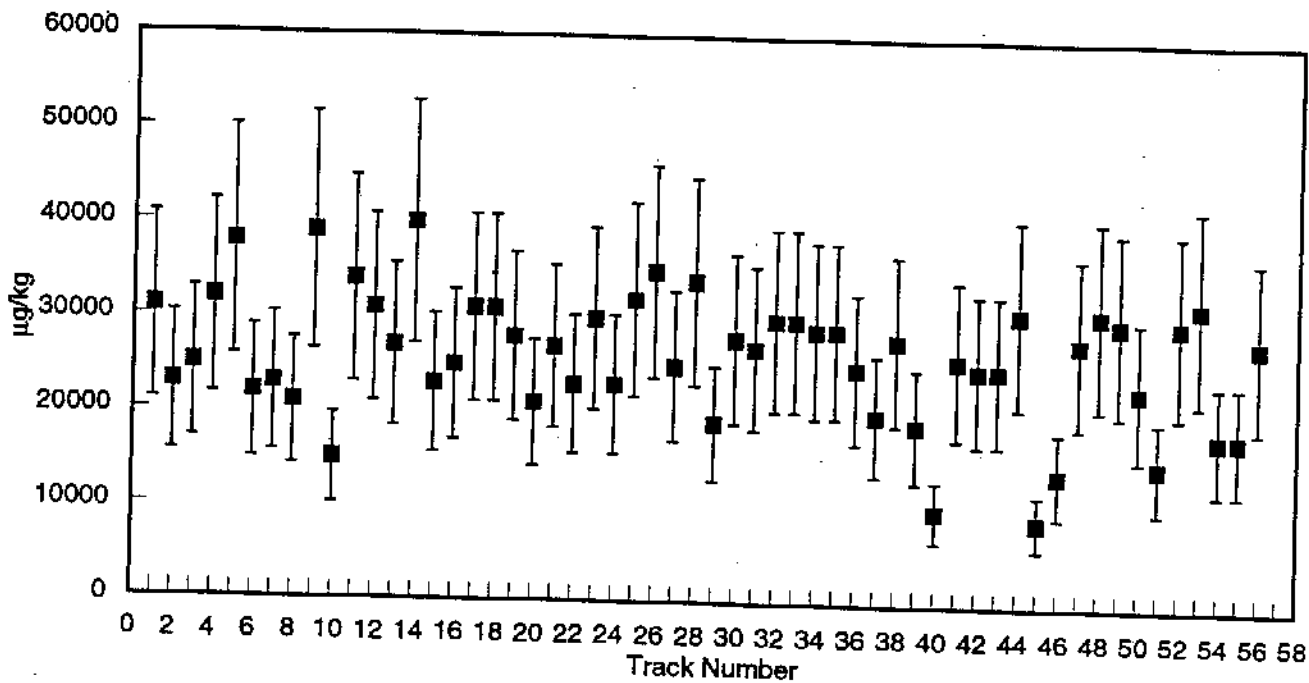


**FIGURE C.2.** Copper Concentrations in Soils

S9306049.32

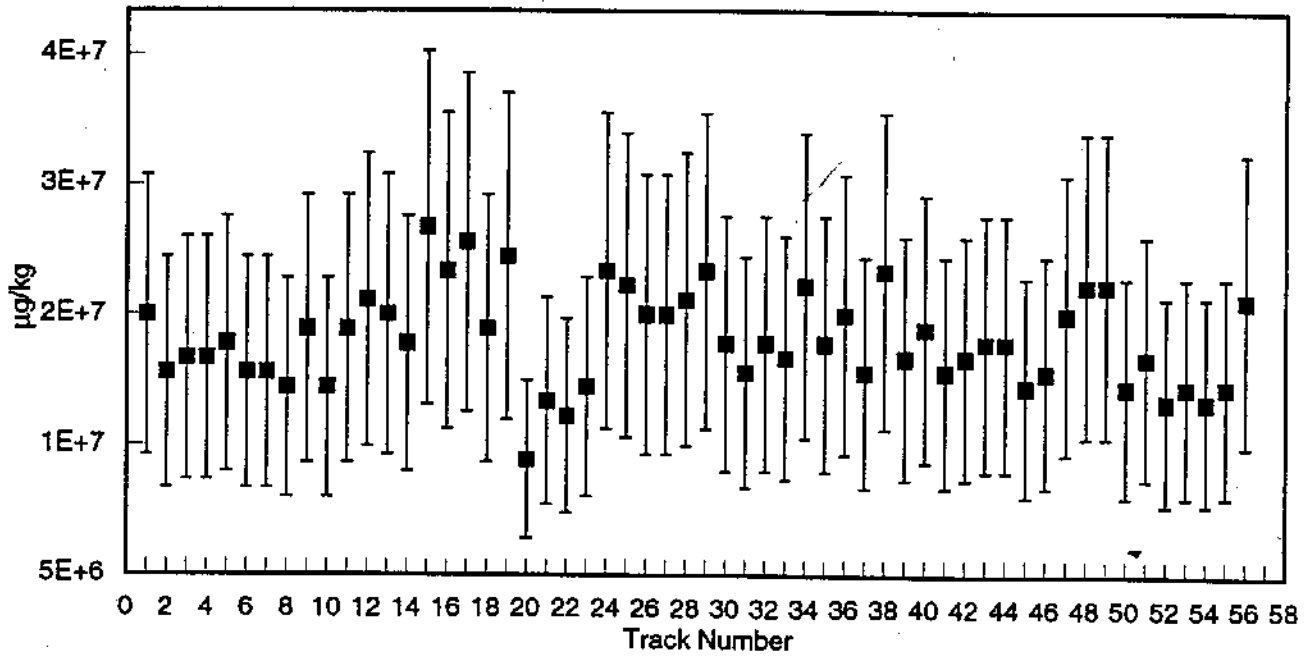


FIGURE C.3. Iron Concentrations in Soils

S9306049.33

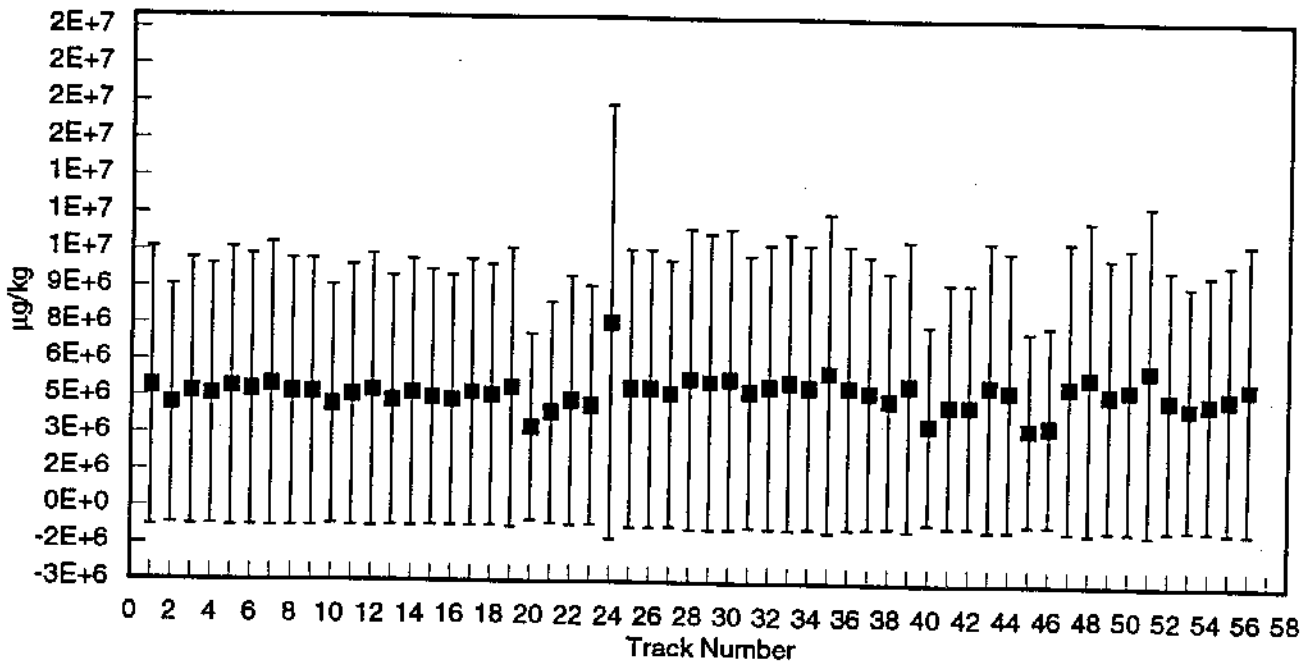


FIGURE C.4. Magnesium Concentrations in Soils

S9306049.34

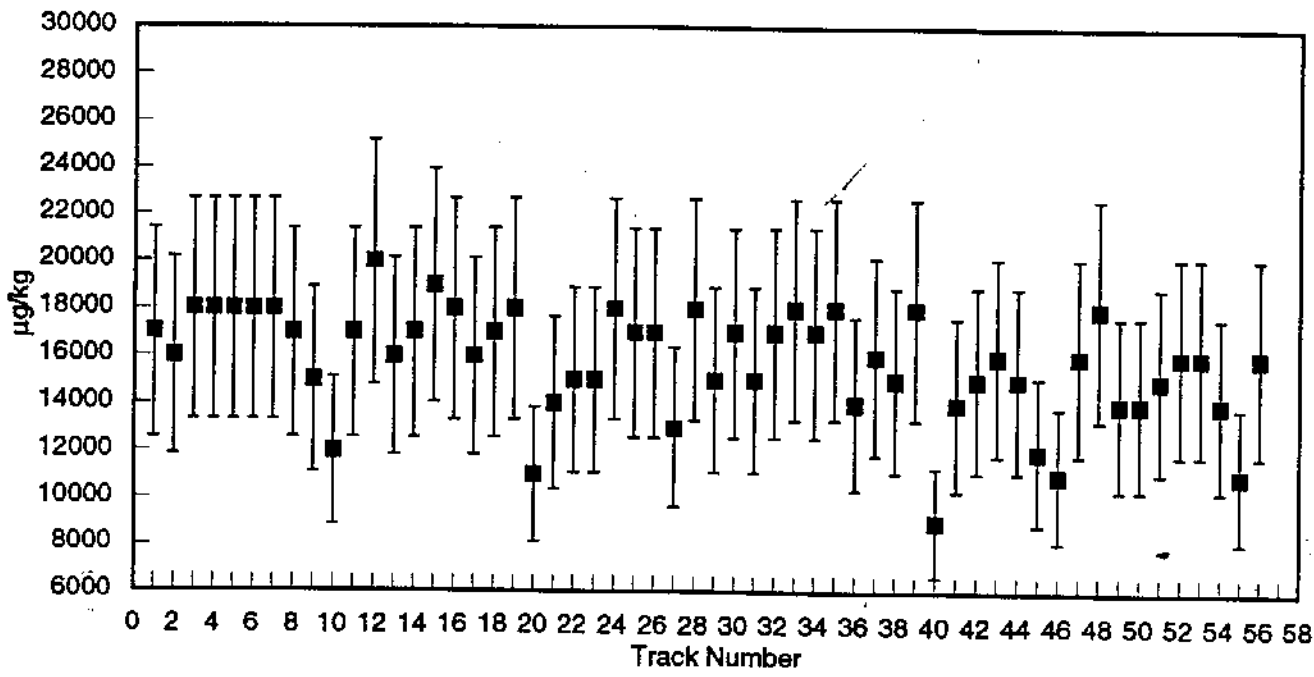


FIGURE C.5. Nickel Concentrations in Soils

S9306049.35

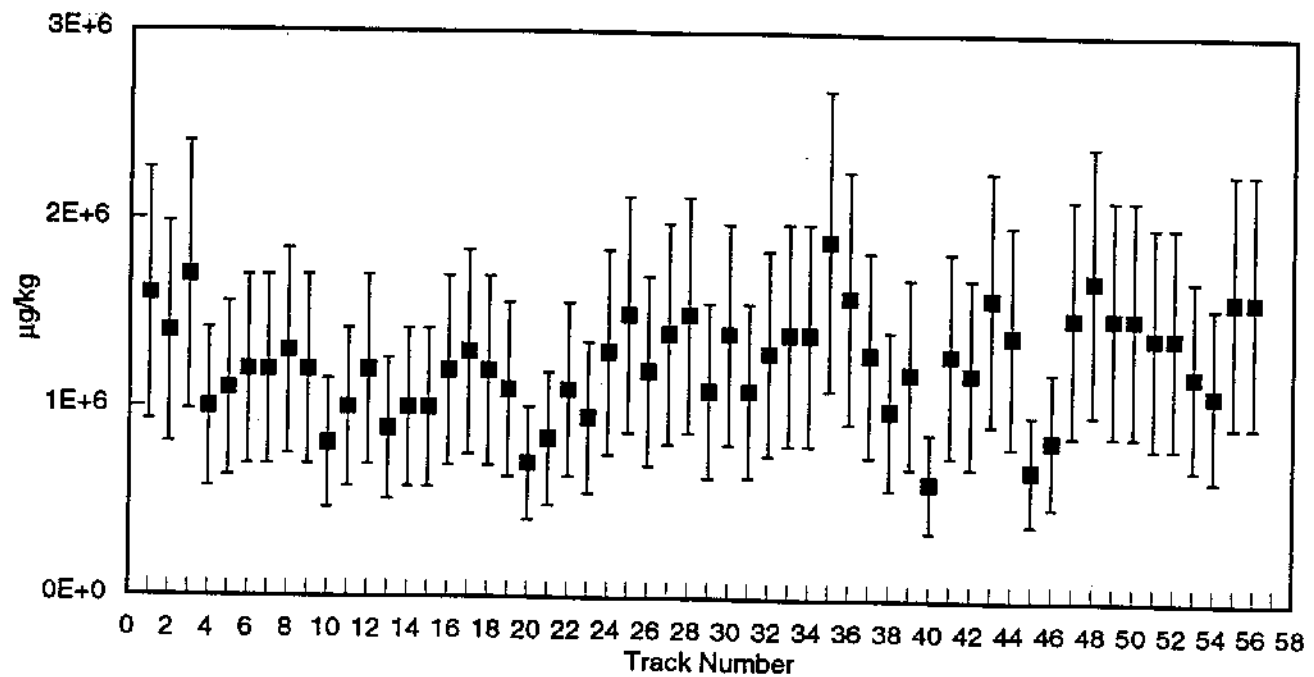
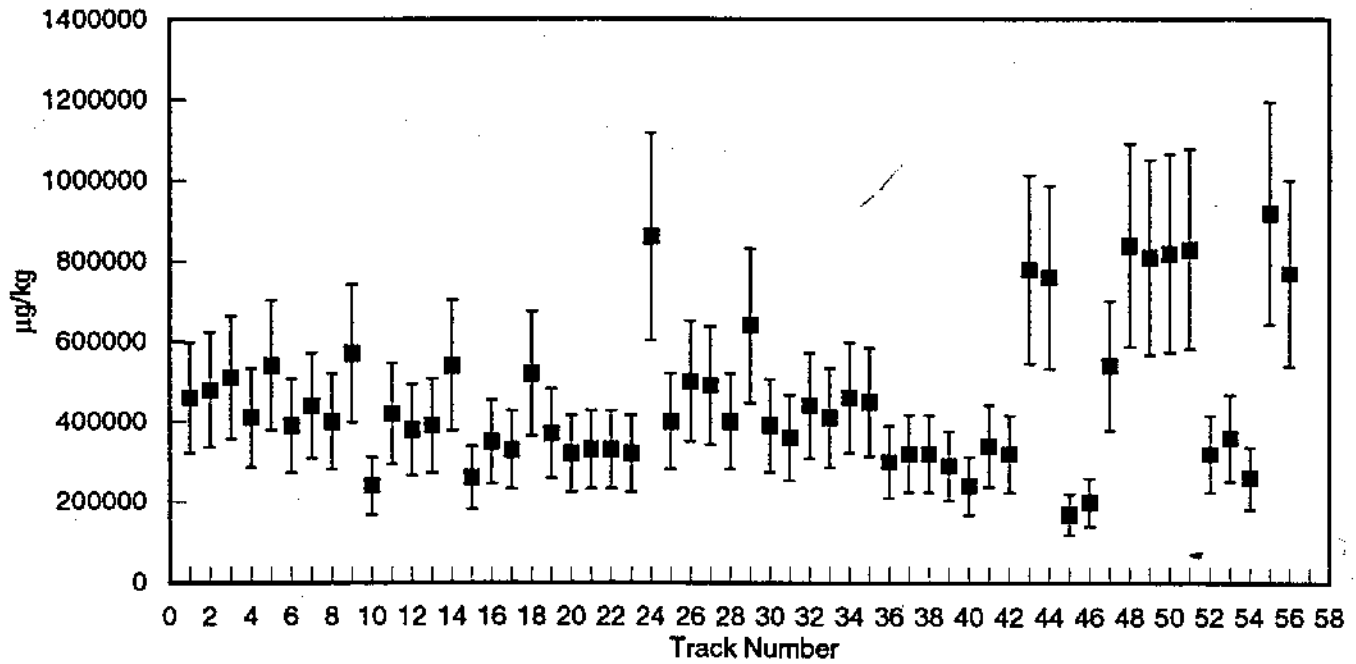


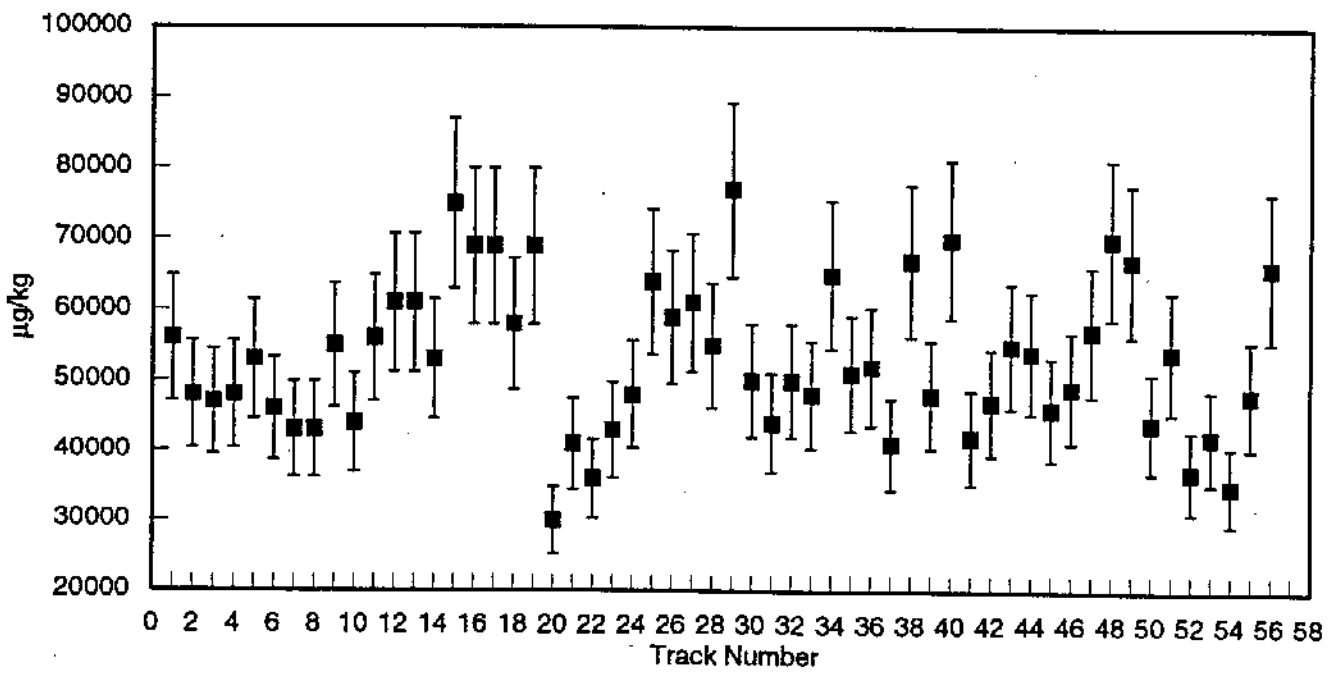
FIGURE C.6. Potassium Concentrations in Soils

S9306049.36



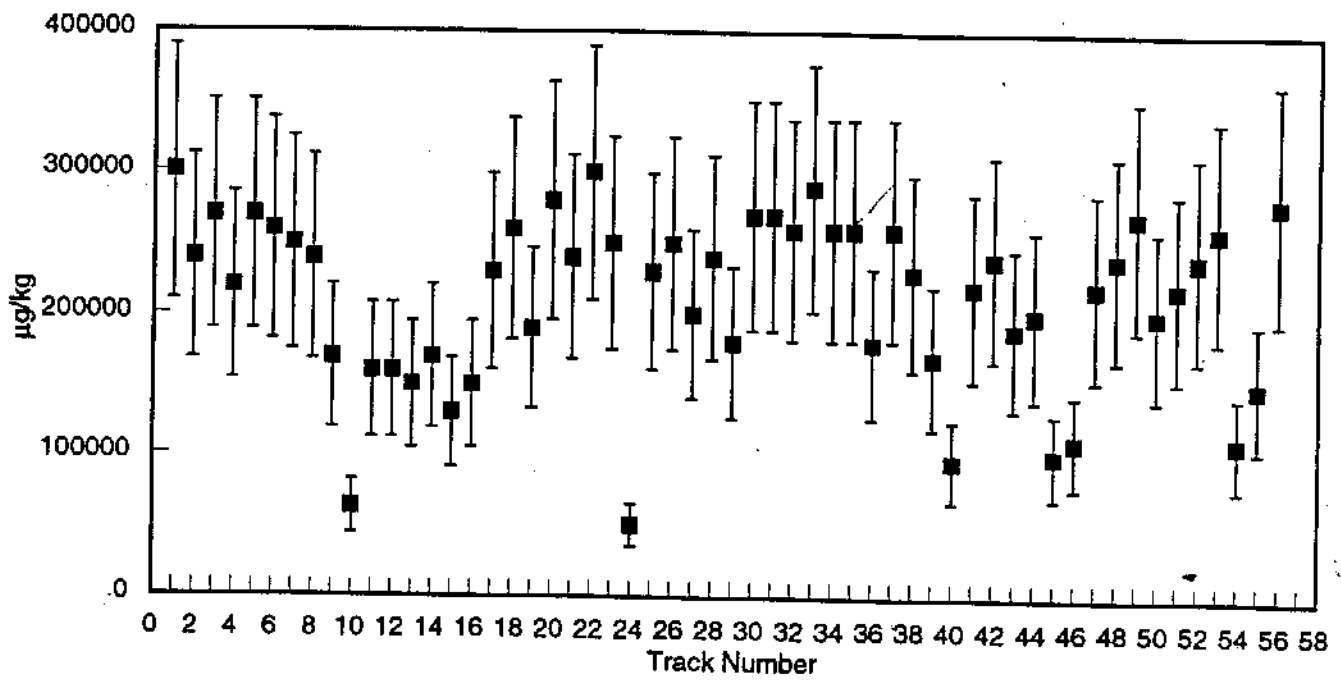
S9306049.37

FIGURE C.7. Sodium Concentrations in Soils



S9306049.38

FIGURE C.8. Vanadium Concentrations in Soils



**FIGURE C.9.** Zinc Concentrations in Soils

S9306049.39

APPENDIX D

ANALYTE CONCENTRATION CORRELATION MATRIX



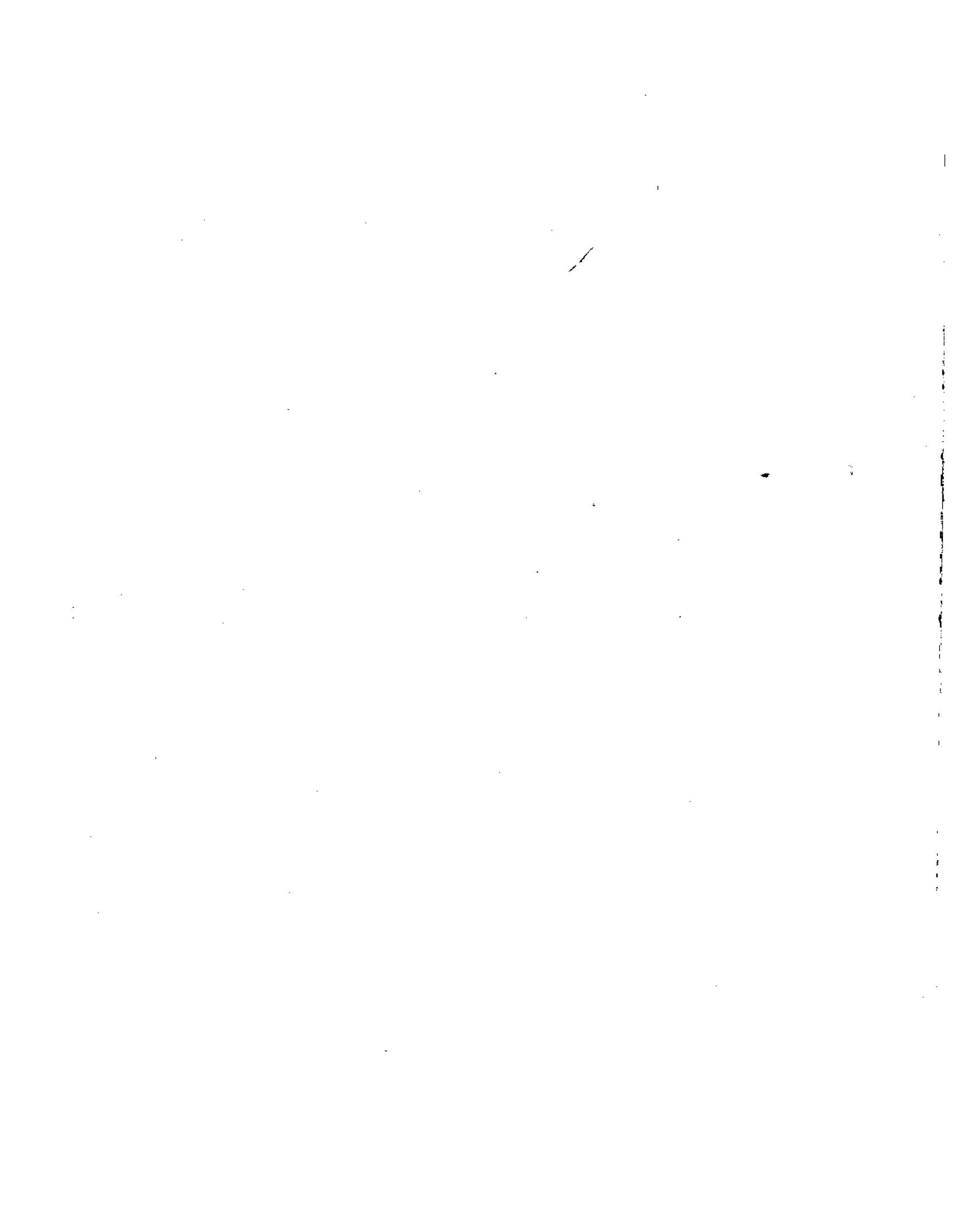
TABLE D.1. Analyte Concentration Correlation Matrix

	Be-7	Na-22	K-40	Co-60	Zn-65	Sr 90	ZrNb-95	Ru-106	Sb-125	Cs-134	Cs-137	CePr-144
Be-7	1.00											
Na-22	0.05	1.00										
K-40	0.19	-0.11	1.00									
Co-60	0.11	0.80	-0.08	1.00								
Zn-65	0.03	-0.43	-0.25	-0.28	1.00							
Sr 90	-0.11	0.12	0.08	0.09	-0.07	1.00						
ZrNb-95	-0.17	0.01	0.22	-0.02	-0.65	-0.02	1.00					
Ru-106	0.03	0.23	0.09	0.29	-0.03	-0.13	0.15	1.00				
Sb-125	0.22	-0.01	-0.06	-0.01	-0.04	-0.13	0.11	0.05	1.00			
Cs-134	-0.03	0.01	-0.51	0.08	0.72	-0.04	-0.73	-0.04	-0.10	1.00		
Cs-137	0.03	0.60	-0.09	0.43	-0.25	0.05	-0.09	-0.13	-0.11	0.09	1.00	
CePr-144	-0.07	-0.03	-0.33	-0.08	0.29	0.13	-0.43	-0.10	-0.22	0.46	-0.06	1.00
Eu-152	0.08	0.87	-0.02	0.77	-0.41	0.12	-0.03	0.13	0.05	0.07	0.73	-0.12
Eu-154	0.08	0.96	-0.09	0.67	-0.45	0.15	0.02	0.21	0.02	0.00	0.57	-0.01
Eu-155	0.18	-0.24	0.17	-0.23	0.11	0.03	-0.25	-0.22	0.20	-0.08	-0.19	0.07
U 234	-0.01	-0.20	0.18	-0.08	0.01	-0.11	0.04	-0.05	0.09	-0.18	-0.19	-0.10
U 235	-0.09	-0.20	0.06	-0.12	-0.04	-0.12	0.04	-0.12	0.07	-0.10	-0.11	-0.03
Pu-238	0.02	0.51	-0.01	0.35	-0.16	0.19	-0.04	0.31	0.14	0.00	0.49	-0.23
U 238	-0.02	-0.24	0.15	-0.13	0.03	-0.13	0.04	-0.07	0.13	-0.16	-0.22	-0.09
Pu 239,240	-0.11	0.64	-0.13	0.52	-0.34	0.45	0.02	0.00	-0.05	0.00	0.67	0.01
Barium	0.00	0.05	-0.01	0.10	0.04	0.20	-0.04	0.09	0.04	0.13	0.04	0.33
Calcium	0.04	-0.05	0.15	0.03	-0.04	0.31	0.15	-0.12	0.04	-0.10	-0.14	-0.31
Chromium	0.01	0.22	-0.01	0.00	-0.13	0.52	-0.01	-0.01	-0.11	-0.08	0.07	0.01
Cobalt	0.23	-0.06	0.18	-0.02	0.12	0.09	-0.08	0.04	-0.19	0.03	-0.06	-0.19
Copper	-0.10	0.15	-0.15	0.21	-0.15	0.23	0.10	-0.17	-0.04	-0.08	0.03	-0.07
Iron	0.09	-0.19	0.13	-0.19	-0.05	0.17	0.10	-0.27	-0.03	-0.29	-0.36	-0.04
Lead	-0.15	0.40	-0.13	0.28	-0.32	0.33	0.03	-0.17	-0.10	-0.01	0.45	0.13
Magnesium	0.09	0.05	0.28	0.05	-0.19	0.23	0.22	0.03	0.00	-0.21	-0.05	-0.43
Manganese	0.12	-0.03	0.03	0.23	0.17	0.11	0.01	0.12	-0.06	0.05	-0.27	-0.10
Nickel	-0.06	0.19	0.04	0.13	-0.36	0.21	0.29	0.05	-0.04	-0.32	0.04	-0.12
Potassium	-0.04	0.02	0.05	0.01	-0.15	0.45	0.17	-0.08	-0.01	-0.08	-0.01	0.01
Sodium	-0.03	0.04	-0.02	0.07	-0.03	0.25	0.15	-0.12	0.16	-0.04	-0.05	-0.26
Vanadium	0.03	-0.17	-0.06	-0.19	0.04	0.16	0.03	-0.28	0.05	-0.16	-0.34	0.14
Zinc	-0.18	0.47	-0.30	0.36	-0.18	0.28	-0.08	-0.20	-0.05	0.13	0.47	0.17

TABLE D.1. (contd)

	Eu-152	Eu-154	Eu-155	U 234	U 235	Pu-238	U 238	Pu 239,240	Barium	Calcium	Chromium
Eu-152	1.00										
Eu-154	0.86	1.00									
Eu-155	-0.19	-0.21	1.00								
U 234	-0.22	-0.26	0.43	1.00							
U 235	-0.17	-0.21	0.32	0.78	1.00						
Pu-238	0.54	0.53	0.00	-0.09	-0.14	1.00					
U 238	-0.26	-0.29	0.42	0.98	0.80	-0.12	1.00				
Pu 239,240	0.68	0.61	-0.24	-0.25	-0.17	0.49	-0.29	1.00			
Barium	0.17	0.04	0.01	-0.07	-0.14	-0.09	-0.04	0.18	1.00		
Calcium	-0.05	-0.07	-0.13	-0.24	-0.09	-0.04	-0.23	0.01	0.07	1.00	
Chromium	0.13	0.23	0.20	-0.06	-0.12	0.44	-0.05	0.20	0.03	0.16	1.00
Cobalt	-0.02	-0.03	0.01	-0.10	-0.29	-0.07	-0.11	-0.03	0.10	0.08	-0.07
Copper	0.08	0.12	0.06	-0.05	0.02	0.04	-0.12	0.17	-0.08	0.40	0.18
Iron	-0.29	-0.18	0.45	0.32	0.14	-0.06	0.32	-0.24	0.01	0.41	0.35
Lead	0.50	0.45	-0.09	-0.34	-0.18	0.37	-0.38	0.58	0.24	0.07	0.23
Magnesium	0.09	0.07	-0.07	-0.30	-0.15	0.16	-0.31	0.04	0.00	0.83	0.19
Manganese	-0.10	-0.16	-0.03	0.08	-0.14	-0.07	0.04	-0.10	0.25	0.49	-0.02
Nickel	0.11	0.18	0.05	-0.11	-0.03	0.17	-0.16	0.28	-0.04	0.34	0.16
Potassium	0.06	0.07	-0.16	-0.42	-0.19	0.05	-0.40	0.21	0.47	0.66	0.24
Sodium	0.01	0.03	-0.26	-0.29	-0.13	0.01	-0.24	0.08	0.04	0.84	0.08
Vanadium	-0.29	-0.16	0.41	0.38	0.17	-0.07	0.40	-0.22	0.14	0.28	0.31
Zinc	0.51	0.50	-0.07	-0.37	-0.17	0.25	-0.39	0.62	0.27	0.04	0.13





APPENDIX E

DOSE CALCULATIONS



## APPENDIX E

### DOSE CALCULATIONS

The potential radiation doses were calculated from several exposure scenarios involving particles of  $^{60}\text{Co}$  recovered during a recent river survey. The dose calculations include inhalation, ingestion, and direct skin exposure for an insoluble stellite particle. The deposition of the particle in the respiratory tract through inhalation, as a function of particle size, was predicted and the resulting dose from the deposition was calculated based on the recently accepted International Council on Radiation Protection (ICRP) respiratory tract model. The dose from ingestion of the particle (swallowing through the mouth) was calculated using MIRDOSE, an internal dosimetry computer code that assumes that the particle does not dissolve within the body. External doses from various realistic exposure scenarios were determined using the skin dose computer code VARSKIN 2. Before discussing the results of the dose calculations, a discussion of regulatory guidance for public exposure to discrete radioactive particles (DRPs) and the likelihood of exposures to DRPs is appropriate.

#### E.1 RADIATION DOSE GUIDANCE

There is no special guidance for skin contamination with DRPs for members of the public. The guidance for doses to the public in DOE Order 5400.5 limits the effective dose equivalent (EDE) to the maximally exposed individual (MEI) from all pathways from U.S. Department of Energy (DOE) sources to 100 mrem/yr EDE. The weighting factor for the skin dose recommended by the ICRP for large areas of skin contamination is 0.01. To contribute an EDE of 100 mrem/yr, the dose averaged over 100 cm<sup>2</sup> of the skin would have to be 10 rem/yr.

Evaluating and recording radiation doses from skin contamination of workers is addressed in the new DOE Radiological Control Manual (DOE 1992). This report does not address the potential health effects of such exposures. The guidance in the DOE Radiological Control Manual for areas <10 cm<sup>2</sup> states

that the dose is to be "averaged over the 1 cm<sup>2</sup> receiving the maximum dose; not added to any other dose equivalent, extremity or shallow dose equivalent (skin) recorded for the annual dose equivalent; and recorded in a person's radiation dose record as a special entry."

The National Council Radiation Protection and Measurements (NCRP) issued Report No. 106 in 1989: Limit for Exposure to Hot Particles on the Skin (NCRP 1989). This report, which addresses only occupational exposure, discusses health effects from irradiation by beta particles. The report describes the principal effect as ulceration of the skin and not skin cancer, and defines a conservative, threshold limit of 1 E+10 beta particles (75  $\mu$ Ci-hr) for ulceration, based on the dose received at a depth of 100  $\mu$ m. The cells in the nasal passage and the skin are not very sensitive to radiation-induced cancer, viz. a risk of 7 E-07 cancers per rad (7 E-05 cancers per Gy), and therefore the recommendations for dose limits are based on deterministic effects.

If radiation doses are extremely high, irradiated tissues can develop burns and other openings called ulcerations. A threshold for ulceration was defined as 230 krads (2300 Gy) evaluated at a depth of 100  $\mu$ m. A highly radioactive particle that remained long enough in the nasal passages or on the skin could lead to such radiation burns and ulceration. At somewhat lower doses temporary cosmetic changes would occur. The report stated that "ulceration of a minute area of skin, such as that which may occur near the threshold for acute deep ulceration, is not considered to be a severe nonstochastic effect." It is not clear how the discussion on health effects and the recommended limit presented in the NCRP report should be translated into guidance for exposure of a member of the public to DRPs on the skin.

A research study involving new experimental work and a literature review was performed by Pacific Northwest Laboratory for the Electric Power Research Institute (EPRI 1992). The authors of this study recommended a different threshold for effects from exposure to DRPs than that given in the NCRP report. The new threshold was based on a new endpoint for skin disruption, "acute necrosis," and given as 10 krads (100 Gy), based on the dose averaged over 1 cm<sup>2</sup> at a depth of 70  $\mu$ m. The authors state that "for stellite particles, which are low-energy beta emitters, the possibility of severe damage is

remote and the area of the skin subject to potential damage would not be cosmetically unacceptable." Once again, the intent of this report is to address the occupational arena, and application to the general public is not straightforward.

However, in contrast to the recommendations in the EPRI report that would allow some minor skin damage to occur, many experts feel that any openings in the skin of an occupational worker are unacceptable. Such openings, while not of a health concern, would prevent the worker from entering a contaminated area. The trend seems to be toward keeping the limit at  $1 \text{ E}+10$  beta particles ( $75 \text{ } \mu\text{Ci-hr}$ ) as published in NCRP (1989). This limit is used by the U.S. Nuclear Regulatory Commission (NRC) in its modified enforcement policy, thus establishing a de facto DRP dose limit. Because this limit is below the dose necessary to produce any skin damage, it seems prudent to use the same limit for the general public. Lowering the limit does not provide an increased level of protection because of the deterministic nature of the risk, and, therefore, a lower limit is not necessary.

At its April 1993 meeting in Washington, D.C., the ICRP approved a new model of the respiratory tract in which they have adopted a weighting factor of  $1 \text{ E}-05$  for the portion of the nose that is most likely to receive a significant dose from a DRP (James et al. 1991). It is possible to use the respiratory tract model to predict the EDE from a DRP that has been inhaled. If the dose to the nasal region is higher than the dose to any other body organ, the nose is further weighted by a factor of 0.025 when its contribution to the EDE is determined. Therefore, the dose to the nasal passages received by a member of the public from a DRP lodged there would have to be  $4 \text{ E}+03$  rem before the EDE limit of 0.1 rem were reached. At doses of this magnitude, significant damage to the tissues of the nose would occur. Thus, the EDE from a particle in the nose should not be the limiting value of acceptable dose. Instead, for exposure of the public to DRPs, a limit of  $10^{10}$  beta particles ( $75 \text{ } \mu\text{Ci-hr}$ ) is considered appropriate.

## E.2 LIKELIHOOD OF EXPOSURE

A study by Schwendiman indicated that the potential for inhalation or pickup of small particles from the ground was very low (Schwendiman 1958). In his study, he scattered fluorescent particles on dry ground and vegetation on the Hanford Site. Although this study is not directly applicable to the location where the two cobalt particles were found, it might be applicable to a scenario where the particles were contained in dry shoreline sediment. The probability of the particles becoming airborne from wet sediments should be less.

The likelihood of exposure to DRPs along the Hanford Reach of the Columbia River is reduced by the small number of such particles found in the several river surveys performed over the years. The likelihood of exposure is further reduced because these particles are not mobile in air or water. In addition, any particles that were present but not detected were probably covered by or buried in sediment. The particles will adhere to the sediment, and the sediment acts as an effective shield. For example, a 1-mm layer of sediment between a particle and the bare skin is sufficient to reduce the skin dose by a factor of 30, and no significant dose is expected from a particle that is buried below 1 cm of sediment.

## E.3 RADIATION DOSIMETRY

According to the supplied information, the particles recovered were stellite (with a typical density of  $8.3 \text{ g/cm}^3$ ), and their activity was  $1.7 \text{ } \mu\text{Ci}$  and  $16 \text{ } \mu\text{Ci}$ . Experience with other stellite DRPs that occur in commercial nuclear power plants indicates that they are essentially insoluble in the gastrointestinal (GI) tract or in any other bodily fluids. Based on measurements performed by Battelle on DRPs isolated at commercial power reactors, the specific activity of stellite averages  $6 \times 10^4 \text{ } \mu\text{Ci/mm}^3$ . From the specific activity for stellite particles, the two particles were estimated to have physical diameters of  $30 \text{ } \mu\text{m}$  and  $70 \text{ } \mu\text{m}$ , respectively. The aerodynamic diameters of particles of this physical size and density were used in the computer code LUDEP (Birchall et al. 1991) to determine the probability of their inhalation. The aerodynamic diameter of the two particles, which is even bigger than the physical diameter, is too large for them to enter the lung.

Therefore, the exposure modes with the highest potential radiation dose rates were found to be those that postulated lodging of the 16- $\mu$ Ci particle in the nasal passages (40 rad/hr averaged over 1 cm<sup>2</sup> at depth of 40  $\mu$ m) and direct contact of that particle with bare skin (30 rad/hr averaged over 1 cm<sup>2</sup> at depth of 70  $\mu$ m). The potential radiation doses from other scenarios were also calculated, including ingestion of the insoluble particles, the dose to several body organs from the passage of the particles through the GI tract, and dose rates to the skin from exposure through intervening layers of cloth. In addition, a calculation was made of the dose to lung tissues from inhalation of a stellite particle small enough to penetrate into the lungs.

#### E.4 INHALATION OF A SMALL PARTICLE

The dose to lung and the extrathoracic (ET) region from inhalation of a DRP depends on the diameter of the particle. To determine the possible effects of inhalation of a DRP, three particle sizes were considered: particles with a physical diameter greater than 10  $\mu$ m, a particle with a diameter of 5  $\mu$ m, and a particle with a diameter of 1  $\mu$ m. The activity of a particle with a diameter of 10  $\mu$ m is 50 nCi, the activity of a particle with a diameter of 5  $\mu$ m is 6 nCi, and the activity of a particle with a diameter of 1  $\mu$ m is 50 pCi. A stellite particle with a diameter of 5  $\mu$ m would probably be barely detectable during a ground survey conducted with a GM meter. The dose from a 1- $\mu$ m particle was deemed to be too small to warrant calculation.

According to the ICRP model, when a person is exposed to a stellite particle that is larger than 10  $\mu$ m there is a 50% probability that the particle will be deposited in the ET region. The probability of deposition in the anterior part of the nose (ET1) region is equally likely as deposition in the naso- and oropharynx (ET2) region. Particles that are deposited in ET1 usually remain there for an average time of about 1 day. They are eventually removed either physically or by sneezing. The average residence time in the ET2 region is about 0.2 hr. Particles that are deposited in ET2 are eventually swallowed.

Using the LUDPE code, doses were calculated for deposition in both the ET1 and ET2 regions. In the following dose calculations, it was assumed that particles would remain in the various compartments for a time equal to twice

the average. For a particle that is deposited in the ET1 region, the potential committed dose factors are about 8 rad/d/ $\mu$ Ci to the nose and 0.2 rad/d/ $\mu$ Ci to the naso- and oropharynx. Therefore, the calculated committed dose from a 16- $\mu$ Ci particle spending 2 days in the ET1 region was calculated to be 250 rad. This same particle would contribute 6 rad to the naso- and oropharynx. Clearly the limiting organ dose is that to the nose. If the regulatory limit for public exposure to these particles were the same as the limit for occupational exposure, i.e., 75  $\mu$ Ci-hr, then the limit would be exceeded for the 16- $\mu$ Ci particle. When credit is taken for self-absorption as permitted in NCRP (1989), the exposure from the 1.7- $\mu$ Ci particle in the nose would be very close to the NCRP limit expressed as 1 E+10 beta particles emitted from the surface of the particle.

Committed doses from a 16- $\mu$ Ci particle in the ET2 region were calculated to be 20 rad to the naso- and oropharynx and 10 rad to the nose. For particles that are deposited in the ET2 region, the naso- and oropharynx dose is limiting. The EDE associated with a particle deposited in the ET2 region was estimated to be <1 mrem, well below the radiation guide for exposure of a member of the public.

Inhaled particles of sufficiently small size can also deposit in the bronchial (BB) region. Stellite particles ranging in size from 5 to 10  $\mu$ m have a small probability of deposition in that region (0.4% maximum). The activity associated with a 10- $\mu$ m particle is calculated to be 50 nCi. The dose factor to the BB region from a  $^{60}\text{Co}$  particle deposited there was calculated to be 60  $\mu$ rad/hr/nCi. Therefore, the dose rate from a 10- $\mu$ m particle in the BB region would be 3 mrad/hr. In the ICRP model, transport from the BB region is composed of two components, fast transport where particles have an average residence time of 0.1 d and a slow transport with an average residence time of about 1 month. However, the probability of slow transport is only 0.7% of the probability of fast transport.

When coupled with the short time that particles are predicted to remain in the BB region (probably 5 hr or less), the total dose (<20 mrad) from a 10- $\mu$ m particle will not produce any adverse deterministic health effects. In

addition, the contribution to the EDE from such a particle in the BB region would be <1 mrem, a dose well below the radiation guides for exposure of a member of the public.

The probability of a 10- $\mu\text{m}$  particle depositing in the BB region and transporting quickly is only 0.004. Because of its long residence time (up to 2 months), the potential dose from a slow-transporting particle in the BB region would be about 300 times that of a fast-transporting particle or just under 5 rad. However, the probability of the particle lodging there is only about 7 E-03 times the probability for deposition in the fast BB region, or 3 E-05. These probabilities must be coupled with the low probability of inhaling the particle.

In summary, if particles stay in the nose for 2 days, then those that are about 1.7  $\mu\text{Ci}$  (corresponding to a physical diameter of 30  $\mu\text{m}$ ) can deliver doses to the nose that approach a limit of 75  $\mu\text{Ci-hr}$ . Particles of this size will not be deposited in the lung. The dose equivalent from a DRP deposited in either the ET or the BB region does not appear to be a health concern.

#### E.5 INGESTION OF A PARTICLE

The impact of ingesting the insoluble particles was evaluated by calculating potential radiation doses to the various organs in the body from passage of the particles through the GI tract. Calculations were performed with the computer code MIRDOSE (Watson et al. 1984). This code uses the ICRP GI tract model to calculate radiation dose to several organs of the body from the gamma radiation ("crossfire") emitted from the radionuclide while it passes through the tract with no absorption into the bloodstream. The results of the MIRDOSE calculation are listed in Table E.1. The code does not generate an EDE. However, the EDE can be calculated from the standard set of organ-dose weighting factors adopted by the U.S. agencies concerned with radiation protection. The calculated EDEs are listed at the bottom of the table; both values are less than the DOE stochastic limit of 100 mrem. The health effects of concern from exposure to such DRP are clearly deterministic (nonstochastic).

**TABLE E.1.** Calculated Radiation Doses from Ingestion of  $^{60}\text{Co}$  Particles

Target Organs	mrad	
	1.7 $\mu\text{Ci}$	16 $\mu\text{Ci}$
Adrenals	<0.5	5
Brain	<0.5	<0.5
Breasts	<0.5	1
Gall Bladder Wall	2	20
Lower Level Intestine	32	300
Small Intestine	7	69
Stomach	2	23
Upper Level Intestine	15	140
Heart Wall	<0.5	2
Kidney	1	10
Liver	1	7
Lungs	<0.5	2
Muscle	1	9
Ovaries	8	74
Pancreas	1	9
Red Marrow	1	13
Bone Surface	1	6
Skin	<0.5	3
Spleen	1	7
Testes	1	7
Thymus	<0.5	1
Thyroid	<0.5	<0.5
Urinary Bladder Wall	2	23
Uterus	3	32
Remainder	1	10
Effective Dose Equiv.	6	60

## E.6 EXTERNAL EXPOSURE

A second set of calculations was performed using the computer code VARSKIN 2 (Durham 1992), written for the U.S. Nuclear Regulatory Commission to calculate dose to skin from DRP. Calculations were performed for a number of exposure scenarios: a particle that is inhaled into the nose, a particle that comes into contact with bare skin, a particle that resides in a person's pocket, a particle that lies below a person's sleeping bag, and the penetrating (deep) dose.

The calculations were performed assuming that the particles had an activity-to-volume ratio of  $5.6 \text{ E}+4 \text{ } \mu\text{Ci}/\text{mm}^3$ , determined based on experience with stellite DRPs found at U.S. nuclear power plants. The geometry of the particles was assumed to be cylindrical with a thickness equal to its diameter. Thus, the 1.7- $\mu\text{Ci}$  particle had a thickness and diameter of  $30 \text{ } \mu\text{m}$ , and the 16- $\mu\text{Ci}$  particle had a thickness and diameter of  $70 \text{ } \mu\text{m}$ . The cylindrical geometry model was chosen to maximize the accuracy of the calculations.

### E.6.1 Exposure Scenarios

As stated above, a particle that is inhaled through the nose must reside in the ET1 region if any regulatory limit is to be approached. Because the depth of the sensitive layer of cells in the nose is  $4 \text{ mg}/\text{cm}^2$ , dose was calculated at that density thickness. The doses calculated using VARSKIN 2 differ from those performed using LUDEP for a number of reasons. First, LUDEP assumes that the activity is spread uniformly throughout the region, while VARSKIN 2 assumes that the source is a particle. Second, LUDEP does not account for particle self-absorption, while this effect is modeled in VARSKIN 2. Finally, the dose calculated by VARSKIN 2 represents the maximum dose to  $1 \text{ cm}^2$  of tissue in the ET1 region.

To simulate the dose to the sensitive layer of cells on the skin, a density thickness of  $7 \text{ mg}/\text{cm}^2$  was chosen. This depth is accepted by international standards committees as the depth at which to calculate skin dose.

To simulate the dose to skin (at a depth of  $7 \text{ mg}/\text{cm}^2$ ) from a particle that has become lodged in a pocket, a layer of clothing was calculated as being placed between the particle and the skin. The clothing was assumed to have a thickness of  $0.4 \text{ mm}$  and a density of  $0.7 \text{ g}/\text{cm}^3$ . These data were

obtained from typical coverall material used in nuclear power plants and represent a conservative value for the thickness of clothing.

The dose to skin from a particle located below a sleeping bag was determined by choosing a clothing thickness that would completely stop the beta radiation emitted from the particle. In this case, a clothing thickness equivalent to two layers of coverall material was sufficient to stop all beta radiation.

The penetrating dose from gamma radiation was calculated by choosing a skin depth of 1 cm. Note that the penetrating dose is calculated to be absorbed by a limited area of the skin and not distributed over the entire body. The penetrating dose should not be used as the dose to the whole body.

#### E.6.2 Results

The doses calculated using VARSKIN 2 represent conservative estimates of dose rate to the skin averaged over 1 cm<sup>2</sup>. The calculated numbers are the maximum possible dose rates for the given scenarios. The results of the calculations are presented in Table E.2.

TABLE E.2. Absorbed Doses from <sup>60</sup>Co Particles<sup>(a)</sup>

Scenario	rad/hr			
	1.7 $\mu$ Ci		16 $\mu$ Ci	
	Beta	Total	Beta	Total
Basal cells in nasal passage	7.3	7.6	38	41
Contact with bare skin	4.4	4.7	23	26
Skin through a pocket	0.11	0.34	0.47	2.6
Skin through sleeping bag	0.0	0.18	0.0	1.7
Deep dose (1 cm)	0.0	0.019	0.0	0.18

(a) Calculated using the VARSKIN 2 code.

## E.7 CONCLUSIONS

Based on calculations using LUDEP, MIRDOSE, and VARSKIN 2, and based on available regulatory guidance, the dose-limiting exposure scenario is a particle that is inhaled into the front part of the nose, where the particle may remain for as long as 48 hr. For a 48-hr residence time, the maximum dose to the nose was calculated by the VARSKIN 2 code to be 2000 rad (41 rads/hr x 48 hr) for the 16- $\mu$ Ci particle and 360 rad for the 1.7- $\mu$ Ci particle. If the regulatory limit for public exposure to these particles was the same as the limit for occupational exposure, i.e., 75  $\mu$ Ci-hr, then the limit would be exceeded by about a factor of ten for the 16- $\mu$ Ci particle. The exposure from the 1.7- $\mu$ Ci particle in the nose would be very close to the NCRP limit expressed as 1 E+10 beta particles emitted from the surface of the particle when credit is taken for self-absorption as permitted in NCRP (1989).

To fully understand the likelihood of a DRP exposure, a detailed radiation survey of the accessible areas along the Columbia River would be prudent. One method of making this determination is to perform a thorough contamination survey of the publicly accessible banks of the Columbia River. An appropriate instrument and scan speed that will allow detection of particles which have an activity of 1  $\mu$ Ci or more should be used. Particles with activities less than 1  $\mu$ Ci should not, in all probability, pose a health hazard and would not result in exposure of the public in excess of limits.

## E.8 REFERENCES

Birchall, A., M. R. Bailey, and A. C. James. 1991. "LUDEP: A Lung Dose Evaluation Program." Radiation Protection Dosimetry 38:167-174.

DOE (U.S. Department of Energy). 1988. Internal Dose Conversion Factors for Calculation of Dose to the Public. DOE/EH-0071, U.S. Department of Energy, Washington, D.C.

DOE (U.S. Department of Energy). 1992. Radiological Control Manual. DOE/EH-0256T, U.S. Department of Energy, Washington, D.C.

Durham, J. S. 1992. VARSKIN Mod 2 and SADDE Mod 2: Computer Codes for Assessing Skin Dose from Skin Contamination. NUREG/CR-5873, U.S. Nuclear Regulatory Commission, Washington, D.C.

EPRI (Electric Power Research Institute). 1992. Threshold Levels for Nonstochastic Skin Effects from Low-Energy Discrete Radioactive Particles. EPRI TR-100048, Electric Power Research Institute, Palo Alto, California.

James, A. C., P. Gehr, R. Masse, R. G. Cuddihy, F. T. Cross, A. Birchell, J. S. Durham, and J. K. Briant. 1991. "Dosimetry Model for Bronchial and Extrathoracic Tissues of the Respiratory Tract." Radiation Protection Dosimetry 37:221-230.

NCRP (National Council on Radiation Protection and Measurements). 1989. Limit for Exposure to Hot Particles on the Skin. NCRP Report No. 106, National Council on Radiation Protection and Measurements, Bethesda, Maryland.

Schwendiman, L. C. 1958. "Probability of Human Contact and Inhalation of Particles." Health Physics 1:352-356.

Watson, E. V., M. G. Stabin, and W. E. Bolch. 1984. Documentation Package for MIRDOSE. Oak Ridge Associated Universities, Oak Ridge, Tennessee.

DISTRIBUTION

<u>No. of Copies</u>		<u>No. of Copies</u>	
<u>OFFSITE</u>		J. W. Schmidt (2)	H6-30
12	DOE/Office of Scientific and Technical Information	C. D. Wade	NI-06
		S. Weiss	H6-02
		52	<u>Pacific Northwest Laboratory</u>
	S. Cross	E. J. Antonio	K6-61
	Washington State Department of Ecology	L. E. Bisping	K6-61
	P.O. Box 57600	L. L. Cadwell	K6-63
	Olympia, WA 98504-7600	A. T. Cooper (7)	K6-61
2	John Erickson	D. D. Dauble	K6-54
	Washington Department of Health	M. K. DeSmet	K6-62
	Airustrial Park	R. L. Dirkes	K6-61
	P.O. Box 47827	J. S. Durham (2)	K3-55
	Olympia, WA 98504-7827	S. L. Friant	K6-52
	L. E. Gadbois	R. O. Gilbert	K7-34
	U.S. Environmental Protection Agency	R. W. Hanf	K6-61
	712 Swift, MS 85-01	L. R. Huesties	K6-61
	Richland, WA 99352	R. E. Jaquish (2)	K1-30
		E. A. Lepel	P8-08
		T. K. Lucas	K6-52
		R. E. Lundgren	K6-62
		E. W. Lusty (2)	K6-78
		G. W. Patton	K6-61
		T. M. Poston	K6-61
		K. M. Probasco	K6-52
6	<u>DOE Richland Operations Office</u>	J. K. Soldat (2)	K3-54
	B. L. Foley	B. L. Tiller	K6-60
	E. D. Goller	H. E. Westerdahl	K6-60
	R. D. Hildebrand	R. K. Woodruff (10)	K6-61
	R. Stewart	Publication Coordination	
	K. M. Thompson	SESP Historical Files/	
	M. W. Tiernan	R. K. Woodruff (2)	
		Technical Report Files (5)	
	<u>U.S. Army Corps of Engineers</u>	<u>Routing</u>	
	A. Foote	R. M. Ecker	
	M. P. Johansen	M. J. Graham	
9	<u>Westinghouse Hanford Company</u>	P. M. Irving	
	J. J. Dorian	C. S. Sloane	
	R. P. Henckel (2)	P. C. Hays (last)	
	N. K. Lane		
	K. M. Leonard		

